



BRNO UNIVERSITY OF TECHNOLOGY

FACULTY OF CIVIL ENGINEERING

INSTITUTE OF STRUCTURAL MECHANICS

**NUMERICAL ANALYSIS OF STRESS FIELD IN THE
VICINITY OF TWO SYMMETRICAL NOTCHES IN
FOUR POINT BENDING TEST: MIXED MODE I+II**

BACHELOR THESIS

AUTHOR

José Antonio Rodríguez Valdés

SUPERVISOR

Prof. Stanislav Seitl, Ph.D.

SUPERVISOR SPECIALIST:

Ing. Petr Miarka

BRNO 2019

ABSTRACT

In this thesis it is described the crack initiation in a four-point bending test with two initial symmetrical notches for concrete, according to the fracture mechanics laws and using the linear elastic theory. The specimen was modelled using the finite element method in software ANSYS. In numerical analysis, the values of the stress intensity factor and the *T*-Stress have been obtained for various geometries and boundary conditions of the concrete specimens. There is only one fixed value, the width of the specimen, the others have been related to it. For this purpose, the distance between cracks, the relative crack length and the specimen size have been varied. Additionally, the values of the displacements in *x* and *y* axes have been obtained for certain geometries, as a method of checking the positive or negative sign of the SIF K_I . The results have been compared according to each particular geometry, showing in graphs the curves obtained for the SIF and for the *T*-Stress. From this results we can extract that all the curves have a similar trend, with bigger or smaller parameters depending on the geometry, also there are repeated single points for all the geometries, where the slope changes from positive to negative or vice versa. In the future this numerical results could be used for evaluation of fracture properties focused on mixed mode I+II.

KEYWORDS (IN ENGLISH)

Crack, concrete, fracture mechanics, Stress intensity factor, T-stress, FEM

ABSTRACT

En este trabajo se describe, según las leyes de mecánica de la fractura elástica lineal, el crecimiento de grieta en un ensayo de flexión en cuatro puntos de una probeta de hormigón. El ensayo se ha modelado mediante el software de elementos finitos, ANSYS. Para ello se han obtenido los valores del factor de intensidad de tensiones y la *T*-Stress, para diferentes geometrías de la probeta, con este fin se ha variado la distancia entre grietas, la longitud de grieta y la longitud de la probeta, únicamente se ha mantenido un valor fijado, el ancho de la probeta. Así mismo se han obtenido los valores de los desplazamientos en los ejes *x* e *y* para ciertas geometrías, como método de comprobación del signo positivo o negativo de la K_I . Los resultados han sido comparados en función de cada geometría particular, exponiendo en gráficos las curvas obtenidas para el factor de intensidad de tensiones y para la *T*-Stress. De los resultados podemos extraer que las curvas siguen siempre una tendencia similar, y que existen puntos singulares que se repiten para todas las geometrías, en los que la pendiente cambia. En un futuro estos resultados podrían usarse para distintos estudios en el campo de la mecánica de la fractura.

KEYWORDS (IN NATIVE LANGUAGE)

Grieta, hormigón, Mecánica de la fractura, Factor de Intensidad de Tensiones, T-stress, Método de Elementos Finitos

BIBLIOGRAPHIC CITATION

José Antonio Rodríguez Valdés *Numerical analysis of stress field in the vicinity of two symmetrical notches in four point bending test: mixed mode I+II. Brno, 2019. 48 p., 15 p. of attachments. Bachelor Thesis. Brno University of Technology, Faculty of civil engineering, Institute of structural mechanics. Supervisor: Prof. Stanislav Seitl, Ph.D. Supervisor Specialist: Ing. Petr Miarka*

ACKNOWLEDGEMENT

This thesis is the final part of my Bachelor's Degree of Mechanical Engineering in the University of Oviedo. It has been done in Brno, Czech Republic during my Erasmus+ Mobility in the Brno University of Technology.

I would like to thank my supervisors, Stanislav Seitl and Petr Miarka, for all their invaluable help during this project. I would also like to thank all the professors from University of Oviedo who help me this years, specially Prof. Maria Jesus Lamela, University of Oviedo Erasmus+ Coordinator. Finally but not less important, I would like to thank my family, for supporting with me this years, and all my friends, for all the good and not so good moments that we share together.

This Bachelor thesis has been written with financial support from "National Sustainability Programme I" project "AdMaS UP – Advanced Materials, Structures and Technologies" (**No. LO1408**) supported by the Ministry of Education, Youth and Sport of the Czech Republic and Brno University of Technology.

TABLE OF CONTENTS

1. Introduction	7
2. Aim.	7
3. Theoretical background.....	8
3.1. Fracture Mechanics.....	8
3.1.1. Simplifying assumptions in Fracture Mechanics.....	8
3.1.2. Griffith`s Theory	8
3.1.3. Stress Field Equations from the Williams` Expansion.....	10
3.1.4. Stress Intensity Factors.	12
3.1.5. <i>T-Stress</i>	13
3.1.6. Mixed Mode Fracture. Parallel cracks.....	14
3.1.7. Crack tip plasticity.....	15
3.1.8. Fracture Mechanical Criteria.....	16
3.2. Concrete characteristics.	18
3.2.1. Concrete as a composite material.....	18
3.2.2. Mechanical properties of concrete.	18
3.2.3. Concrete Testing.	20
4. Numerical Model.....	20
4.1. Geometry and basic boundary conditions.	20
4.2. Material properties.....	21
4.3. Element type.	22
4.4. Modelling the specimen.	22
4.4.1. Keypoints.....	22
4.4.2. Lines.....	23
4.4.3. Areas.....	24
4.4.4. Meshing.....	25
4.5. Boundary conditions.....	26
4.6. Solution and postprocessing in ANSYS.	26
4.7. Calculate the <i>T-Stress</i> from S_x and S_y	27
5. Various boundary conditions used for numerical study.....	29
6. Numerical results and discussion.....	31
6.1. Constant <i>D/S</i> ratio curves.....	32
6.2. Analysis of the graphs for constant <i>D/S</i> ratio.....	37

6.3. Constant S/W ratio curves.	38
6.4. Analysis of the graphs for constant S/W ratio.	45
6.5. K_I sign discussion.	46
7. Conclusions.	50
References	51
List of abbreviations.	53
List of symbols.....	54
List of figures.	55
List of graphs.	56
List of tables.....	57
Curriculum vitae.....	58
Annexes.....	60
Annexe I: Macro.	60
Annexe II: Results.....	67
Stress Intensity Factors for mixed Mode I/II and T -Stress.....	67
Displacements.	71

1. Introduction

If we talk about fracture mechanics, the main way of studying a material's behaviour is checking his crack growth. With this purpose it should be considered, characteristic parameters of the lineal elastic fracture mechanics as stress intensity factor and *T-Stress*.

Actually, the concrete is the most used material in civil engineering, for this reason it is so important to know deeply, everything related to the crack growth in beams with different geometries. In this thesis, it has been studied the crack growth in a concrete specimen with four supports and two notches. To define the material, it has been used two elastic properties of concrete, the Young's Modulus and the Poisson's ratio. The results of this work could be used as a reference for different studies in fracture mechanics or just for a didactic use, but that's not useful for real structures or in a different field of engineering, because it considers lineal elastic theory and additionally, in a real structure it is used reinforced concrete and it is steel the material which supports the bending.

With a set of graphs, it have been compared how the geometric parameters affects to this type of samples. This way of working have been improved over time, from the laboratory real tests to the current simulation software using the finite elements method. Actually, before performing the laboratory analysis, it should be modelled and studied how it works in a computer in order to save money and time. In this job, the different geometries have been tested just in the finite element software, ANSYS. ANSYS provides directly the values of the stress intensity factor, and the stress values needed to calculate the T-Stress.

The stress intensity factor K is a fundamental parameter in fracture mechanics field, it express the stress state in the crack tip, when it arrives to a critical value which makes the crack collapse, it is called fracture toughness K_c . There are three modes of cracking, K_I , K_{II} and K_{III} , each one represents a stress direction in the crack tip. In the results it is proved that in this work it has been obtained just K_I and K_{II} .

The *T-Stress* is also a concept which is tightly related to fracture mechanics, it is used for different functions in this field, but mainly it can be considered as a parameter to control the stress stability of the crack.

The objective of this thesis is about extracting some results and conclusions, which can be useful in a future in this field of concrete fracture mechanics.

2. Aim.

The main aim of this thesis is to describe the the stress field in the vicinity of two symmetrical initial notches in a four point bending specimen during the static load.

Partially, numerical study is focused on the influence of various boundary conditions on three main fracture mechanics parameters. The parameters in case of mixed mode I+II are Stress Intensity Factor for mode I and for mode II and factor describe the constraint *T-Stress*.

This numerical analysis was done in the Finite Element Method software, ANSYS.

3. Theoretical background.

3.1. Fracture Mechanics.

All the thesis is based on fracture mechanics [1], but there are two basic theories in this field; linear elastic fracture mechanics (LEFM) and elastic-plastic fracture mechanics (EPFM) theories. In this thesis, the introduced study is performed in LEFM.

3.1.1. Simplifying assumptions in Fracture Mechanics.

In Fracture Mechanics there are simplified concepts which are common in the works, the following are used in this thesis:

- The material is homogenous isotropic and continuum, its behaviour, as it is said before, is linear elastic, and displacements and strains are small.
- The material is free from internal stresses and body forces such as those due to gravity.
- The initial notch is like crack that is flat.
- The body being considered is of constant thickness.

The last assumption results in considerable mathematical simplification, because it turns a three-dimensional situation in a two-dimensional one. [2][1]

3.1.2. Griffith's Theory

Griffith energy balance consists in applying the first law of thermodynamics to fracture mechanics, when a system goes from a nonequilibrium state to equilibrium, there is a net decrease in energy, he applies this idea to a crack growth. Furthermore, Griffiths says that the low resistances in brittle bodies are due to little cracks produced on the manufacturing process. [3]

An existing crack can grow only if such a process causes the total energy to overcome the material resistance in the crack tip, where the presence of the crack induces a concentration of stresses. That is why the critical conditions for fracture can be defined as the point where crack growth occurs under equilibrium conditions, with no net change in total energy. [3]

Located stress on crack tip is defined as follows:

$$\sigma_A = \sigma_\infty \left(1 + \frac{2a}{b}\right) \quad (1)$$

where σ_A is the located stress at the crack tip, σ_∞ is the applied stress and a and b are the two axes of the ellipse.

Inglis modified the formula, adding the curvature radius ρ ,

$$\sigma_A = \sigma_\infty \left(1 + 2\sqrt{\frac{a}{\rho}}\right) \quad (2)$$

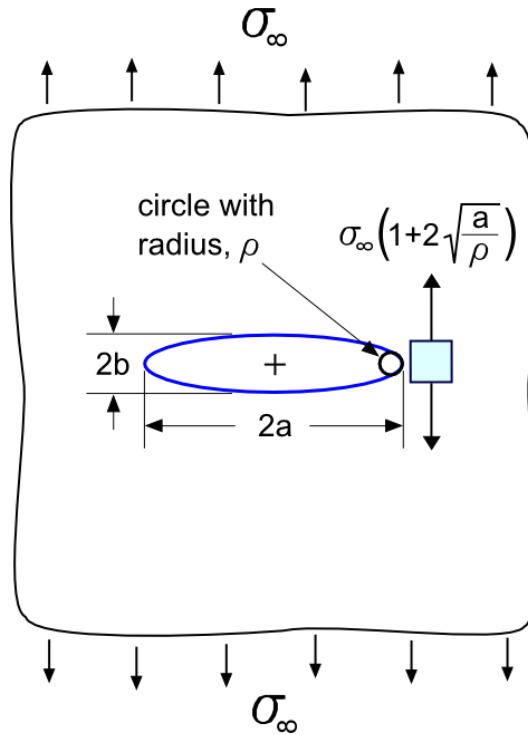


Figure 1: Elliptical crack retaken from [4].

Then, assuming $a \gg \gg b$ and $\rho = b^2/a$, the located stress at the crack tip is:

$$\sigma_{loc} = 2\sigma_\infty \left(\frac{a}{\rho}\right)^{\frac{1}{2}} \quad (3)$$

This equation predicts an infinite stress when $\rho=0$ that is wrong, so Griffith improves his theory, including energy in the equation. It results in the next expression:

$$\sigma_f = \left(\frac{E \gamma_s}{4a}\right)^{\frac{1}{2}} \quad (4)$$

where σ_f is the remote stress at failure, E is the Young's modulus, γ_s is the surface energy per unit area.

The equation (4) was developed by Gehlen and Kanninen [5] in order to use it at atomic level:

$$\sigma_R = \sigma_{max} = \left(\frac{E \gamma_s}{a}\right)^{\frac{1}{2}} \quad (5)$$

where a is the crack length, γ_s and E are the same terms as the previous equation. Matching $\sigma_R = \sigma_{loc}$ it is obtained:

$$\sigma_R = \left[\left(\frac{E\gamma}{4a} \right) \left(\frac{\rho}{a} \right) \right]^{\frac{1}{2}} \quad (6)$$

Finally if $\rho=a$ and $\gamma = \frac{Ea}{100}$, it is possible to say that $\sigma_R = 10^{-3} E$.

3.1.3. Stress Field Equations from the Williams' Expansion.

Applying the elasticity theory to the case of a random geometry body, which contains a crack and supports different external pressures or forces, it is possible to obtain the stress field in the vicinity of the crack tip. The position in this stress field is defined by polar coordinates (r, θ) and the origin is on the crack tip.

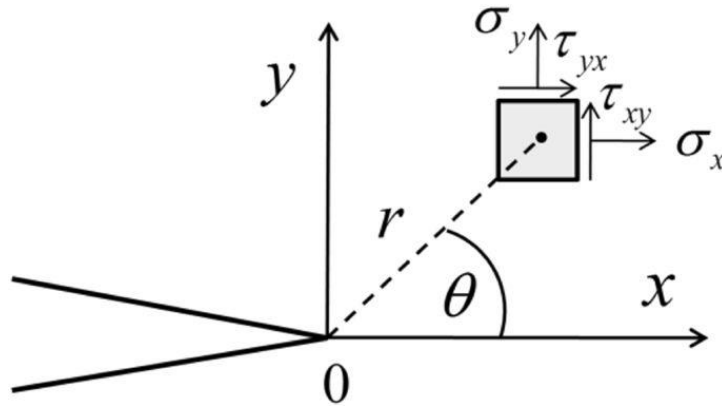


Figure 2: A point defined in the vicinity of the crack tip.^[1]

The Williams's expansion [6] is an infinite power series which describes the stress field by the following function:

$$\phi(r, \theta) = \sum_{n=0}^{\infty} r^{\lambda_n+1} F_n(\theta) \quad (7)$$

In this function we can express the $F_n(\theta)$ as:

$$F_n(\theta) = A_n \sin(\lambda_n + 1) \theta + B_n \cos(\lambda_n + 1) \theta + C_n \sin(\lambda_n + 1) \theta + D_n \cos(\lambda_n + 1) \theta \quad (8)$$

A_n, B_n, C_n and D_n are constants and nonzero, the displacements must be finite in all regions of the body so λ must be up to 0. Assuming traction free in the crack faces, $\sigma_{\theta\theta}(0) = \sigma_{\theta\theta}(2\pi) = \sigma_{r\theta}(0) = \sigma_{r\theta}(2\pi) = 0$ which implies $F(0)=F(2\pi)=F'(0)=F'(2\pi)$ as boundary condition. We have the next eigenvalues for λ_n :

$$\lambda_n = \frac{n}{2} \text{ where } n = 1, 2, 3, \dots \quad (9)$$

Then it is obtained :

$$\phi(r, \theta) = r^{\frac{n}{2}+1} \left\{ \left[\sin\left(\frac{n}{2} + 1\right) \theta^* - \frac{n-2}{n+2} \sin\left(\frac{n}{2} + 1\right) \theta^* \right] + D_n \left[\cos\left(\frac{n}{2} - 1\right) \theta - \cos\left(\frac{n}{2} + 1\right) \theta \right] \right\} \quad (10)$$

Substituting in equation (9), $\theta = \theta^* - \pi$, giving the first values of n and after some mathematical manipulations, the next equation represents the stress field in the vicinity of the crack tip:

$$\sigma_{i,j} = \frac{K_I}{\sqrt{2\pi r}} f_{i,j}^I(\theta) + \frac{K_{II}}{\sqrt{2\pi r}} f_{i,j}^{II}(\theta) + T + O_{i,j}(r, \theta) \quad (11)$$

where K_I and K_{II} are the stress intensity factors (SIF), $f_{i,j}^I(\theta)$ and $f_{i,j}^{II}(\theta)$ are dimensionless functions, usually written as Y_I and Y_{II} , which are used to consider the geometry in the equation, the T or T -Stress is an independent term and $O_{i,j}(r, \theta)$ represent the higher order terms which are negligible.

Table 1: Stress field equations. Mode I and II. [7]

	Mode I	Mode II
σ_{xx}	$\frac{K_I}{\sqrt{2\pi r}} \cos\left(\frac{\theta}{2}\right) \left[1 - \sin\left(\frac{\theta}{2}\right) \sin\left(\frac{3\theta}{2}\right) \right]$	$\frac{K_{II}}{\sqrt{2\pi r}} \cos\left(\frac{\theta}{2}\right) \left[2 + \cos\left(\frac{\theta}{2}\right) \cos\left(\frac{3\theta}{2}\right) \right]$
σ_{yy}	$\frac{K_I}{\sqrt{2\pi r}} \cos\left(\frac{\theta}{2}\right) \left[1 + \sin\left(\frac{\theta}{2}\right) \sin\left(\frac{3\theta}{2}\right) \right]$	$\frac{K_{II}}{\sqrt{2\pi r}} \cos\left(\frac{\theta}{2}\right) \sin\left(\frac{\theta}{2}\right) \cos\left(\frac{3\theta}{2}\right)$
τ_{xy}	$\frac{K_I}{\sqrt{2\pi r}} \cos\left(\frac{\theta}{2}\right) \sin\left(\frac{\theta}{2}\right) \cos\left(\frac{3\theta}{2}\right)$	$\frac{K_{II}}{\sqrt{2\pi r}} \cos\left(\frac{\theta}{2}\right) \left[1 - \sin\left(\frac{\theta}{2}\right) \sin\left(\frac{3\theta}{2}\right) \right]$
σ_{zz}	0 (Plane Stress) $\nu (\sigma_{xx} + \sigma_{yy})$ (Plane Strain)	0 (Plane Stress) $\nu (\sigma_{xx} + \sigma_{yy})$ (Plane Strain)
τ_{xz}, τ_{yz}	0	0

where ν is Poisson's ratio

Table 2: Displacements equations. Mode I and II. [7]

	Mode I	Mode II
u_x	$\frac{K_I}{2\mu} \sqrt{\frac{r}{2\pi}} \cos\left(\frac{\theta}{2}\right) \left[\kappa - 1 + 2 \sin^2\left(\frac{\theta}{2}\right)\right]$	$\frac{K_{II}}{2\mu} \sqrt{\frac{r}{2\pi}} \sin\left(\frac{\theta}{2}\right) \left[\kappa + 1 + 2 \cos^2\left(\frac{\theta}{2}\right)\right]$
u_y	$\frac{K_I}{2\mu} \sqrt{\frac{r}{2\pi}} \sin\left(\frac{\theta}{2}\right) \left[\kappa + 1 - 2 \cos^2\left(\frac{\theta}{2}\right)\right]$	$\frac{K_{II}}{2\mu} \sqrt{\frac{r}{2\pi}} \cos\left(\frac{\theta}{2}\right) \left[\kappa - 1 - 2 \sin^2\left(\frac{\theta}{2}\right)\right]$

μ is the shear modulus

$\kappa=3-4\nu$ (plane strain)

$\kappa=(3-\nu)/(1+\nu)$ (plane stress)

Table 3: Tangential Stresses and displacement. Mode III. [7]

Mode III
$\tau_{xz} = -\frac{K_{III}}{\sqrt{2\pi r}} \sin\left(\frac{\theta}{2}\right)$
$\tau_{yz} = \frac{K_{III}}{\sqrt{2\pi r}} \cos\left(\frac{\theta}{2}\right)$
$u_z = \frac{K_{III}}{\mu} \sqrt{\frac{r}{2\pi}} \sin\left(\frac{\theta}{2}\right)$

3.1.4. Stress Intensity Factors.

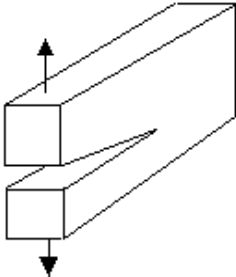
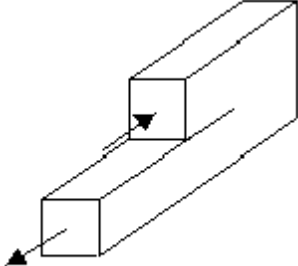
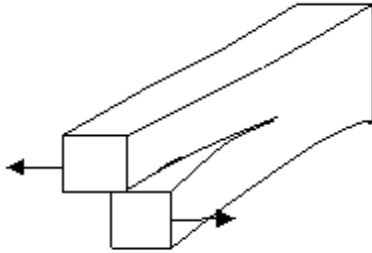
The stress intensity factor (K) defines the amplitude of the crack-tip singularity. That is, stresses near the crack tip increase in proportion to K. Furthermore, the stress intensity factor defines the crack tip conditions, if K is known, it is possible to obtain stress, strain, and displacement as a function of r and θ . This single-parameter description of crack tip conditions turns out to be one of the most important concepts in fracture mechanics [8].

Stress intensity factor is an expression that only depends on the stress applied σ , the crack length a , and the specimen's geometry C .

$$K = C\sigma\sqrt{\pi a} \quad (12)$$

When a pressure is applied to a cracked body, the crack surfaces moves in different directions, it depends on the type of load, the direction of the load, etc. There are three possible modes of crack surface displacement. The stress intensity factor is evaluated in each mode (K_I , K_{II} , K_{III}).

Table 4: Modes of crack tip surface displacement

Mode I (Opening mode)	
Mode II (Edge sliding mode)	
Mode III (Shear mode)	

For linear elastic materials, stress, strain and displacement are additive, the stress intensity factor is additive in each mode too, but it is not correct to sum a K_I with a K_{II} .

$$K_I^{Total} = K_I^{(A)} + K_I^{(B)} + K_I^{(C)} \quad (13)$$

$$K_{Total} \neq K_I + K_{II} + K_{III} \quad (14)$$

For Mode I the sign is important, if K_I is positive the crack will be opening, if K_I is negative the crack will be closing. For Modes II and III the sign is a matter of convention, it is usually taken as positive [9]. In this thesis it is only obtained stress intensity factors from Mode I and Mode II, that is due to the load direction, the crack surface does not move out of the pressure plane.

3.1.5. *T-Stress*

The value of the *T-Stress* is the independent term on r of the Stress Field equations obtained from the Williams's expansion. It have been studied for many different researchers and it is used to many different things in the field of FM. [10]

- *T-Stress* is used as a correction to the Westergaards solution in order to eliminate the effect of the transverse stress which arises in uniaxial loading. [11]
- *T-Stress* is used as a crack path prediction in compact tension (CT) specimens, but there are several studies that contradict this theory [11].
- The plastic zone (PZ) is affected by the *T-Stress*, it corrects the PZ as a consequence of the crack-tip constraint mechanism, its effects on PZ are analogous to the fringes lobes. [14]
- Because of its role in improving the PZ size at the crack tip in SSY and its mathematical origin to compensate the σ_{0x} that arises due to Westergaards function in uniaxial loading, *T-stress* can be considered as a parameter affecting the stiffness of the material under uniaxial loading, thus influencing the crack tip opening displacement and the crack tip constraint [15]. The *T-stress* sign and magnitude are affected by the material non-homogeneity. *T-stress* in anisotropic materials is affected by the anisotropy and elastic mismatched [16].
- In *T-stress* studies on piezoelectric and pressure-sensitive materials [17] it was shown to be affected by the elastic and electric constants (positive charge increased the *T-stress*), affected the crack kinking behaviour, and the PZ shapes
- *T-Stress* is not useful to predict crack paths in dynamic crack growth. [18]
- The sign of *T-stress* determines the shielding or anti-shielding behavior of the plastic zone shape and size at the crack tip [19].

One of the methods to calculate the *T-Stress* is as follows:

$$T = \lim_{r \rightarrow 0} (\sigma_{xx} - \sigma_{yy})_{\theta=0} \quad (16)$$

where σ_{xx} and σ_{yy} are the stress components and θ is the polar coordinate angle. In this thesis, *T-Stress* is calculated by the difference between σ_{xx} and σ_{yy} , that is possible for θ equal to zero.

3.1.6. Mixed Mode Fracture. Parallel cracks.

When there are more than one mode of loading, the energy release rate contributions is given by the next expression:

$$G = \frac{K_I^2}{E'} + \frac{K_{II}^2}{E'} + \frac{K_{III}^2}{2\mu'} \quad (17)$$

K_I , K_{II} and K_{III} are the stress intensity factors, $E=E'$ for plane stress, $E' = \frac{E}{1-\nu^2}$ for plane strain and μ is the shear modulus.

For parallel cracks [20], cracks tend to shield each other, which results in a decrease of K_I in each crack. As a consequence multiple cracks parallel one to another are less concern than multiple cracks in the same plane.

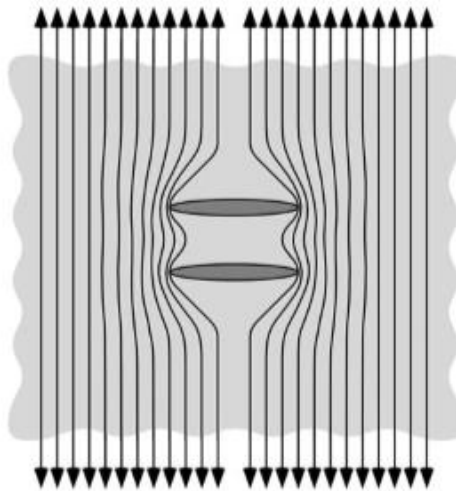


Figure 3: Parallel cracks with stress lines.[21]

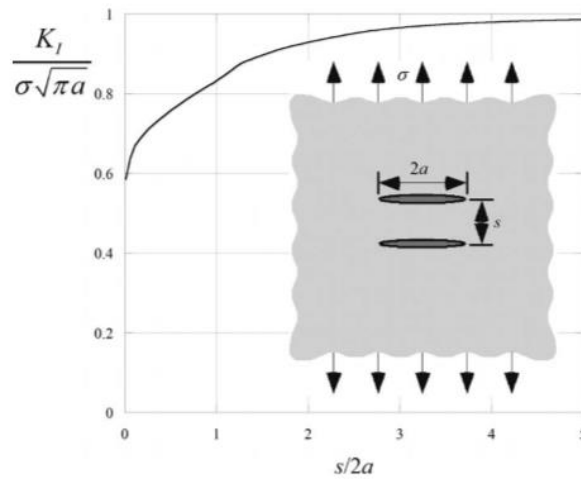


Figure 4: Stress intensity factor analysis, for different geometrical conditions in a parallel cracks case. [22]

That is an important concept in this thesis, because the specimen has two cracks parallel one to the another.

3.1.7. Crack tip plasticity.

LEFM predicts in the crack tip infinite stresses, that is because of the PZ which appears in the crack tip. The size of this PZ can be calculated by the Irwin approach. [23]

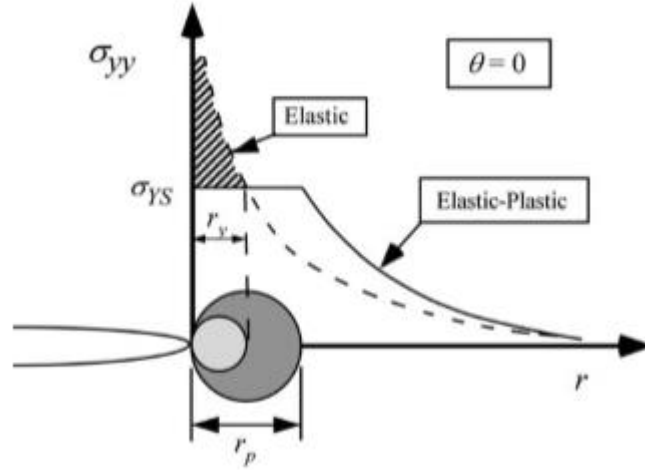


Figure 5: Plastic zone for plane stress (r_y) and plain strain (r_p). [24]

Following the Irwin approach, assuming spherical PZ, plain stress and matching $\sigma_{yy} = \frac{K}{\sqrt{2\pi r}}$ to the yield stress, σ_{ys} , it is obtained the following expression:

$$r_y = \frac{1}{2\pi} \left(\frac{K}{\sigma_{ys}} \right)^2 \quad (\text{plane stress}) \quad (18)$$

For plain strain, the radius of the PZ is three times less:

$$r_p = \frac{1}{6\pi} \left(\frac{K}{\sigma_{ys}} \right)^2 \quad (\text{plane strain}) \quad (19)$$

3.1.8. Fracture Mechanical Criterions.

It is possible to use different fracture mechanical criteria in studies of fracture resistance under the mixed mode on concrete, some of them are maximum tangential stress criterion (MTS) [25], generalised maximum tangential stress (GMTS), maximum tangential strain (MTSN), etc. [26]. Some of them are described on the next paragraphs.

According to MTS criterion there are two important postulations:

- The crack extension starts in the plane perpendicular to the direction of the greatest tangential stress.
- The maximum tangential stress at a certain radius r_c reaches its critical value σ_c for crack extension initiation under combined plane loading.

For single mode I it is easy to get the expression:

$$K_{IC} = \sigma_c \sqrt{2\pi r_c} \quad (20)$$

where K_{IC} represents the fracture toughness.

The GMTS is based on MTS. For mixed mode I/II, the elastic tangential stress is:

$$\sigma_{\theta\theta} = \frac{1}{\sqrt{2\pi r}} \cos \frac{\theta}{2} \left(K_I \cos^2 \frac{\theta}{2} - \frac{3}{2} K_{II} \sin \theta \right) + T \sin^2 \theta + O_{i,j} \left(r^{\frac{1}{2}} \right) \quad (21)$$

where r and θ are the polar coordinates with the origin located at the crack tip; K_I , K_{II} and T denote the mixed-mode first terms and T -stress, respectively. The higher-order terms $O(r^{1/2})$ can be considered negligible comparing to the first three terms.

Now, according to the first postulation of MTS:

$$K_I \sin \theta_0 + K_{II} (3 \cos \theta_0 - 1) = \frac{16}{3} T \sqrt{2\pi r_c} \cos \theta_0 \sin \frac{\theta_0}{2} \quad (22)$$

substituting θ_0 from (21) and σ_c from (20) into (19), we get a parametric equation of initiation cracking curve in $K_I/K_{IC} - K_{II}/K_{IC}$ plane.

$$\left\{ \begin{array}{l} \frac{K_I}{K_{IC}} = \gamma \frac{K_{II}}{K_{IC}} \\ \frac{K_{II}}{K_{IC}} = \frac{1}{\cos \frac{\theta_0}{2} \left(\gamma \cos^2 \frac{\theta_0}{2} - \frac{3}{2} \sin \theta_0 \right) + B \sqrt{\frac{2\pi r_c}{a}} \sqrt{1 + \gamma^2} \sin^2 \theta_0} \end{array} \right. \quad (23)$$

$$B = \frac{T \sqrt{\pi a}}{\sqrt{K_I^2 + K_{II}^2}} \quad (24)$$

a represents crack length, and $\gamma = K_I/K_{II}$ is the ratio of first terms for a crack under mixed mode loading. The biaxiality B indicates how important is the T -Stress. [27]

In some materials, the strain based criteria provides more realistic description of the failure mechanism than stress and energy based criteria [28]. The MTSN criterion was developed by Chang [29] based on St. Venant Theory.

The main postulate is that crack propagates in the direction, θ_0 , where the tangential strain, $\varepsilon_{\theta\theta}$, attains its maximum value, ε_T , at a critical distance, r_c , from the crack tip. It could be represented as [30]; **Error! No se encuentra el origen de la referencia.:**

$$\left\{ \begin{array}{l} \left. \frac{\partial \varepsilon_{\theta\theta}}{\partial \theta} \right|_{r=r_c; \theta=\theta_0} = 0 \\ \left. \frac{\partial^2 \varepsilon_{\theta\theta}}{\partial \theta^2} \right|_{r=r_c; \theta=\theta_0} < 0 \end{array} \right. \quad (25)$$

$$\varepsilon_{\theta\theta}(r_c, \theta_0) = \varepsilon_T = \sigma_T/E \quad (26)$$

σ_T is the tensile fracture strength, E is the Young's modulus, r_c is the damaged zone around the crack tip, a material property.

Tangential stress and strain can be related by:

$$\epsilon_{\theta\theta} = \frac{1}{E} (\sigma_{\theta\theta} - \nu \sigma_{rr}) \quad (27)$$

where ν is the Poisson's ratio and $\sigma_{\theta\theta}$ and σ_{rr} are the components in polar coordinates of the stress field, with origin in the crack tip.

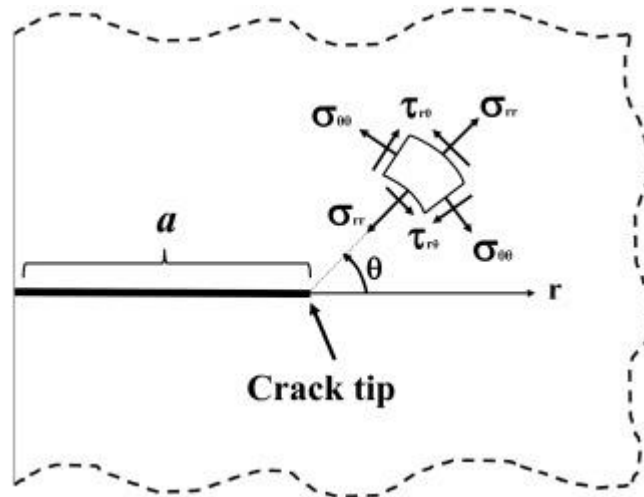


Figure 6: Crack tip stress components.

3.2. Concrete characteristics.

3.2.1. Concrete as a composite material.

Composites materials are macroscopic combinations of different materials. They are made-up by a matrix and reinforcements, together it is obtained a new material with the benefits of its components.

Concrete is a ceramic composite material made by cement, aggregate, water and admixtures. The cement is a binder, a substance used to set and harden the other materials, there are different cements as Portland cement or calcium aluminate cement. About water just say that it is possible to use any water acceptable by practice and for reinforced concrete it cannot be used sea water. In aggregates, the common ones are sand and gravel, but it depends on the application of the concrete. An important parameter about aggregates is the size, the d/D is a ratio which shows the smallest and largest square mesh grating that the particles can pass, this ratio is useful in order to create the suitable concrete needed for each application. The admixtures are different substances used to improve the quality or the manageability of concrete, for example set retarding concrete admixtures or water-reducing concrete admixtures.

3.2.2. Mechanical properties of concrete.

The most important characteristic of concrete is its high compressive strength, that is why concrete is one of the most important materials in construction. Its main lack is

tensile strength, in order to supply this tensile strength steel is used as a reinforcement. Steel has a good behaviour at traction and bending loads, so together it is obtained a material which resists all types of loads. In this thesis, it is studied mass concrete specimens, it means, without reinforcement.

The characteristic compressive strength of each type of concrete, f_{ck} , is calculated from a normal distribution of the strengths of different samples from the same concrete, 95% of tested specimens should not have a value less than f_{ck} . For routine uses it can be used from 20 MPa to 32 MPa. In the Eurocode 2: Design of concrete structures there are different tables to choose this parameter for each type of concrete [31].

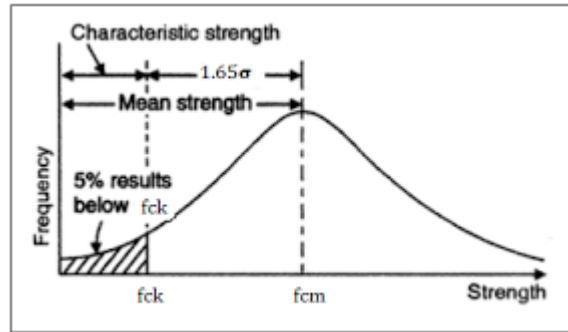


Figure 7: Normal distribution for determining characteristic compressive strength.

Then for design in construction, it is used the f_{cd} , characteristic specific compressive strength:

$$f_{cd} = \alpha_{cc} \frac{f_{ck}}{\gamma_c} \quad (28)$$

where α_{cc} is a value which takes care of the fatigue of the concrete when it is under big stresses, it is assigned by the manager of each construction project and it must be between 0.85 and 1; f_{ck} is the characteristic strength of the concrete project and γ_c is the factor of safety.

An estimated Young's Modulus for design, could be calculated following the next expression:

$$E_{cm} = 8500 \sqrt[3]{f_{cm}} \quad (29)$$

where f_{cm} is the characteristic compressive strength at 28 days, this strength can be estimated as $f_{cm} = f_{ck} + 8 \text{ N/mm}^2$ [31].

An usual value for Young's Modulus is 27000 MPa, but there is a significant variation depending on the concrete composition [32], concrete age [33], etc.

For the Poisson's Ratio it is used a value of $\nu = 0.2$ in elastic strain, for plastic strain it could be used a value until 0.5 [31].

3.2.3. Concrete Testing.

To evaluate the mechanical properties of concrete it is needed to test it in multiple different ways. There are two main categories, before and after cured.

Before cured, some important factors to keep in mind are the consistency, which depends on the water/cement ratio, the docility, how easy is to handle the concrete, and the density and homogeneity, which depends on the aggregate of the concrete.

A common test is the slump test, which measures the consistency of concrete by a Abrams cone filled with fresh concrete, when the cone is removed, the concrete slumps, checking the height of the sample is known the consistency of the concrete.

After cured, the testing could be destructive or non-destructive. Destructive tests are made with normalized specimens, some of them are the three point bending test, the four point bending test, the Brazilian test or the compression test. Actually, with the finite element methods, it is possible to obtain similar results without destructive methods. Furthermore, there are other non-destructive methods as testing with a sclerometer to know the strength deducing it from hardness, or magnetic resonance tests, which gives information about Young's Modulus or Poisson's Ratio.

All this tests are really useful to obtain compressive strength, Young's Modulus, flexural strength, etc, but they should follow European standards [34].

4. Numerical Model.

Numerical models were prepared in finite element software ANSYS. In following subchapters the modelling is introduced.

4.1. Geometry and basic boundary conditions.

This thesis exposes the results for a four point bending test with a parallel cracks specimen. The model has been done with relative dimensions which have been varied in order to obtain the stress intensity factors and the *T-Stress* for each geometry.

The main dimensions is the width (W) and the another varying dimensions are the span (S), the crack length (a), and the distance between cracks (D).

It minds, there is only one dimension with a constant value, the width, which size is always 100 mm, all the others are related between them; a/W is the relative crack length-width ratio, S/W is the span-width ratio and D/S is the distance between cracks-span ratio.



Figure 8: : Sketch of the specimen.

Table 5: Values of the dimension ratios.

Ratio	Values
a/W	0.1, 0.2, 0.3, 0.35, 0.4, 0.45, 0.5, 0.6, 0.7, 0.8
S/W	1, 2, 3, 4, 6
D/S	0.33, 0.4, 0.5, 0.8

The modelling in ANSYS have been done in 2D, so the third dimension is going to be one millimetre in all cases.

Finally the value v has been defined as:

$$v = \frac{(S - D)}{2} \quad (30)$$

4.2. Material properties

After define the input parameters, the next step consists in setting the material properties. In ANSYS, it is needed two values to define a linear isotropic material, Young's Modulus and Poisson's ratio. For Young's Modulus an accepted value is 30000 MPa which corresponds to a C20/25 concrete, following the Eurocode 2. The Poisson's ratio for concrete is 0.2 [31].

In the macro it is used the command *UIMP*, to define this values.

Table 6: Material properties for ANSYS.

	Young`s Modulus	Poisson`s ratio
Concrete C20/25	30000 MPa	0.2

4.3. Element type.

The element type is defined with the command *ET*. It is used a *PLANE82* 2D solid element with eight nodes. This element have been used in plane strain, in ANSYS , this is defined by the command *KEYOPT*.

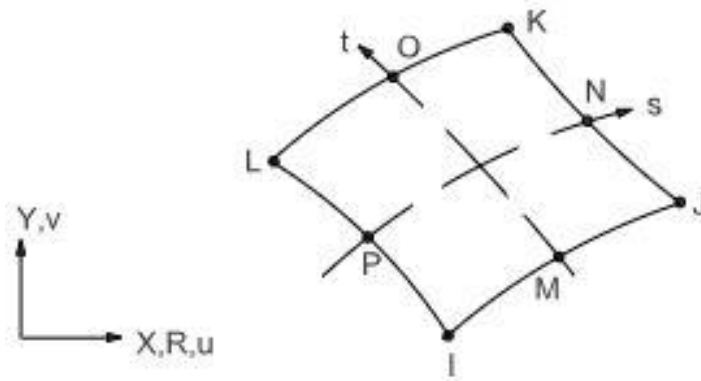


Figure 9 : PLANE82 2D 8 Node Structural Solid.

4.4. Modelling the specimen.

To model a specimen in ANSYS, we must create its geometry in four steps: Keypoints, Lines, Areas and Meshing.

4.4.1. Keypoints.

The keypoints are the starting parameters of the modelling. They are located in the main positions of the specimen, as corners, centres, start and end of the crack, etc. The command to create keypoints is *K*, there are 22 keypoints in the macro, all of them created in cartesian coordinate system with the relative dimensions defined before.

To create the crack tip, there are keypoints located in the same position, this is the method to study the behaviour of the crack.

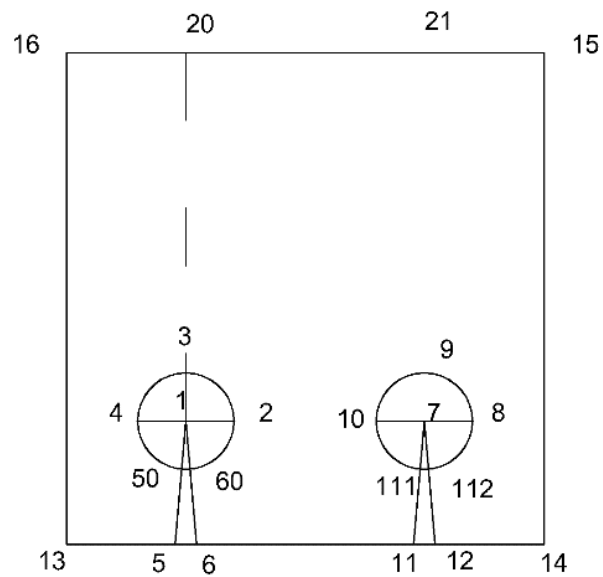


Figure 10: Keypoints number in macro.

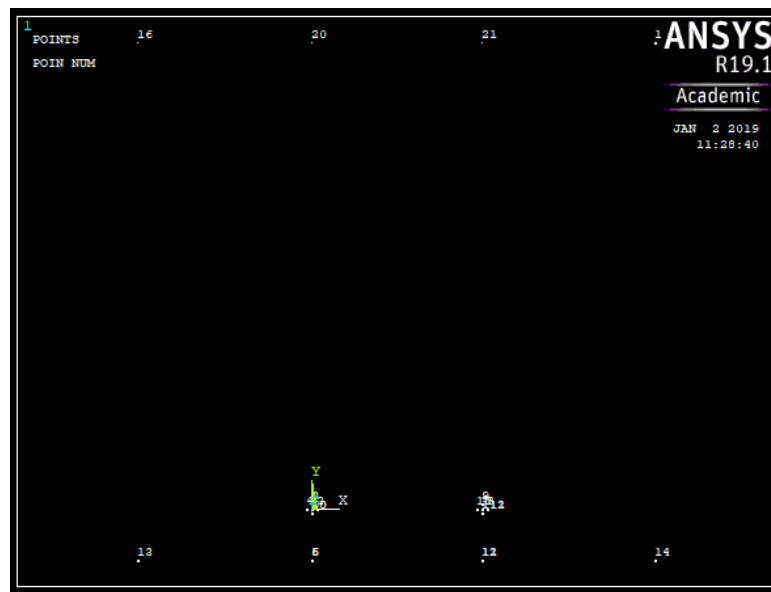


Figure 11: Keypoints in ANSYS.

4.4.2. Lines.

The lines are used to link the keypoints. Some of them represent the geometry, and others are created to divide all the specimen in areas in the next step. There are 32 lines in the macro, all of them created with the command *L* or the command *arc*, if it is part of a circumference.

The crack is modelled by two lines one on top of the other. These two lines will represent the open of the crack at the end of the test.

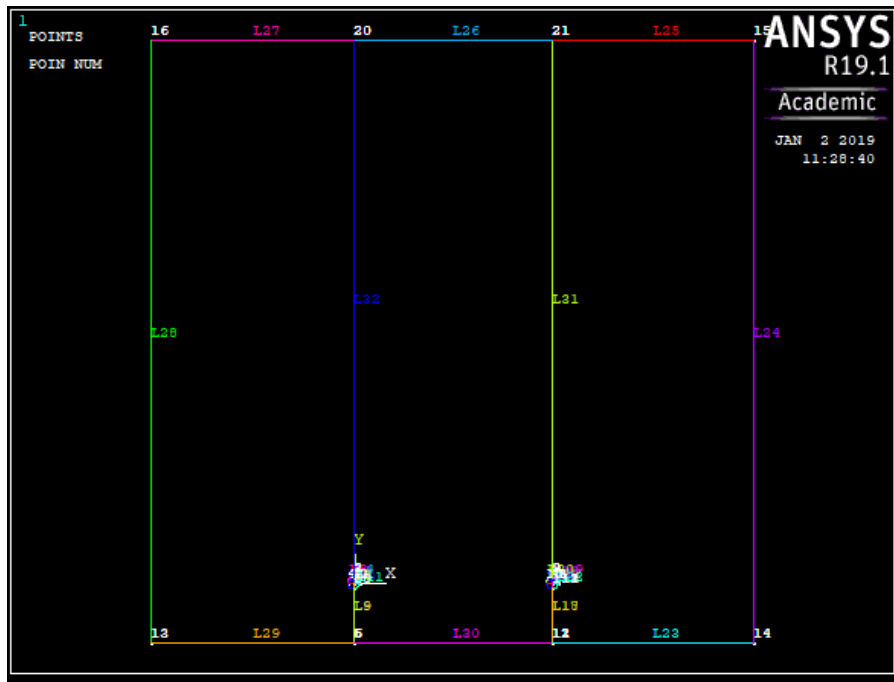


Figure 12: Lines in ANSYS

4.4.3. Areas.

The Areas are the third step of the modelling, they are created using the lines with the command *AL*. There are 11 areas in the macro.

At the tip of the cracks, there are circular areas to study the behaviour at the important zone of the specimen.

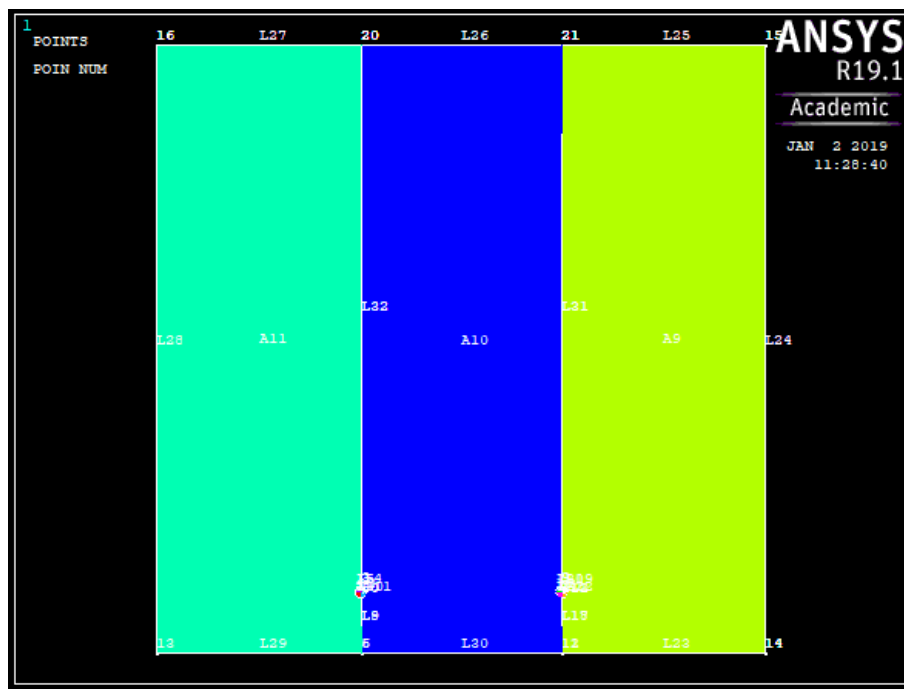


Figure 13: Areas in ANSYS

4.4.4. Meshing.

The meshing consists in dividing the whole specimen in elements, the commands used are *KESIZE* which specifies the edge lengths of the elements near to each keypoint, *LESIZE* which specifies the divisions and spacing ratio on unmeshed lines, then *KSCON* is used to create all the mesh radially from a keypoint, in the macro from two points, the tip of both cracks; finally the command *AMESH* creates all the mesh in each area.

The elements of the mesh should be as small and plenty as possible, in order to guarantee an accuracy on the results.

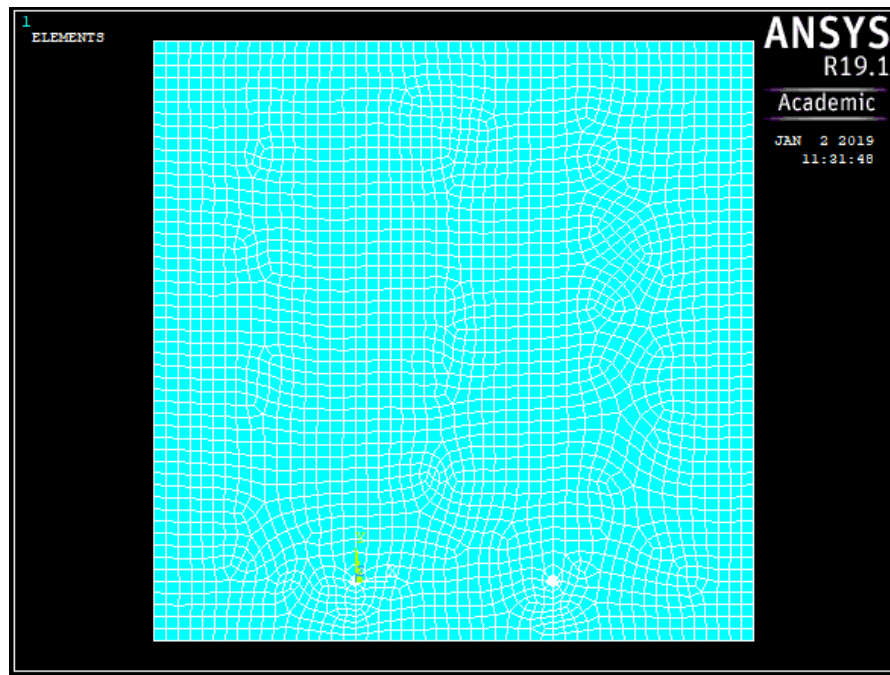


Figure 14: Meshing in ANSYS

4.5. Boundary conditions.

The boundary conditions are the loads and supports. In ANSYS, as the load the forces in node and compression pressure on line are used, and for supports the selected displacement in X or Y direction for nodes were zero.

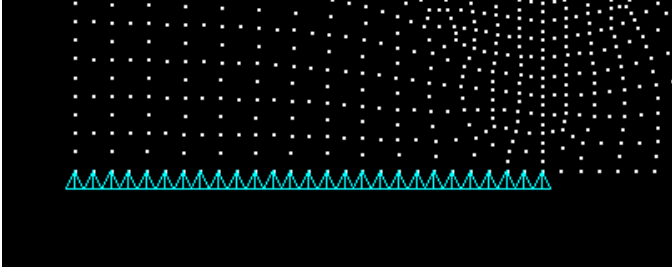


Figure 15: Boundary condition ($u_y=0$) plotted in ANSYS

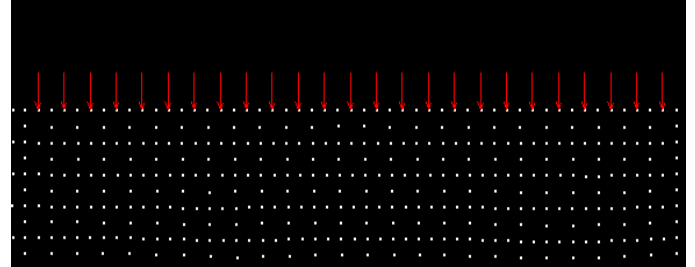


Figure 16: Pressure plotted in ANSYS.

4.6. Solution and postprocessing in ANSYS.

For the solution in ANSYS it is used the command, *SOLVE*, after this command starts the postprocessing step. In this last step, are obtained the results of the test: Stress Intensity Factors, stresses, displacements and graphs of deformation.

To obtain this results, it is necessary to set a path where the solution will be calculated. Also it is needed to create a new cartesian coordinates system, the path must be parallel to the x axis, so the calculation path is going to be defined in the new coordinates system; the command to create it is *CSKP*, then to activate it we use the command *RSYS*. After that, the path is defined with the command *LPATH*. The path is defined by 5 nodes, it starts in the crack tip and continues with two nodes at each side of the crack.

Then the command *KCALC* is used to get the SIF in plane strain. The displacements of the crack tip and the closest nodes of the path for each side of the crack, are obtained with command **GET*, for both directions x and y. The stresses S_x and S_y , are obtained in an output file as a table, in the table it is possible to see each stress at different distances from the crack tip. From these tables are going to be calculated the *T-Stress*. Also it is possible to plot the deformed shape in *General Postprocessor* → *Plot Results* → *Deformed Shape*.

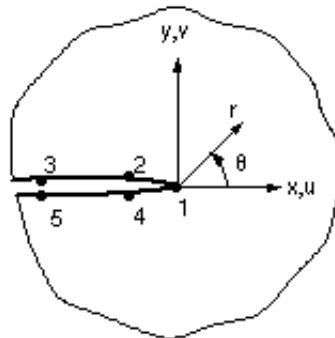
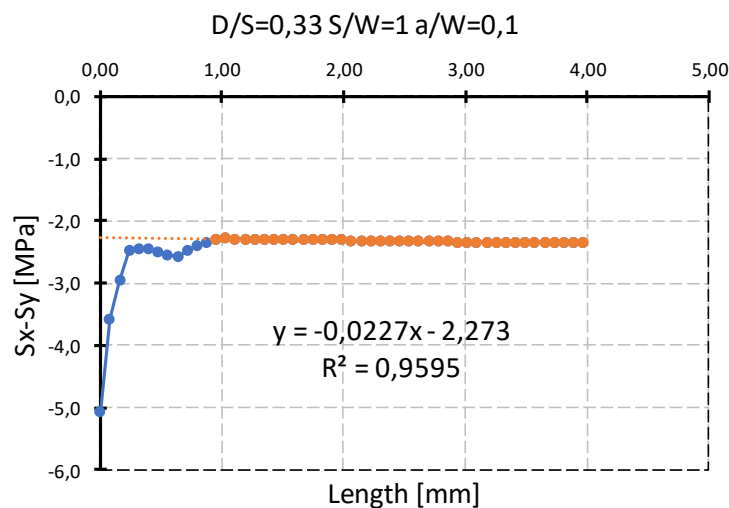


Figure 17 : Path definition in ANSYS [35].

4.7. Calculate the *T-Stress* from S_x and S_y .

As it is known the *T-Stress* is the independent term of the Williams's expansion, the easiest way to calculate it is extracting the values of S_x and S_y in ANSYS on tables, this values are calculated at different distances from the crack tip. Then, it is necessary to calculate the difference S_x-S_y and plot this difference in a graph, with the value S_x-S_y in the y axis and the value of the length in the x axis. Extracting the linear trend line from the graph and choosing the independent term of this line, we get the *T-Stress*. This process have been done for each different geometry of the specimen.

The next table and the next graph are examples of how to apply the method explained above this paragraph:



Graph 1: Values extracted from ANSYS plotted to calculate the *T-Stress* for $D/S=0.33$ $S/W=1$ and $a/W=0$ (*T-Stress*=-2.273).

Table 7: Values extracted from ANSYS to calculate the T-Stress

	D/S=0,33	S/W=1	a/W=0,1	
LENGHT	SX	SY	SX-SY	SX-SY
0,00	2,65	7,73	-5,08	
0,08	0,87	4,45	-3,58	
0,16	0,13	3,10	-2,97	
0,24	-0,43	2,06	-2,49	
0,32	-0,55	1,90	-2,45	
0,40	-0,60	1,87	-2,47	
0,48	-0,69	1,81	-2,50	
0,56	-0,84	1,70	-2,55	
0,63	-0,98	1,60	-2,57	
0,71	-1,00	1,48	-2,49	
0,79	-1,03	1,37	-2,40	
0,87	-1,06	1,29	-2,35	
0,95	-1,09	1,22	-2,31	-2,31
1,03	-1,12	1,17	-2,29	-2,29
1,11	-1,14	1,15	-2,29	-2,29
1,19	-1,16	1,14	-2,30	-2,30
1,27	-1,18	1,12	-2,30	-2,30
1,35	-1,20	1,10	-2,30	-2,30
1,43	-1,21	1,09	-2,30	-2,30
1,51	-1,23	1,07	-2,30	-2,30
1,59	-1,25	1,06	-2,31	-2,31
1,67	-1,27	1,04	-2,31	-2,31
1,75	-1,29	1,02	-2,31	-2,31
1,82	-1,31	1,01	-2,31	-2,31
1,90	-1,32	0,99	-2,32	-2,32
1,98	-1,34	0,97	-2,32	-2,32
2,06	-1,36	0,96	-2,32	-2,32
2,14	-1,38	0,94	-2,32	-2,32
2,22	-1,40	0,93	-2,32	-2,32
2,30	-1,42	0,91	-2,33	-2,33
2,38	-1,44	0,89	-2,33	-2,33
2,46	-1,45	0,88	-2,33	-2,33
2,54	-1,47	0,86	-2,33	-2,33
2,62	-1,49	0,84	-2,34	-2,34
2,70	-1,51	0,83	-2,34	-2,34
2,78	-1,53	0,81	-2,34	-2,34
2,86	-1,55	0,80	-2,34	-2,34
2,94	-1,56	0,78	-2,34	-2,34
3,01	-1,58	0,77	-2,35	-2,35
3,09	-1,58	0,77	-2,35	-2,35
3,17	-1,59	0,76	-2,35	-2,35
3,25	-1,59	0,76	-2,35	-2,35
3,33	-1,60	0,75	-2,35	-2,35
3,41	-1,60	0,75	-2,35	-2,35
3,49	-1,61	0,74	-2,35	-2,35
3,57	-1,61	0,74	-2,35	-2,35
3,65	-1,62	0,74	-2,35	-2,35
3,73	-1,62	0,73	-2,35	-2,35
3,81	-1,63	0,73	-2,36	-2,36
3,89	-1,63	0,72	-2,36	-2,36
3,97	-1,64	0,72	-2,36	-2,36

5. Various boundary conditions used for numerical study.

At the beginning of the study there were four different types of boundary conditions. In this first four types the laboratory conditions were represented with point loads and point constraints. It is difficult to get these point conditions in a real test, that is why in this thesis it is used distributed loads and constraints which represent better the real test. There were two different combinations with distributed conditions, both of them give similar results, so it is not a vital decision to choose one or the other. Finally, it is used BC 5 to get the results.

Modelling the boundary conditions in ANSYS is easy, using the commands LSEL, NSEL and KSEL, it is possible to select lines, nodes or keypoints, respectively. Then the commands D, F and SF, are used to create the boundary condition ($u_x=0$ or $u_y=0$), the loads or the pressures, in the selected entity.

For the loads, in the point boundary conditions, there are two forces of 100N each one, on the top of the specimen each one line up with one crack. In the distributed boundary conditions, there is a pressure with different values depending on the dimensions of each case, but the load is always 200 N in all.

Table 8: Values of the dimension ratios.

Ratio	Values
a/W	[0.1; 0.8]
S/W	1, 2, 3, 4, 6
D/S	0.33, 0.4, 0.5, 0.8

Table 9: Boundary conditions of two initial symmetrical notches in four point bending specimen.

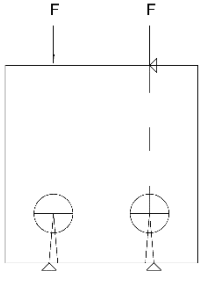
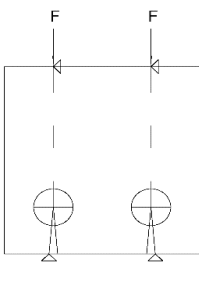
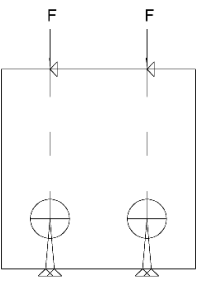
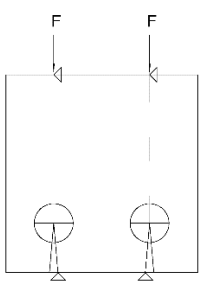
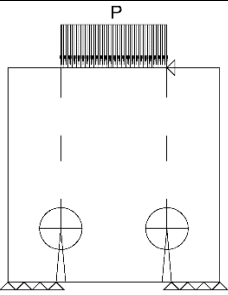
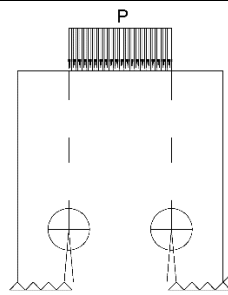
Boundary conditions	Model
1	
2	
3	
4	

Table 10: Distributed boundary conditions.

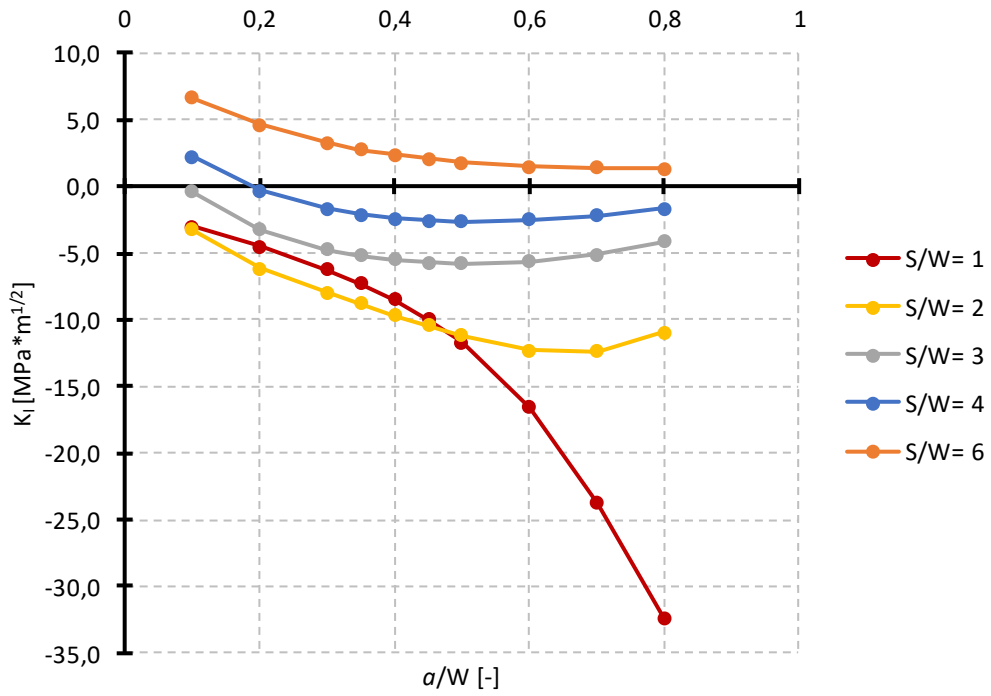
5	
6	

6. Numerical results and discussion.

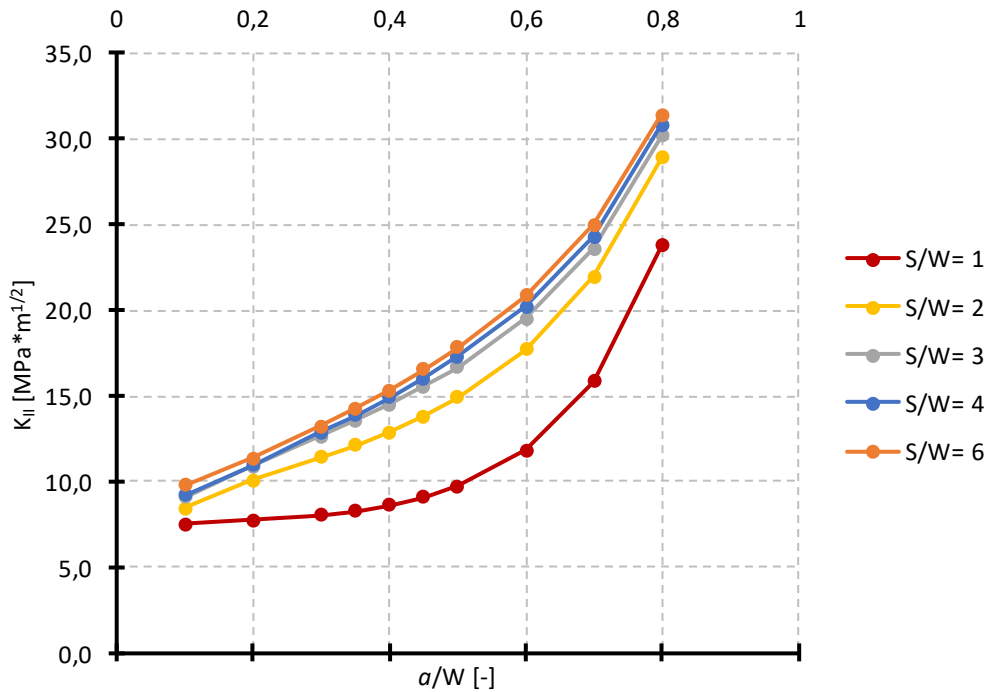
All the numerical results are presented in graphs, where the x axis always represents relative crack length (a/W ratio). Then the y axis represents the parameter obtained in ANSYS (SIF or T -Stress). Each graph is for a constant value of a dimension ratio (S/W or D/S), and the curves represent the values of the dimension ratios which are not constant, this values are showed in the legend.

6.1. Constant D/S ratio curves.

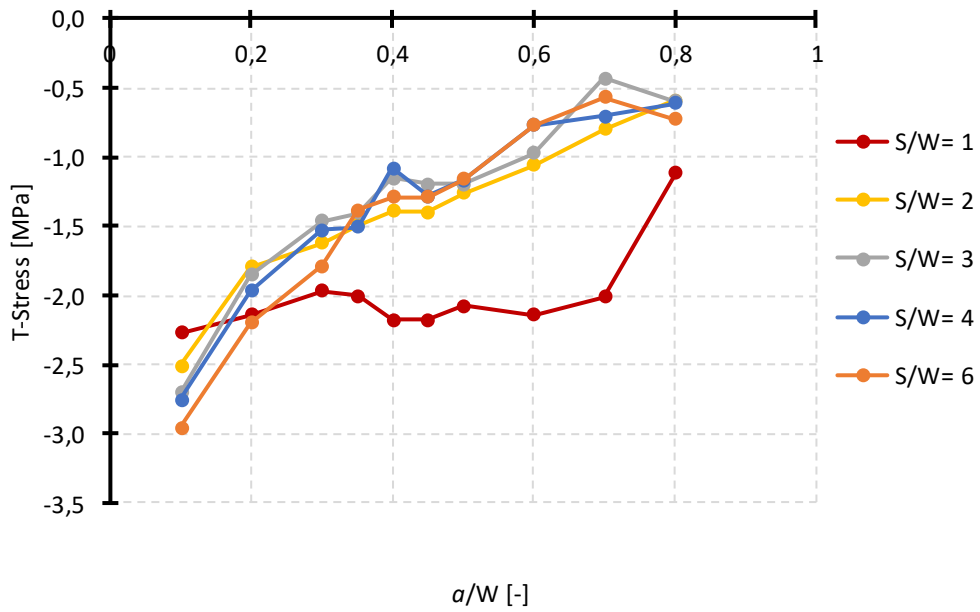
For a constant distance between cracks to span $D/S=0.33$, next graphs represent the values of K_I , K_{II} and T -Stress, for different values of crack length.



Graph 2: K_I variation for $D/S=0.33$

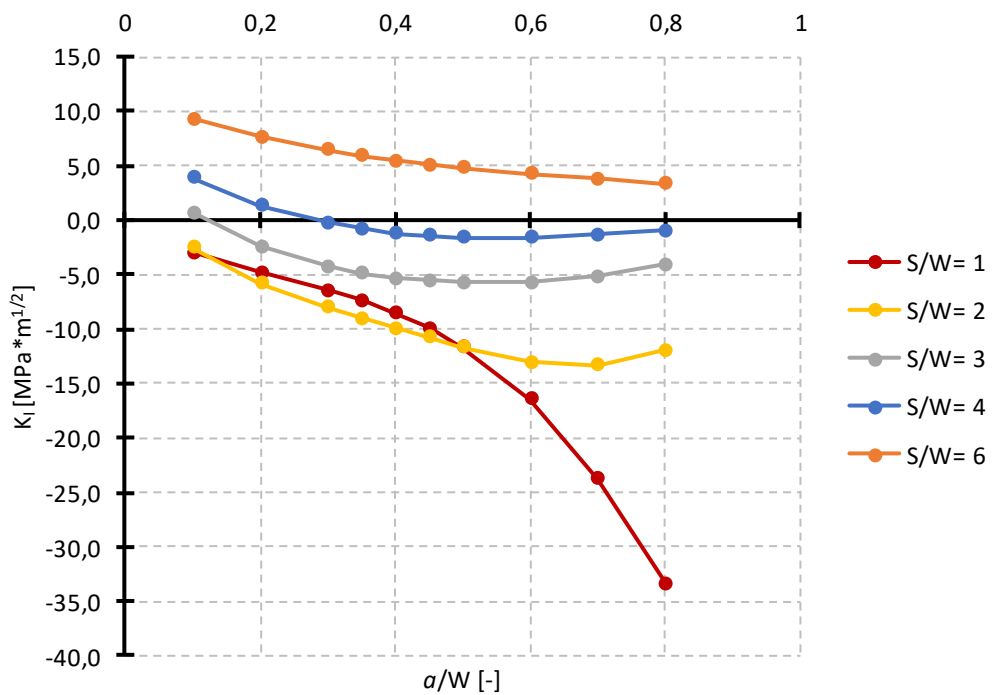


Graph 3: K_{II} variation for $D/S=0.33$

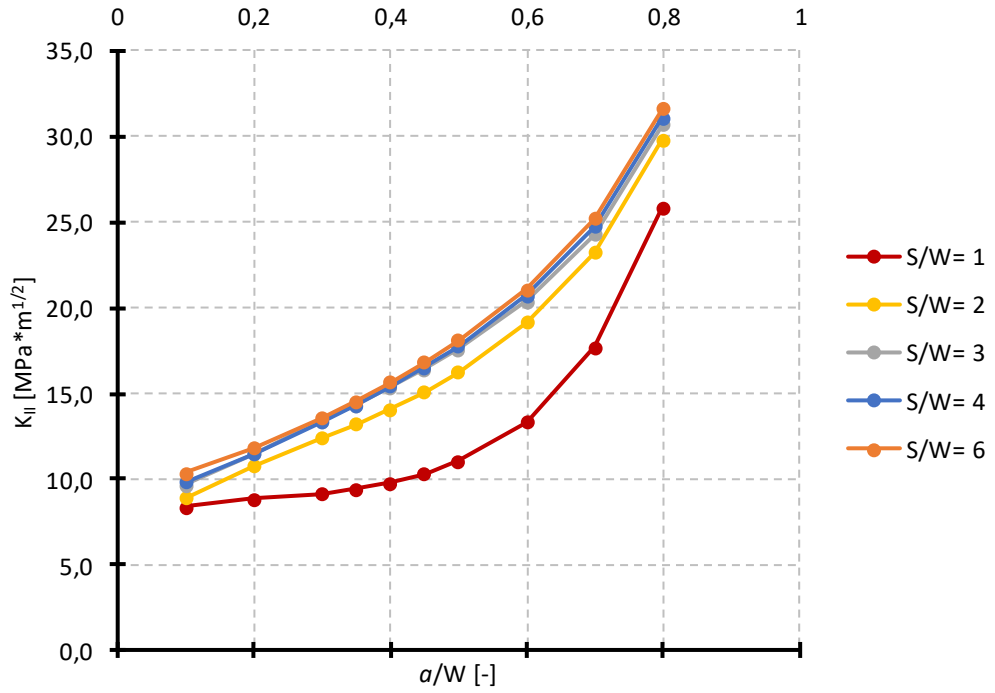


Graph 4 T-Stress variation for $D/S=0.33$

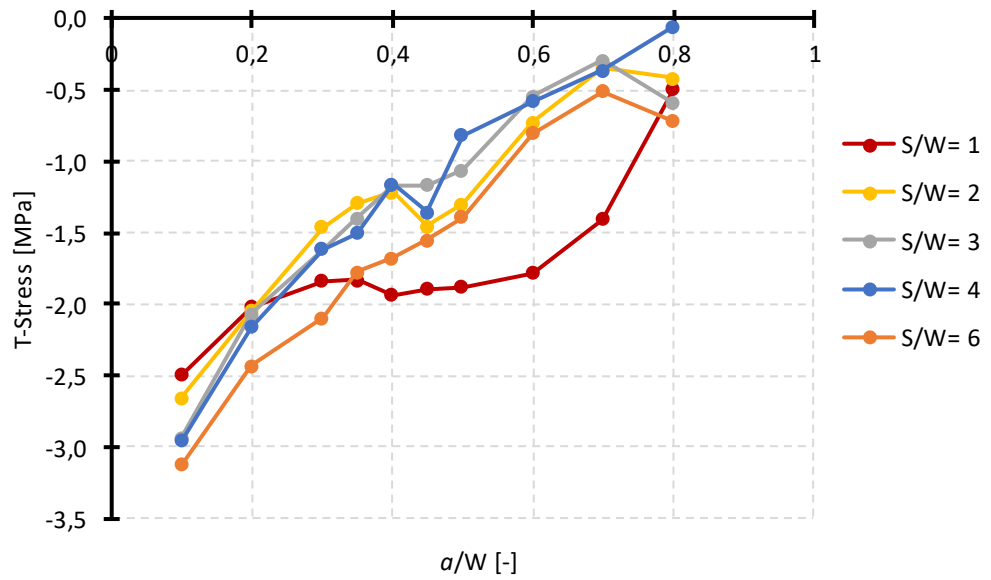
For a constant $D/S=0.4$, next graphs represent the values of K_I , K_{II} and T-Stress, for different values of crack length.



Graph 5 : K_I variation for $D/S=0.4$

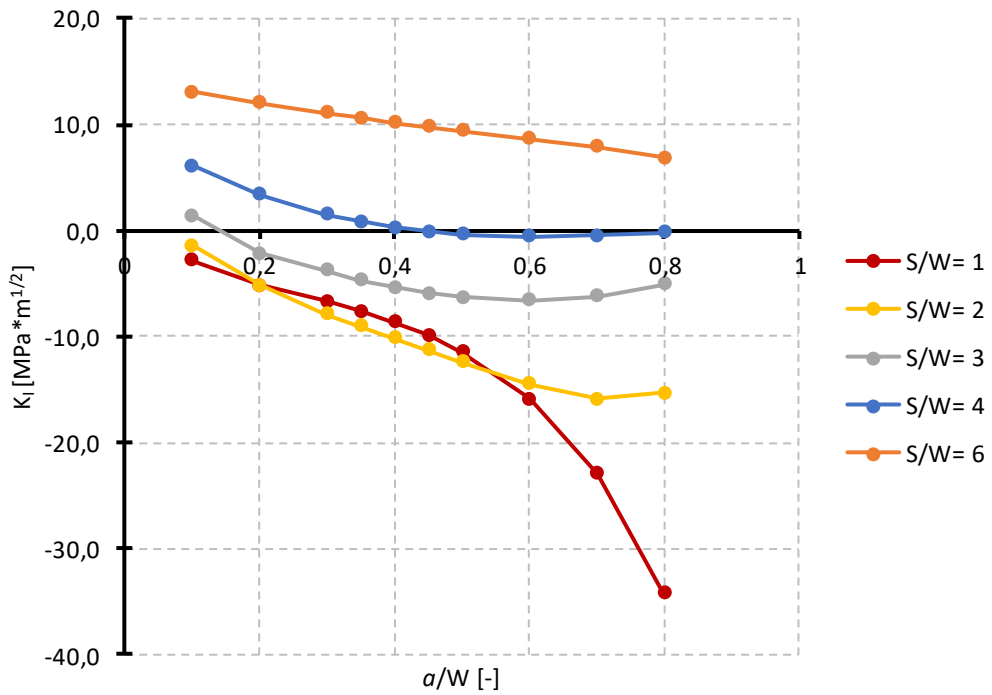


Graph 6: K_{II} variation for $D/S=0.4$

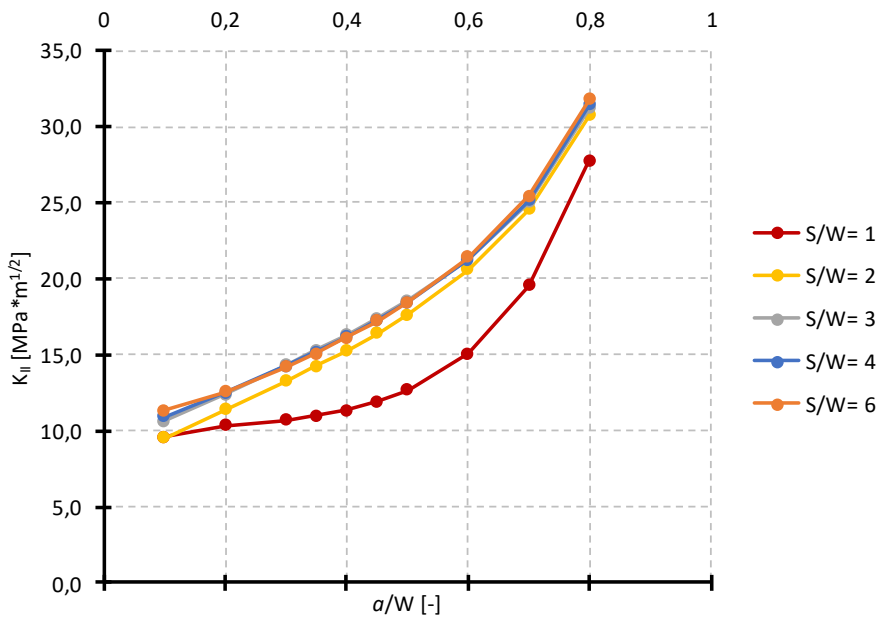


Graph 7: T-Stress variation for $D/S=0.4$

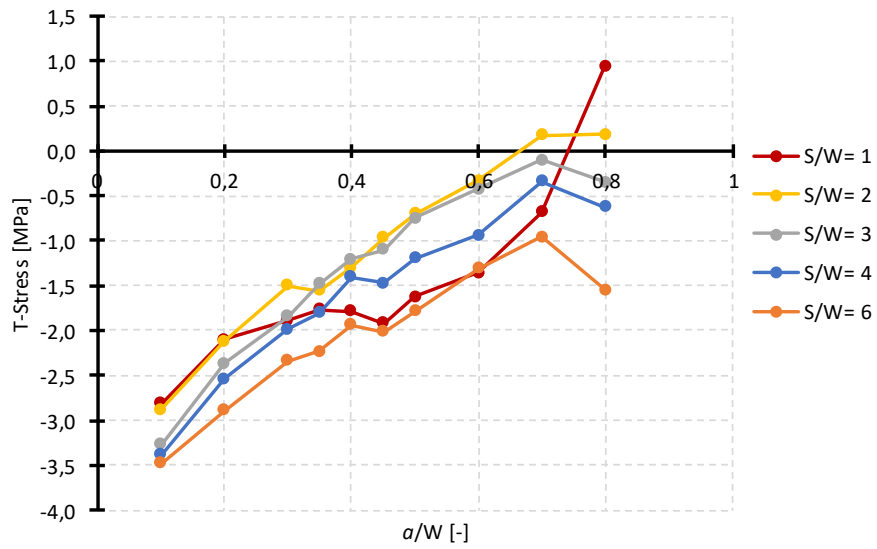
For a constant $D/S=0.5$, next graphs represent the values of K_I , K_{II} and T -Stress, for different values of crack length.



Graph 8: K_I variation for $D/S=0.5$

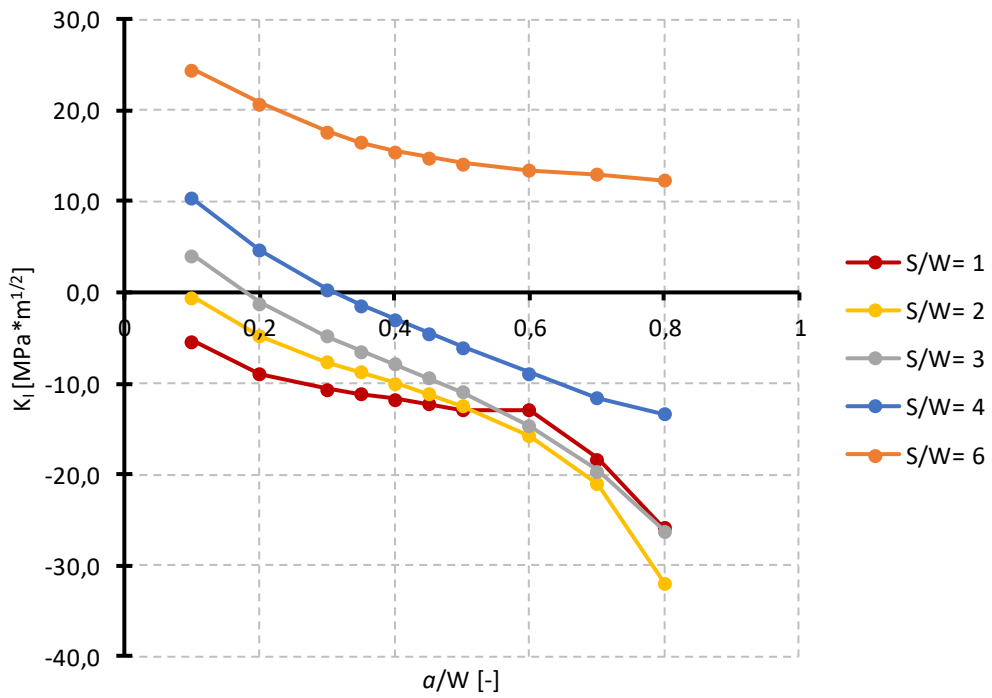


Graph 9: K_{II} variation for $D/S=0.5$

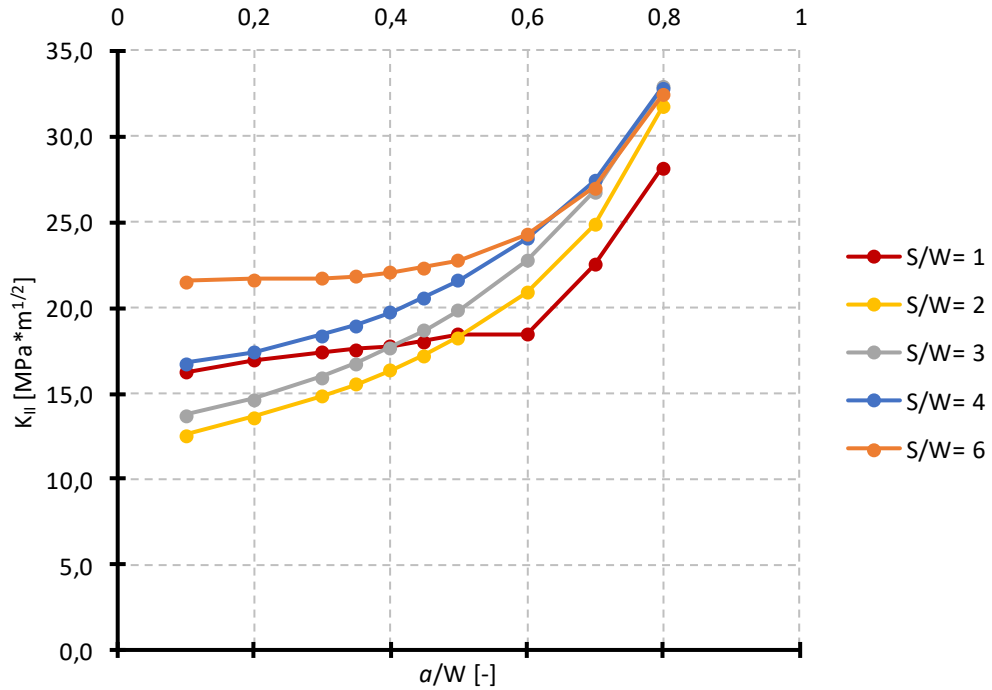


Graph 10: T-Stress variation for $D/S=0.5$

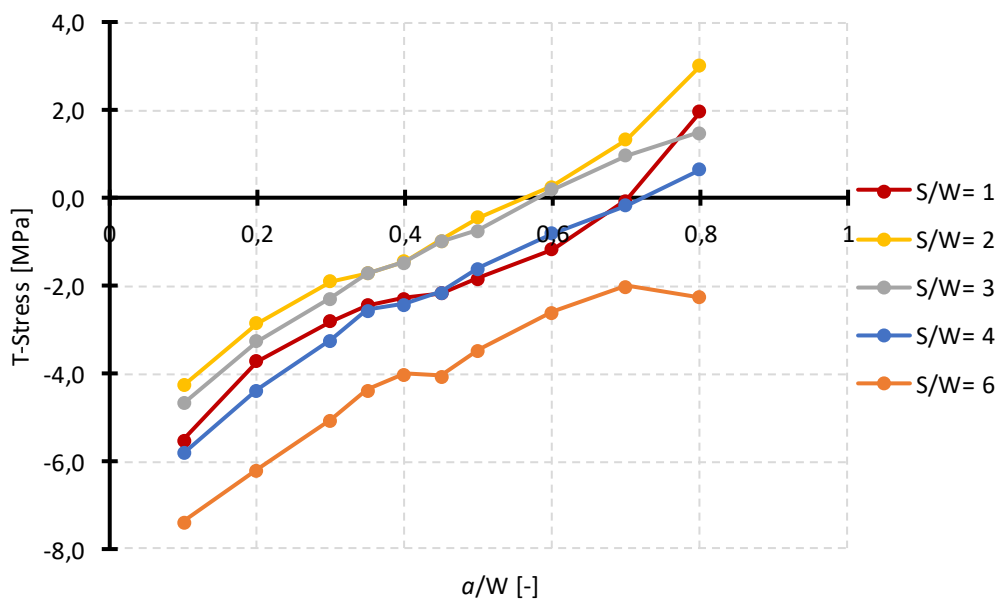
For a constant $D/S=0.8$, next graphs represent the values of K_I , K_{II} and T-Stress, for different values of crack length.



Graph 11: K_I variation for $D/S=0.8$



Graph 12: K_{II} variation for $D/S=0.8$



Graph 13: T-Stress variation for $D/S=0.8$

6.2. Analysis of the graphs for constant D/S ratio.

For the first three D/S cases, $D/S=0.33$; 0.4 ; 0.5 , the K_I has a very clear trend line for all the S/W ratios except for $S/W=1$. With a bigger S/W ratio the value of K_I is going up from a closed crack to an open crack. With smaller a/W ratio the value of K_I is bigger, so the crack tend to open with small crack lengths. For $S/W=1$ the K_I has a different slope in the last three a/W ratios, $a/W=0.6$; 0.7 ; 0.8 , this case studies an square specimen, so that is

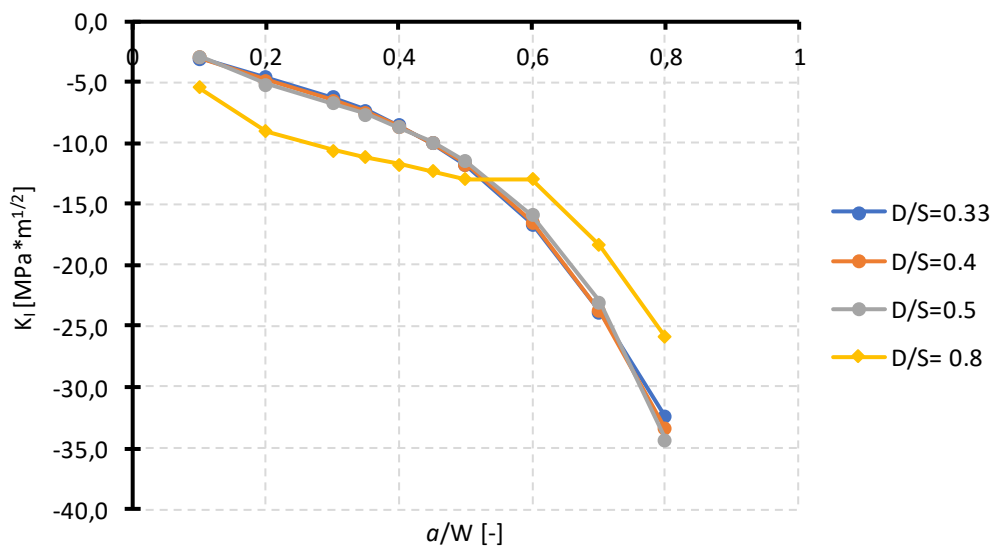
probably the reason to give different results. For the last D/S case, $D/S=0.8$, the slopes of all the S/W ratios, except $S/W=6$, become similar to $S/W=1$ slope.

For K_{II} the trend line is very clear for all the values of S/W , even it gives similar results for $S/W= 2;3;4;6$ in the first three series, $D/S= 0.33; 0.4; 0.5$. In the $D/S=0.8$ the results change respect to the other series, especially the trend line of $S/W=1$. Furthermore, we can see that K_{II} unlike K_I , tends to go up with bigger crack lengths.

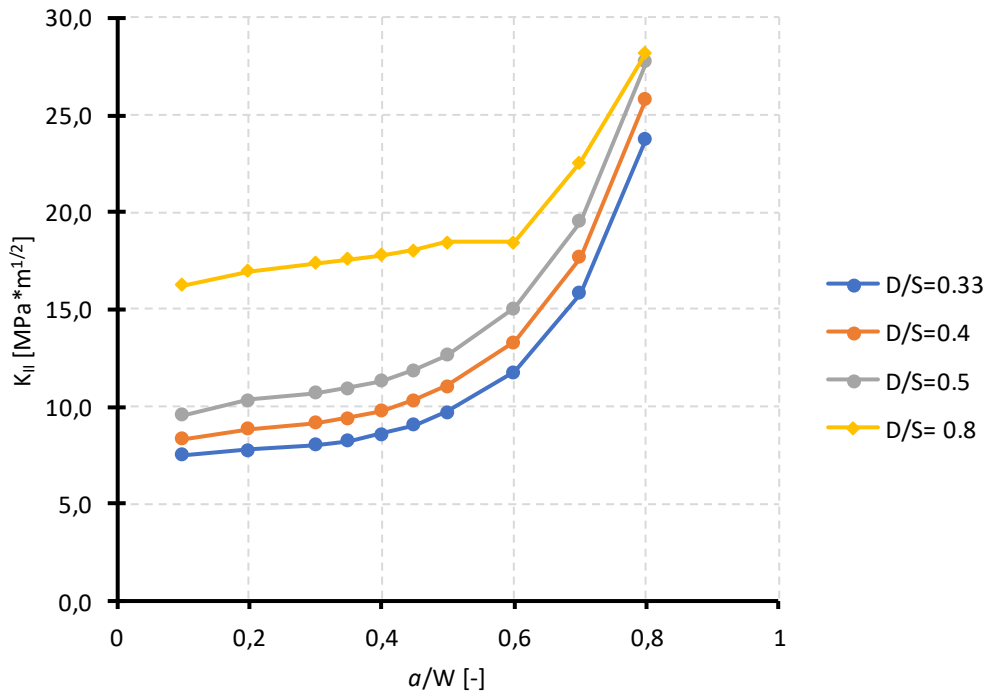
T -Stresses tend to be smaller with bigger values of S/W , and as K_{II} goes up with bigger crack lengths.

6.3. Constant S/W ratio curves.

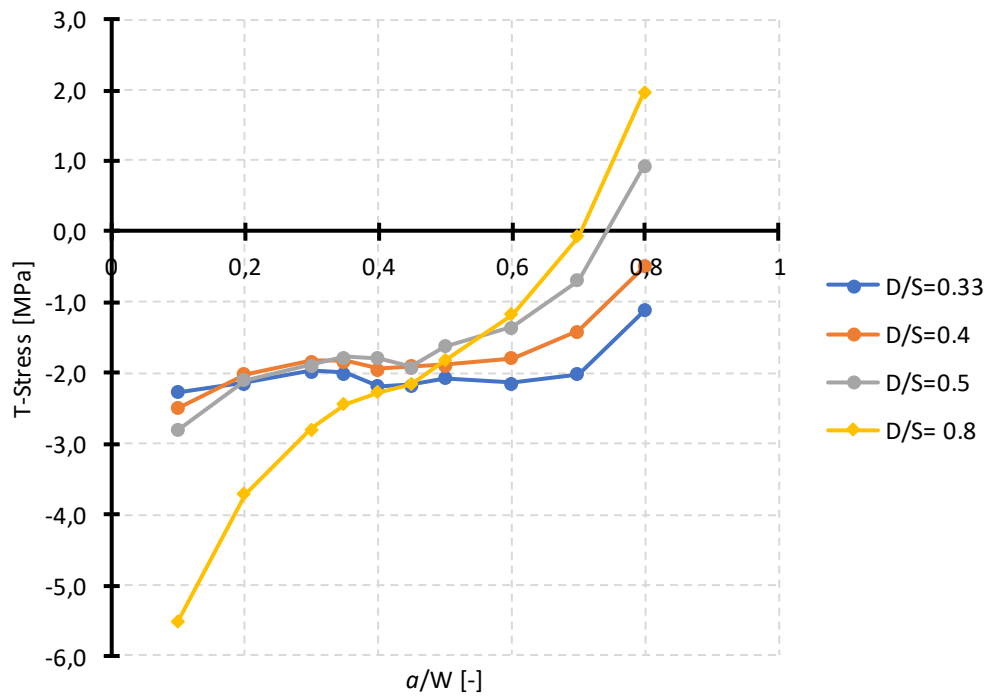
For a constant $S/W=1$, next graphs represent the values of K_I , K_{II} and T -Stress, for different values of crack length.



Graph 14: K_I variation for $S/W=1$

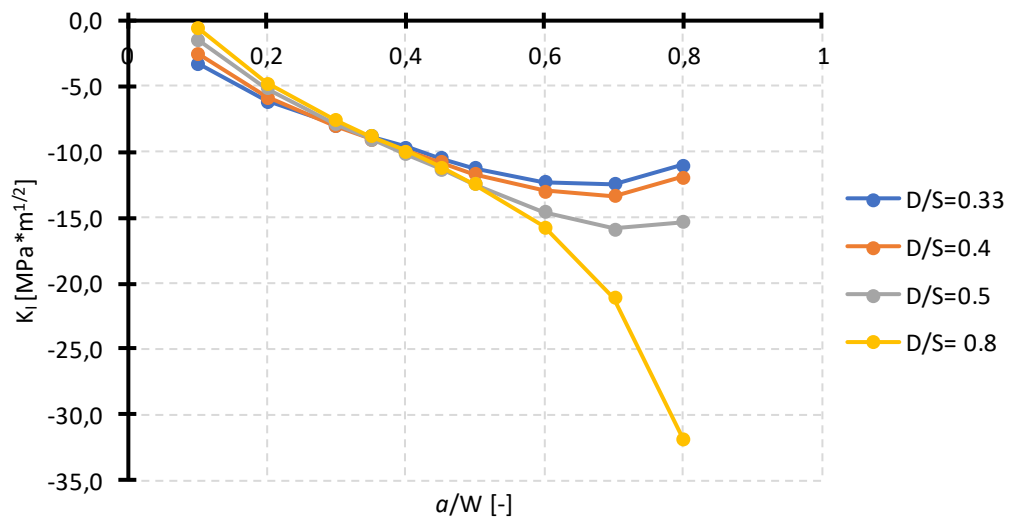


Graph 15: K_{II} variation for $S/W=1$

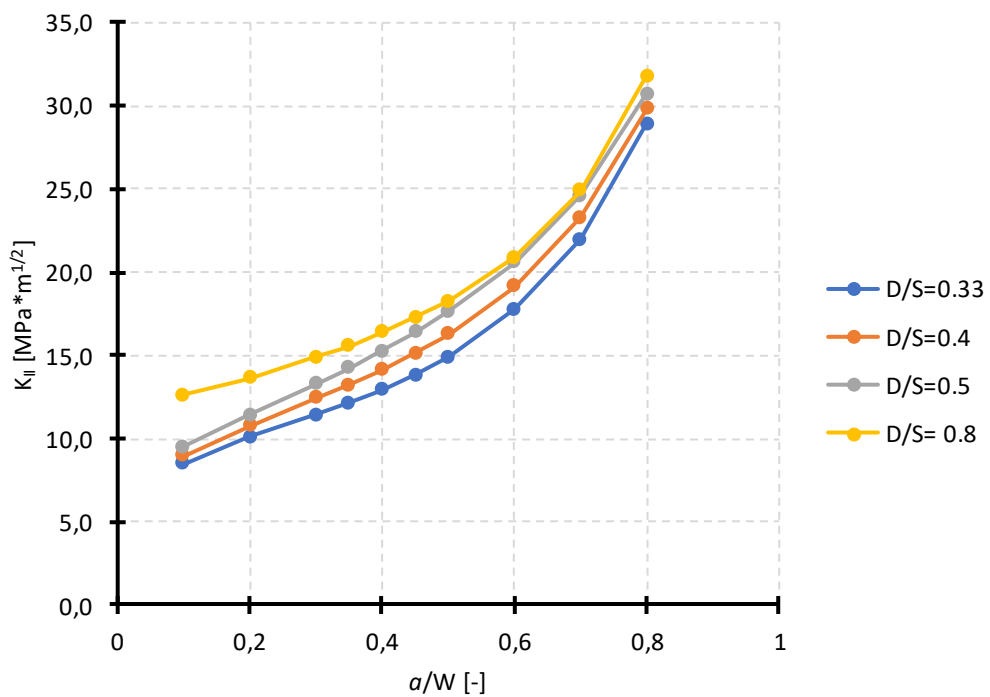


Graph 16: T-Stress variation for $S/W=1$

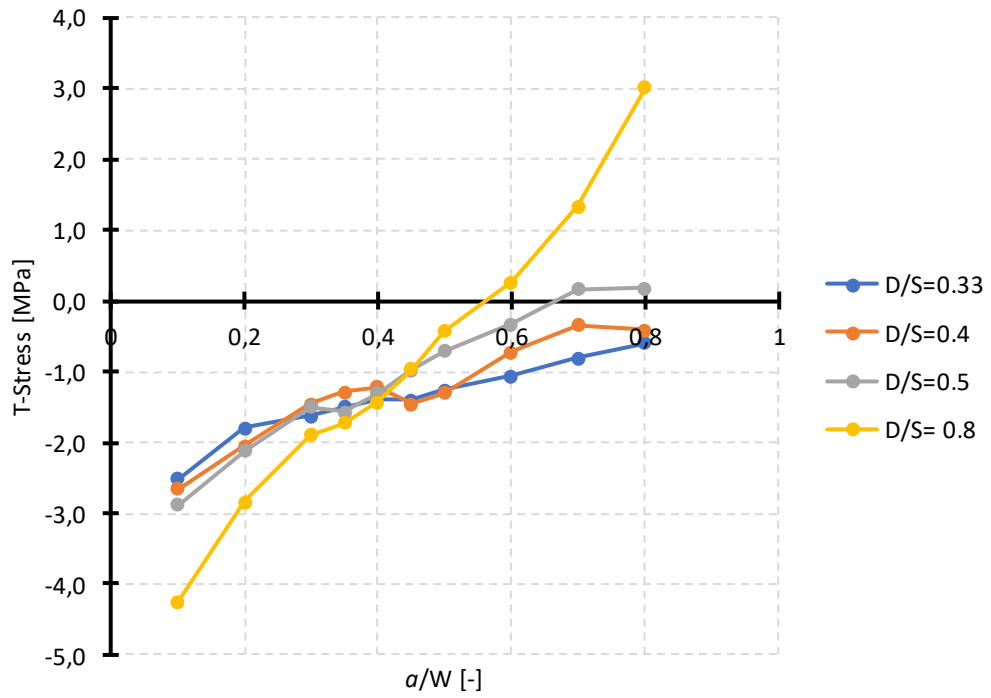
For a constant $S/W=2$, next graphs represent the values of K_I , K_{II} and T -Stress, for different values of crack length.



Graph 17: K_I variation for $S/W=2$

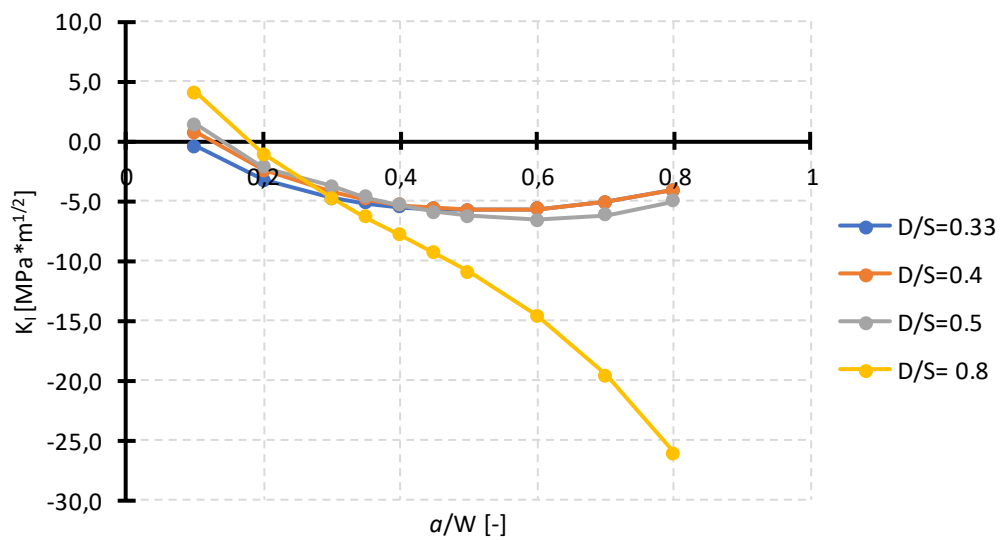


Graph 18: K_{II} variation for $S/W=2$

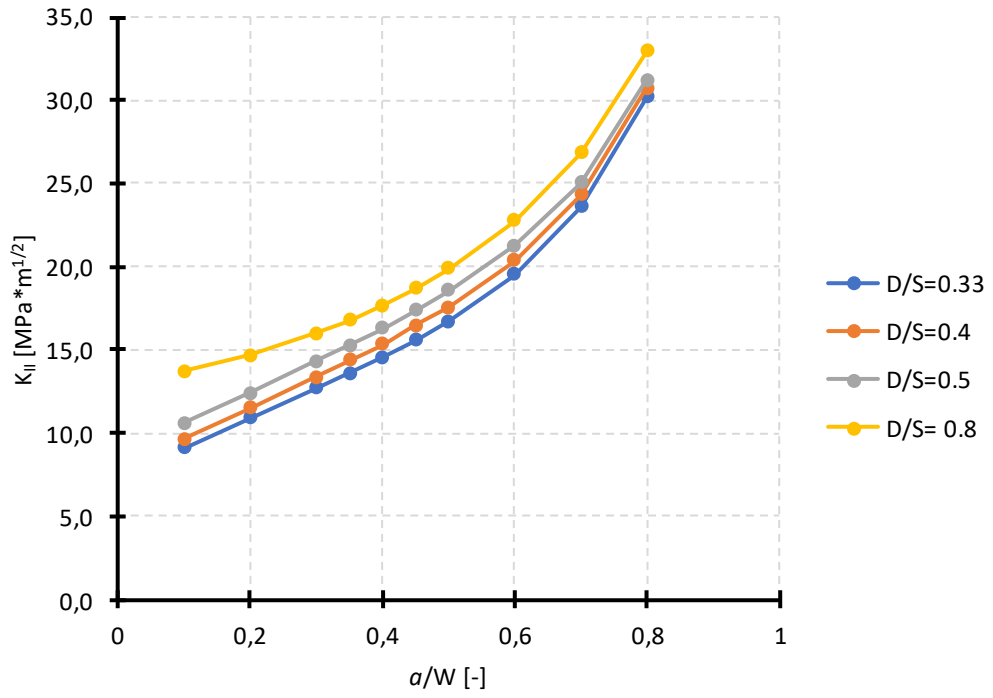


Graph 19: T-Stress variation for S/W=2

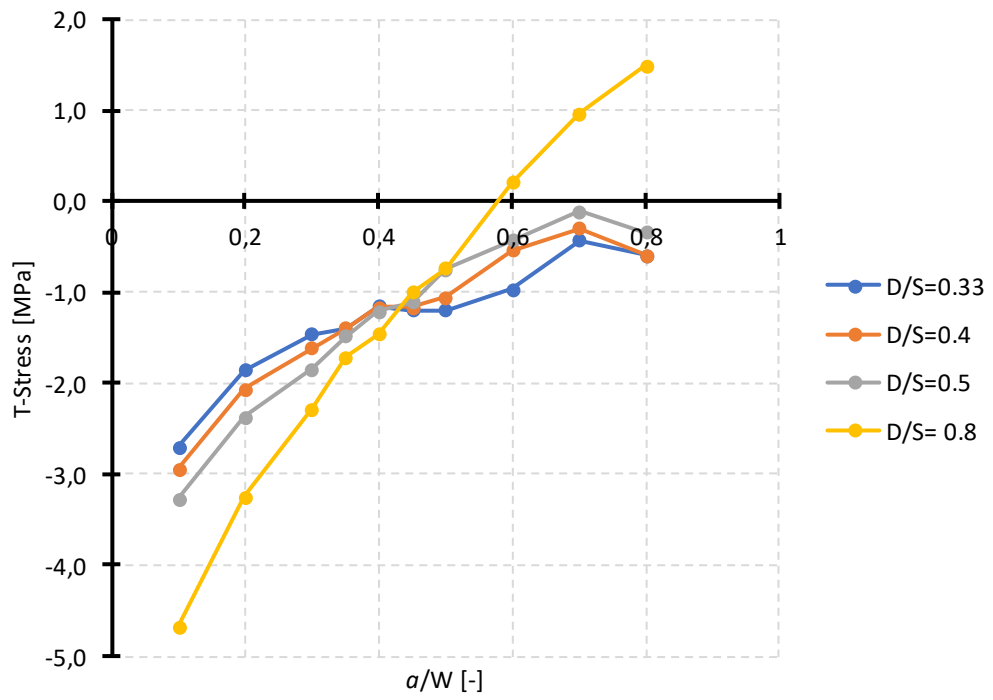
For a constant S/W=3, next graphs represent the values of K_I , K_{II} and T-Stress, for different values of crack length.



Graph 20: K_I variation for S/W=3

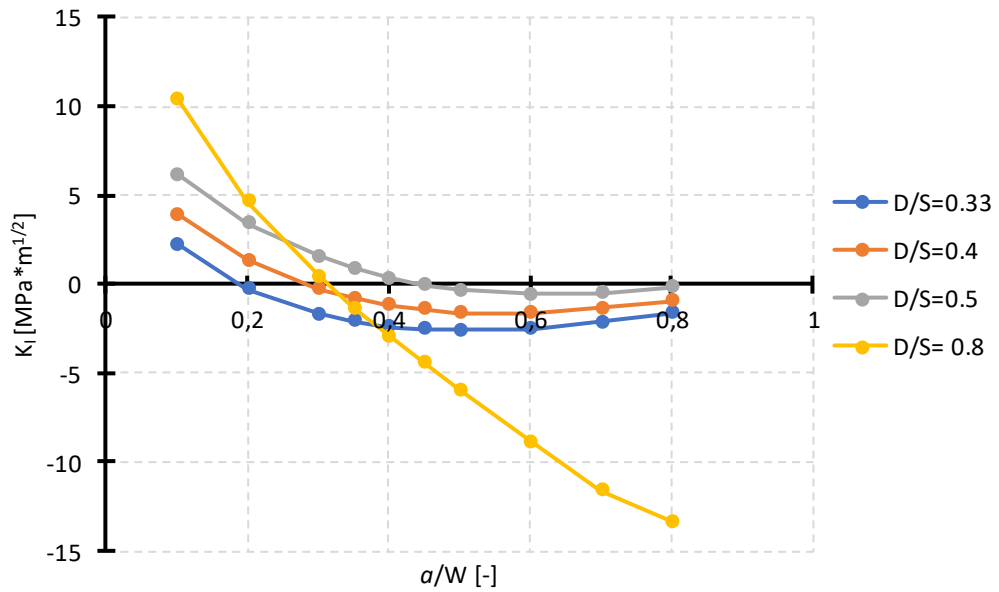


Graph 21: K_{II} variation for $S/W=3$

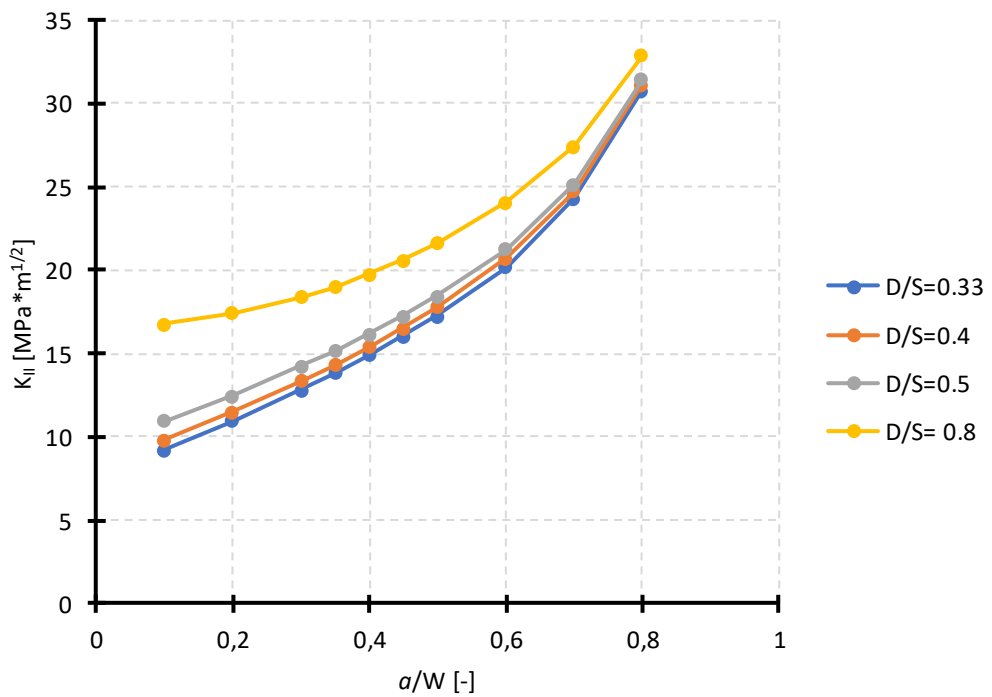


Graph 22: T-Stress variation for $S/W=3$

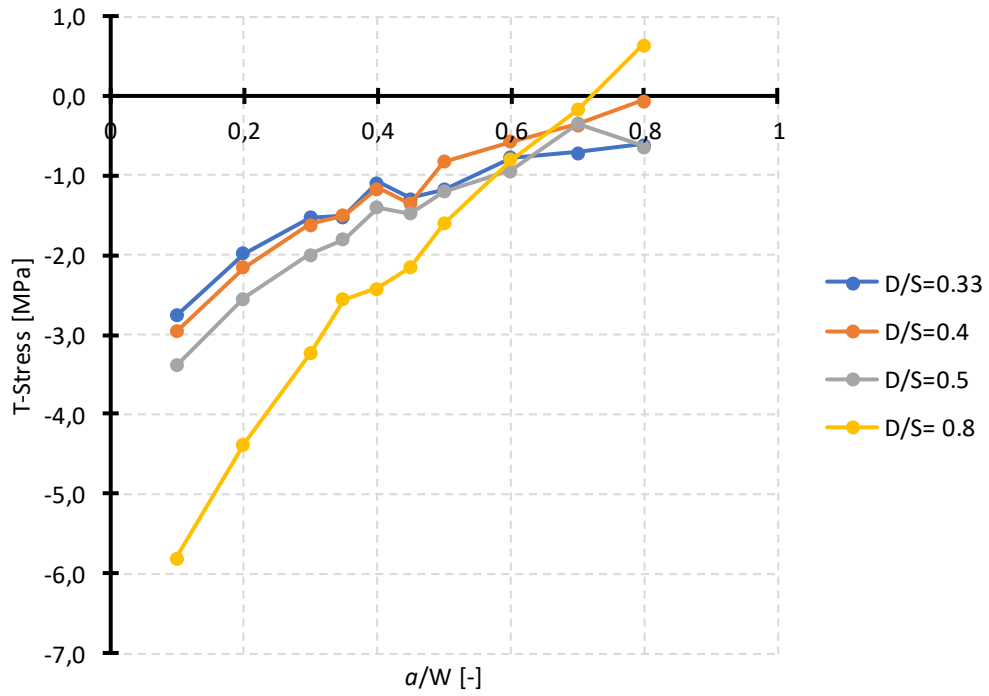
For a constant $S/W=4$, next graphs represent the values of K_I , K_{II} and T -Stress, for different values of crack length.



Graph 23: K_I variation for $S/W=4$

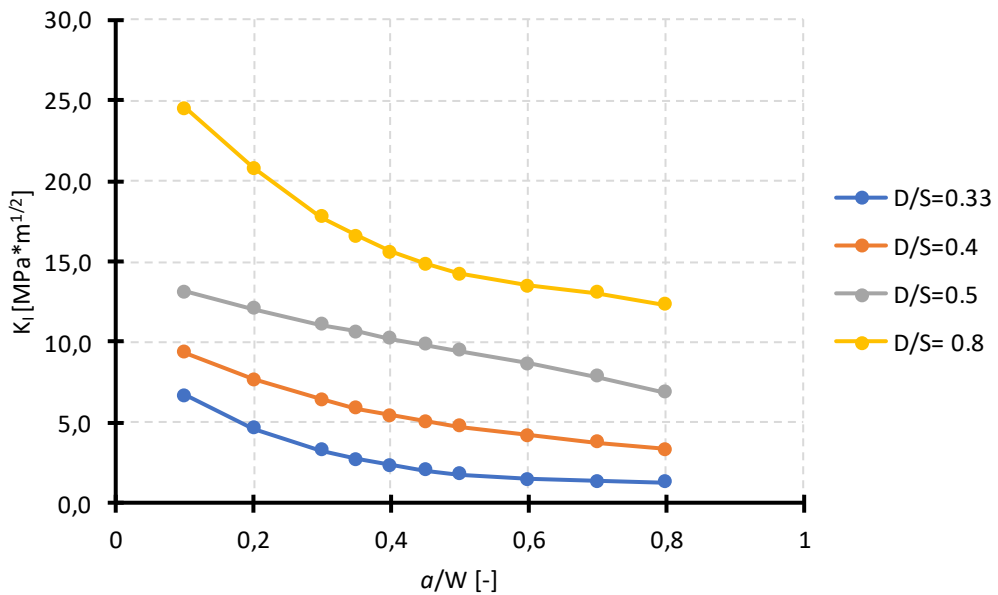


Graph 24: K_{II} variation for $S/W=4$

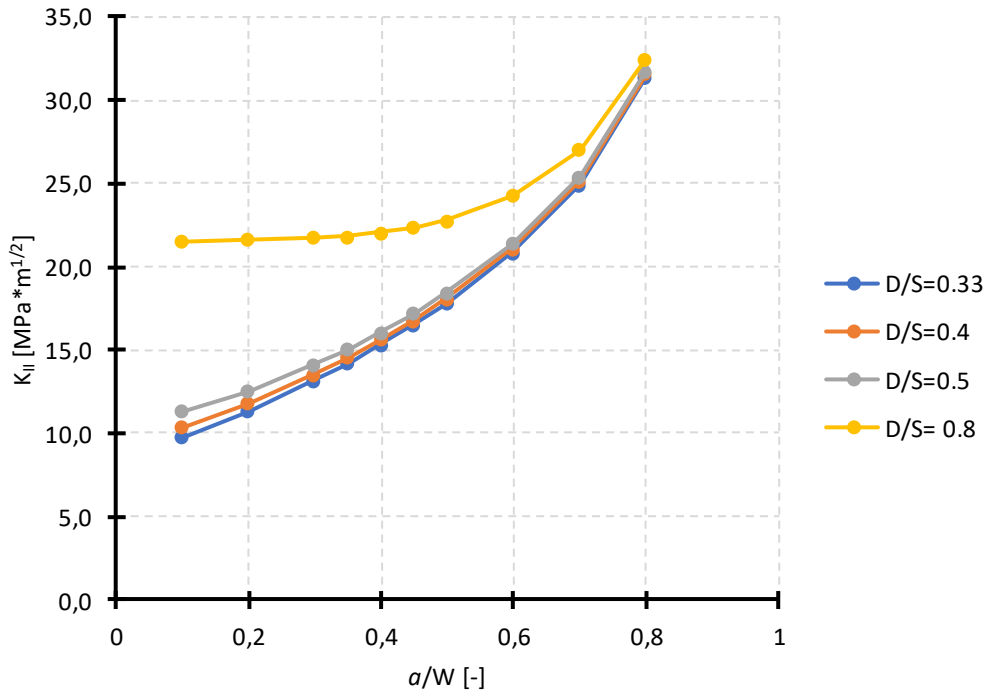


Graph 25: T-Stress variation for S/W=4

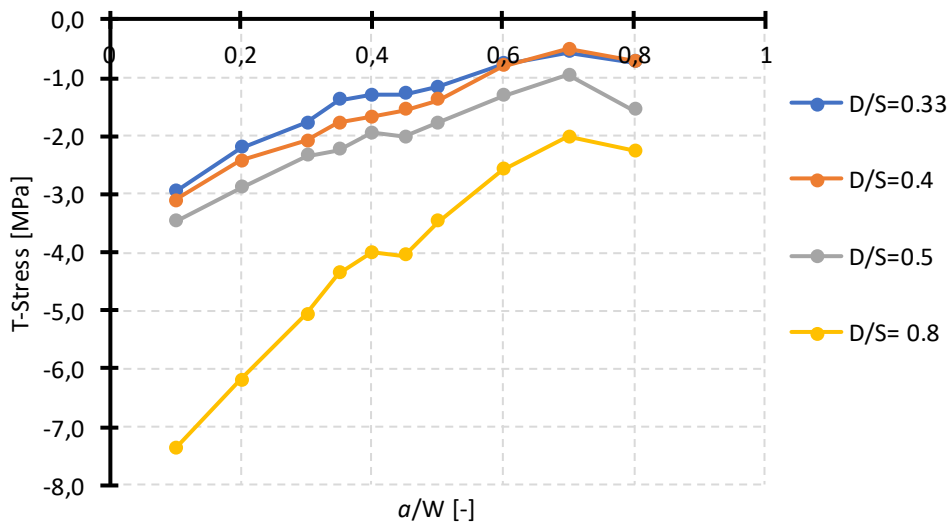
For a constant S/W=6, next graphs represent the values of K_I , K_{II} and T-Stress, for different values of crack length.



Graph 26: K_I variation for S/W=6



Graph 27: K_{II} variation for $S/W=6$



Graph 28: T-Stress variation for $S/W=6$

6.4. Analysis of the graphs for constant S/W ratio.

For K_I , the trend lines are so different depending on the geometry. For $S/W=1$ all the curves are similar, as it is said before this is a special case for a square specimen. All the values are negative, it means that the crack is always closing, additionally, with bigger cracks the K_I gives more important values. For $S/W=2; 3; 4$, all the series are similar with almost constant values for all the crack lengths, except for $D/S=0.8$. For $D/S=0.8$ the curve

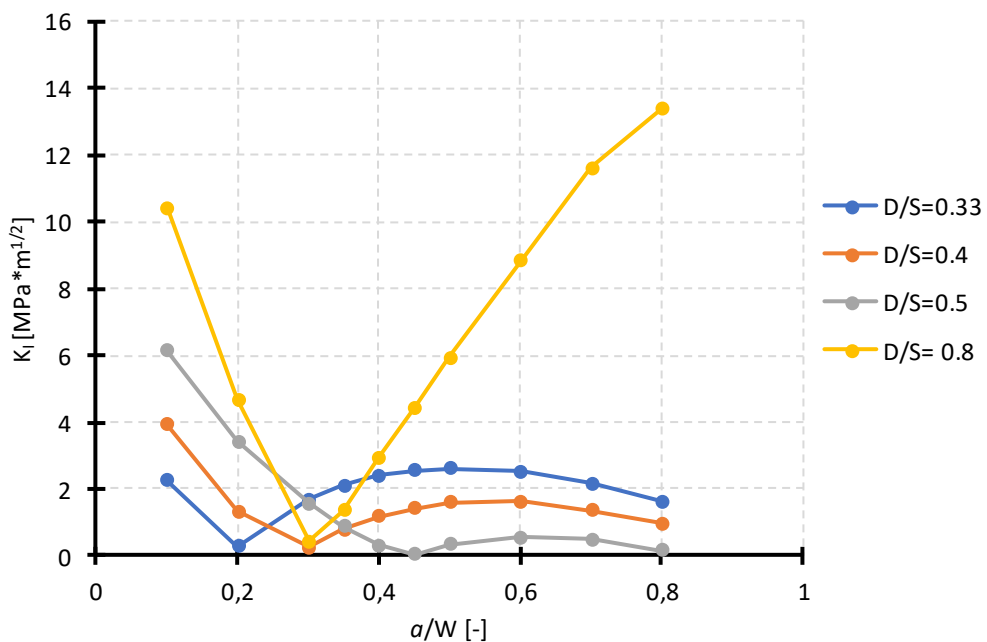
has a bigger slope, and it tends to close the crack for bigger crack lengths. Finally, for $S/W=6$, all the series are positive, then the cracks are opening always. Furthermore, in this last case, it is proved that the K_I grows up with bigger D/S ratios, and goes down with bigger crack lengths.

The K_{II} curves are very similar for all the cases. It is always growing up with the crack length and it gives similar values for all the D/S ratios in each S/W case. The only remarkable difference could be the $D/S=0.8$, which is bigger than the other curves always, especially with $S/W=1$ and $S/W=6$.

The T -Stress curves are similar for all the D/S cases except for $D/S=0.8$. In all S/W cases, the T -Stress grows up from -3 to nearly 0, with bigger crack lengths. For $D/S=0.8$ it is different, the curve has the same trend line but it grows up with an accentuated slope. Additionally, for different values of S/W , the $D/S=0.8$ curve keeps the slope but it drops in the graph for bigger S/W values.

6.5. K_I sign discussion.

When the K_I results extracted by ANSYS were plotted, some of the graphs gave strange trend lines and it seems to be wrong. As it is showed in the next figure:



Graph 29: K_I variation in absolute value for a constant $S/W=4$.

These strange trend lines are caused by the software ANSYS, it calculates the SIF as an absolute value. The appropriated sign for each K_I obtained by ANSYS, is known checking the displacements in the crack.

In the macro, using the command *GET the displacements are obtained for both axis, this values are for the coordinates system 14, which have his axes exchanged, so it is necessary to check the y displacements. This displacements are both with the same sign always, that is an important fact to apply the next equation.

Calculating the difference between u_y of each node as the next equation:

$$u_{y208} - u_{y144}$$

(31)

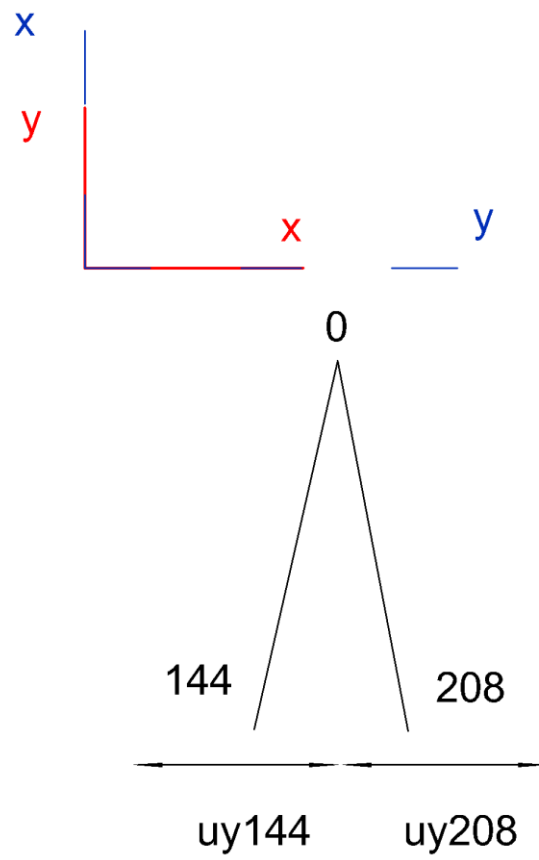


Figure 18: Crack and nodes which its displacements were studied.

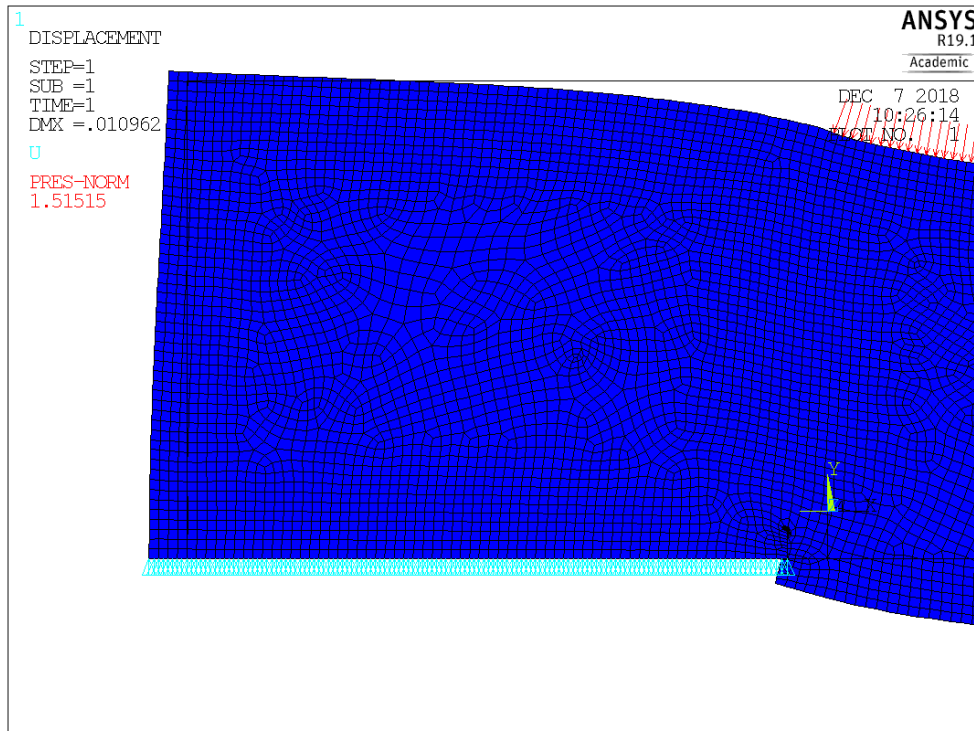


Figure 19: Deformed shape of a specimen with a closing crack.

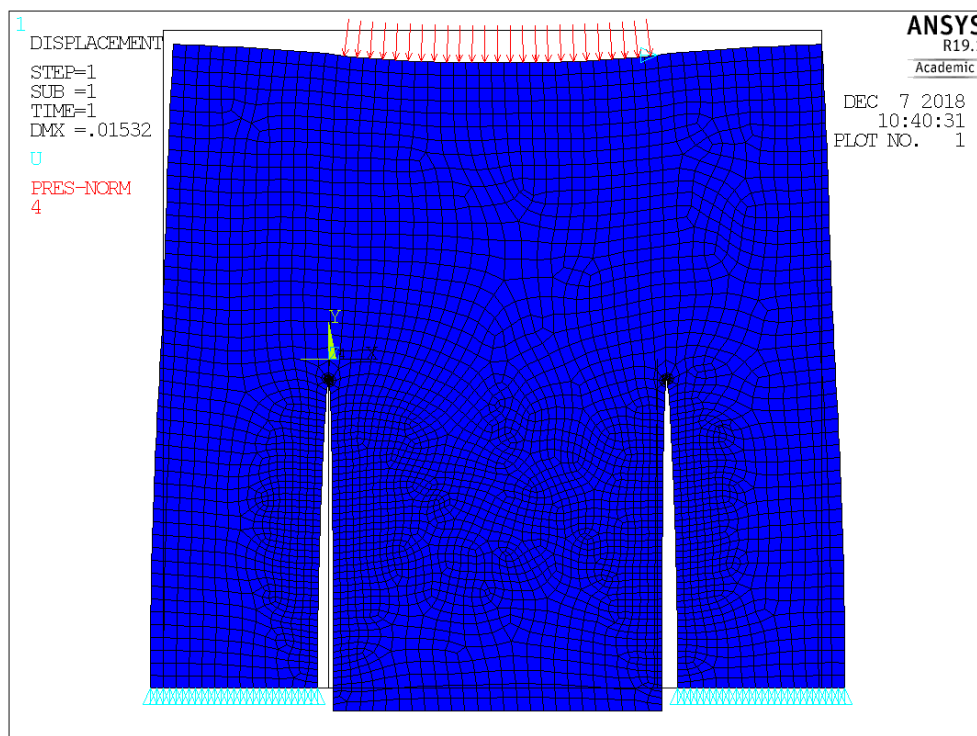


Figure 20: Deformed shape of a specimen with an opening crack.

If the value from the equation 31 is positive the crack is opening, because the node 144 does not exceed the value of the node 208, so the K_I must be positive. If the value is negative, the value of the node 144 has exceeded the value of the node 208, so the crack is closing. Showing some examples is easy to get it.

At the start of the test, both nodes are in the same position. Once the load have been applied the displacements are:

Table 11: Displacements for $D/S=0.8$ $S/W=6$ $a/W=0.1$

Uy node 1	Uy node 144	Uy node 208	Uy208-uy144	sign
-0.004	-0.0043	-0.0036	0.0007	positive

It is possible to check that the node 208 have moved to left, but it have move his position less than the node 144, and there is a distance between them, so the crack is opened.

The next case is the same but with positive displacements:

Table 12: Displacements for $D/S=0.33$ $S/W=6$ $a/W=0.1$

Uy node 1	Uy node 144	Uy node 208	Uy208-uy144	sign
0.0046	0.0045	0.0047	0.0002	positive

In this case the nodes have moved to the right, but node 208 have moved his position more than node 144, so there is a distance between them and the crack is opened.

Now the case of a closed crack:

Table 13: Displacements for $D/S=0.4$ $S/W=2$ $a/W=0.1$

Uy node 1	Uy node 144	Uy node 208	Uy208-uy144	sign
-0.00065	-0.00062	-0.00068	-0.000060	negative

In this case the nodes have moved to the left, the node 208 have moved his position more than the node 144, so it have reach and exceed his position, the crack is closed.

Last case for a closed crack with positive displacements:

Table 14: Displacements for $D/S=0.4$ $S/W=2$ $a/W=0.7$

Uy node 1	Uy node 144	Uy node 208	Uy208-uy144	sign
0.017	0.018	0.017	-0.0010	negative

Now the nodes have moved to the right, the node 144 have moved his position more than the node 208, so the crack is closed.

For K_{II} it is not necessary to check the sign, because the sign in Mode II does not represent the opening or closing of the crack, it is just a relative value, furthermore it is always taken as positive.

For the T -Stress the sign is not given by ANSYS, it is the independent term of an linear equation, so Excel gives the appropriated sign.

7. Conclusions.

In this thesis, three parameters were studied in order to define the stress conditions on the crack tip for different dimensions in four point bending test, Stress Intensity Factor for mixed Mode I/II and *T-Stress*. The results were obtained in the Finite Element Method software, ANSYS, and then they were plotted in graphs. Comparing the curves it is possible to obtain some conclusions.

For square specimens ($S/W=1$), the curves have different behaviours because this is a special case.

The K_I changes its behaviour depending on the dimensions, but it is proved that for bigger crack lengths, the SIF Mode I tend to negative values, this means that the crack is closing.

For K_{II} , the curves are very clear, always with the same shape. The curve always grows for bigger crack lengths.

T-Stress has clear trend lines too, and as K_{II} , the curves are always growing up for bigger crack lengths.

The values obtained in ANSYS are just mathematical results, which have to be analysed to prove its veracity, as it is done with K_I sign proved with displacements.

All the results extracted in this thesis could be improved in the future or used in different documents to get more conclusions in four point bending test. To prove the accuracy of this values, they should be compared with real numbers obtained in laboratory.

References

- [1] Anderson, T. L., Fracture Mechanics. Fundamentals and Applications, Third Edition, 2005.
- [2] Pook, L. P., Linear Elastic Fracture Mechanics for Engineers Theory and Applications. WITPress. 2000. p. 3. ISBN 1 85312 7035.
- [3] Anderson, T. L., Fracture Mechanics. Fundamentals and Applications, Third Edition, 2005, p. 29.
- [4] <http://www.fracturemechanics.org/ellipse.html>
- [5] Gehlen, P.C., Kanninen, M.F., An Atomic Model for Cleavage Crack Propagation in Iron, Inelastic Behaviour of Solids, McGraw-Hill, New York, 1970, pp. 587–603.
- [6] Miarka. P., Seitl. S., Analysis of mixed Mode I/II failure of selected structural concrete grades, Institute of Structural Mechanics, Brno, 2018, p. 8.
- [7] Belzunce, J., Tecnología de materiales: Comportamiento en servicio de materiales, Escuela Politécnica de Ingeniería de Gijón, Gijón, 2012, p.48.
- [8] Anderson, T. L., Fracture Mechanics. Fundamentals and Applications, Third Edition, 2005, p. 44.
- [9] Pook, L. P., Linear Elastic Fracture Mechanics for Engineers Theory and Applications. WITPress. 2000. p. 22. ISBN 1 85312 7035.
- [10] M. Gupta, R.C. Alderliesten, R. Benedictus, A review of *T-stress* and its effects in fracture mechanics, Engineering Fracture Mechanics, Volume 134, 2015, Pages 218-241, ISSN 0013-7944.
- [11] R.J. Sanford, A critical re-examination of the Westergaard method for solving opening-mode crack problems, Mech Res Commun, 6 (5) (1979), pp. 289-294.
- [12] Cotterell, B. (1966). Notes on the paths and stability of cracks. International Journal of Fracture Mechanics, 2(3), 526-533.
- [13] Melin, S., The influence of the T-stress on the directional stability of cracks, Int J Fract, 114 (3) (2002), pp. 259-265.
- [14] S.G. Larsson, A.J. Carlsson, Influence of non-singular stress terms and specimen geometry on small-scale yielding at crack tips in elastic-plastic materials, J Mech Phys Solids, 21 (4) (1973), pp. 263-277.
- [15] T. Nakamura, D.M. Parks, Determination of elastic *T-stress* along 3-dimensional crack fronts using an interaction integral, Int J Solids Struct, 29 (13) (1992), pp. 1597-1611.
- [16] J.-H. Kim, G. Paulino, *T-stress* in orthotropic functionally graded materials: Lekhnitskii and Stroh formalisms, Int J Fract, 126 (4) (2004), pp. 345-384.
- [17] X.F. Li, K.Y. Lee, Fracture analysis of cracked piezoelectric materials, Int J Solids Struct, 41 (15) (2004), pp. 4137-4161.
- [18] B. Yang, K. Ravi-Chandar, Evaluation of elastic *T-stress* by the stress difference method, Eng Fract Mech, 64 (5) (1999), pp. 589-605.

- [19] R. Zhou, P. Zhu, Z. Li, The Shielding Effect of the Plastic Zone at Mode-II Crack Tip, *Int J Fract*, 171 (2) (2011), pp. 195-200
- [20] Anderson, T. L., *Fracture Mechanics. Fundamentals and Applications*, Third Edition, 2005, p. 88.
- [21] Anderson, T. L., *Fracture Mechanics. Fundamentals and Applications*, Third Edition, 2005, Figure 2.57., p. 86.
- [22] Anderson, T. L., *Fracture Mechanics. Fundamentals and Applications*, Third Edition, 2005, Figure 2.58., p. 87.
- [23] Anderson, T. L., *Fracture Mechanics. Fundamentals and Applications*, Third Edition, 2005, p. 61.
- [24] <https://slideplayer.com/slide/13869782/>
- [25] Erdogan, F., Sih, G.C., On the crack extension in plates under plane loading and transverse shear, *Journal of Basic Engineering*, Volume 85, Issue 4, pp. 525-527
- [26] Miarka. P., Seitzl. S., Analysis of mixed Mode I/II failure of selected structural concrete grades, *Institute of Structural Mechanics, Brno*, 2018, p. 9.
- [27] Yanhua Zhao, Wei Dong, Bohan Xu, Jin Liu, Effect of *T-stress* on the initial fracture toughness of concrete under I/II mixed-mode loading, *Theoretical and Applied Fracture Mechanics*, Volume 96, 2018, Pages 699-706, ISSN 0167-8442.
- [28] R.K. Nalla, J.H. Kinney, R.O. Ritchie, Mechanistic fracture criteria for the failure of human cortical bone, *Nat. Mater.*, 2 (2003), pp. 164-168.
- [29] K.J. Chang, On the maximum strain criterion — a new approach to the angled crack problem, *Eng. Fract. Mech.*, 14 (1981), pp. 107-124.
- [30] M.M. Mirsayar, Mixed mode fracture analysis using extended maximum tangential strain criterion, *Materials & Design*, Volume 86, 2015, Pages 941-947, ISSN 0264-1275.
- [31] EN 1992-1-1: Eurocode 2: 2004, *Design of concrete structures - Part 1-1: General rules and rules for buildings*, European Committee for Standardization Brussels, Belgium.
- [32] Krystian Jurowski, Stefania Grzeszczyk, The Influence of Concrete Composition on Young's Modulus, *Procedia Engineering*, Volume 108, 2015, Pages 584-591, ISSN 1877-7058.
- [33] Dalibor Kocab, Barbara Kucharczykova, Petr Misak, Petr Zitt, Monika Kralikova, Development of the Elastic Modulus of Concrete under Different Curing Conditions, *Procedia Engineering*, Volume 195, 2017, Pages 96-101, ISSN 1877-7058.
- [34] Aenlle M., *Propiedades del Hormigón, Estructuras de Hormigón*, Escuela Politécnica de Gijón, Gijón, 2018.
- [35] <http://www.ansys.stuba.sk> , Chapter 10: Fracture Mechanics, Bratislava, Slovakia.

List of abbreviations.

LEFM	Linear elastic fracture mechanics.
EPFM	Elastic plastic fracture mechanics.
FM	Fracture mechanics.
FEA	Finite element analysis.
SIF	Stress intensity factor.
PZ	Plastic zone.
CT	Compact tension.
GMTS	Generalized maximum tangential stress.
MTS	Maximum tangential stress.
MTSN	Maximum tangential strain.

List of symbols.

σ	Applied stress.
K_{Ic}	Fracture toughness.
C	Specimen's geometry constant.
a	Crack length.
σ_{ij}	Stress tensor.
σ_A, σ_{LOC}	Located stress at A.
ρ	Radius of curvature.
σ_f	Remote stress at failure.
E	Young's modulus.
x	x axis.
y	y axis.
γ_s	Surface energy per unit area.
f_{ij}	Dimensionless function.
K	Stress intensity factor.
σ_{ij}	Stress tensor.
r. θ	Polar coordinates.
$\sigma_{\theta\theta}$	Tangential stress.
$\epsilon_{\theta\theta}$	Tangential strain.
K_I	Stress intensity factor for Mode I.
K_{II}	Stress intensity factor for Mode II.
K_{III}	Stress intensity factor for Mode III.
ν	Poisson's ratio.
σ_{ys}	Yield strength.
r	Radius of the plastic zone.
T	T-stress.
P	Applied load.
x. y	Cartesian coordinates.
fcd	Characteristic compressive strength of concrete.
fck	Characteristic specific compressive strength of concrete.
fcm	Characteristic compressive strength of concrete at 28 days.
a/W	Crack length-Width ratio.
S/D	Span-Distance between cracks ratio.
S/W	Span-Width ratio.
ux	Displacement in x axis.
uy	Displacement in y axis.

List of figures.

Figure 1: Elliptical crack retaken from [4].	9
Figure 2: A point defined in the vicinity of the crack tip. ^[1]	10
Figure 3: Parallel cracks with stress lines.[21]	15
Figure 4: Stress intensity factor analysis, for different geometrical conditions in a parallel cracks case. [22]	15
Figure 5: Plastic zone for plane stress (r_y) and plain strain (r_p). [24]	16
Figure 6: Crack tip stress components.	18
Figure 7: Normal distribution for determining characteristic compressive strength.	19
Figure 8: : Sketch of the specimen.	21
Figure 9 : PLANE82 2D 8 Node Structural Solid.	22
Figure 10: Keypoints number in macro.	23
Figure 11: Keypoints in ANSYS.	23
Figure 12: Lines in ANSYS	24
Figure 13: Areas in ANSYS.	24
Figure 14: Meshing in ANSYS.	25
Figure 15: Boundary condition ($u_y=0$) plotted in ANSYS	26
Figure 16: Pressure plotted in ANSYS.	26
Figure 17 : Path definition in ANSYS [35].	26
Figure 18: Crack and nodes which its displacements were studied.	47
Figure 19: Deformed shape of a specimen with a closing crack.	48
Figure 20: Deformed shape of a specimen with an opening crack.	48

List of graphs.

Graph 1: Values extracted from ANSYS plotted to calculate the T-Stress for $D/S=0.33$ $S/W=1$ and $a/W=0$ ($T\text{-Stress}=-2.273$).	27
Graph 2: K_I variation for $D/S=0.33$	32
Graph 3: K_{II} variation for $D/S=0.33$	32
Graph 4 $T\text{-Stress}$ variation for $D/S=0.33$	33
Graph 5 : K_I variation for $D/S=0.4$	33
Graph 6: K_{II} variation for $D/S=0.4$	34
Graph 7: $T\text{-Stress}$ variation for $D/S=0.4$	34
Graph 8: K_I variation for $D/S=0.5$	35
Graph 9: K_{II} variation for $D/S=0.5$	35
Graph 10: $T\text{-Stress}$ variation for $D/S=0.5$	36
Graph 11: K_I variation for $D/S=0.8$	36
Graph 12: K_{II} variation for $D/S=0.8$	37
Graph 13: $T\text{-Stress}$ variation for $D/S=0.8$	37
Graph 14: K_I variation for $S/W=1$	38
Graph 15: K_{II} variation for $S/W=1$	39
Graph 16: $T\text{-Stress}$ variation for $S/W=1$	39
Graph 17: K_I variation for $S/W=2$	40
Graph 18: K_{II} variation for $S/W=2$	40
Graph 19: $T\text{-Stress}$ variation for $S/W=2$	41
Graph 20: K_I variation for $S/W=3$	41
Graph 21: K_{II} variation for $S/W=3$	42
Graph 22: $T\text{-Stress}$ variation for $S/W=3$	42
Graph 23: K_I variation for $S/W=4$	43
Graph 24: K_{II} variation for $S/W=4$	43
Graph 25: $T\text{-Stress}$ variation for $S/W=4$	44
Graph 26: K_I variation for $S/W=6$	44
Graph 27: K_{II} variation for $S/W=6$	45
Graph 28: $T\text{-Stress}$ variation for $S/W=6$	45
Graph 29: K_I variation in absolute value for a constant $S/W=4$	46

List of tables.

Table 1: Stress field equations. Mode I and II. [7]	11
Table 2: Displacements equations. Mode I and II. [7]	12
Table 3: Tangential Stresses and displacement. Mode III. [7]	12
Table 4: Modes of crack tip surface displacement.....	13
Table 5: Values of the dimension ratios.	21
Table 6 : Material properties for ANSYS.	21
Table 7: Values extracted from ANSYS to calculate the <i>T-Stress</i>	28
Table 8: Values of the dimension ratios.	29
Table 9: Boundary conditions of two initial symmetrical notches in four point bending specimen.	30
Table 10: Distributed boundary conditions.	31
Table 11: Displacements for $D/S=0.8$ $S/W=6$ $a/W=0.1$	49
Table 12: Displacements for $D/S=0.33$ $S/W=6$ $a/W=0.1$	49
Table 13: Displacements for $D/S=0.4$ $S/W=2$ $a/W=0.1$	49
Table 14: Displacements for $D/S=0.4$ $S/W=2$ $a/W=0.7$	49
Table 15: Results for $D/S=0.33$	67
Table 16: Results for $D/S=0.4$	68
Table 17: Results for $D/S=0.5$	69
Table 18: Results for $D/S=0.8$	70
Table 19: Displacements for $D/S=0.33$	71
Table 20: Displacements for $D/S=0.4$	72
Table 21: Displacements for $D/S=0.5$	73
Table 22: Displacements for $D/S=0.8$	74

Curriculum vitae.

José Antonio Rodríguez Valdés

Birth: November 10th, 1995 (23 years)

ID: 71902970W

Address: Doctor Marañón 14 5ºA, 33400 Avilés, Asturias, Spain

Contact: +34678872911

E-mail: joseguez23@gmail.com

STUDIES

- **MECHANICAL ENGINEERING BACHELOR**
University of Oviedo
Escuela Politecnica de Gijón (Gijón Polytechnic School of Engineering)
Mention in Construction
2013-2019
- **ERASMUS+ MOBILITY IN BRNO (CZECH REPUBLIC)**
Brno University of Technology
Vysoké učení technické v Brně (Faculty of Civil Engineering)
Realization of the Final Bachelor Project and one subject from last year
Final Bachelor Project: Numerical Analysis of stress field in the vicinity of two symmetrical notches in four point bending test: mixed mode I+II
Year 2018–2019
Stay duration: 4 months
- **SHIELD METAL ARC WELDING COURSE CERTIFIED**
Forteastur S.L.
200 practical hours

LANGUAGES

- **SPANISH**
Native
- **ENGLISH**
B2 First Certificate in English - Cambridge

SKILLS AND APTITUDES

SOFTWARE SKILLS

- **MICROSOFT OFFICE**
Excel, PowerPoint, Word
- **AUTODESK**
Inventor, Autocad
- **CYPE**
- **ANSYS**
- **LISAFEA**

PRACTICAL EXPERIENCE

- **ARCELOR MITTAL.** Duration of the internship: Two months. Year: 2018.
Place: ArcelorMittal University, Avilés, Asturias.

SKILLS

- Dedication.
- Eagerness to learn.
- Teamwork.
- Adaptive capability

OTHER INTERESTING DATA

- European driving license
- Own car
- Willingness to travel

Annexes.

Annexe I: Macro.

```
!Macro for Four Point Bending Test in concrete
!Jose Antonio Rodriguez Valdes
!-----
!Primary Orders
!-----
/clear
/PREP7
/PNUM,KP,1
/PNUM,LINE,1
/PNUM,AREA,1
/PNUM,VOLU,1
/PSF,PRES,NORM,2,0,1
/PBC,ALL,,1
!-----
!INPUT PARAMETERS
!-----
W=100      !Width of the specimen
S_W=6      !S/W ratio S_W=1 square specimen
S=S_W*W    !Span
a_W=0.8    !a/W ratio
a = a_W*W  !crack length
D_S=0.8    !D/S ratio
D=D_S*S    !Distance between cracks
v=(S-D)/2
Q=200      !Distributed force
P = Q/D    !Input force
n = 6
r_C = 0.25
!-----
!Material parameters and element typ
!-----
UIMP,1,EX, , ,30e3,  !Youngs modulus
UIMP,1,NUXY, , ,0.2, !Poissons ratio
ET,1,82             !Element type
KEYOPT,1,3,2       !Plane strain 1,3,2;
```

!-----

!Keypoints

!-----

K,1,0,0

K,2,1,0

K,3,0,1

K,4,-1,0

K,50,0,-1

K,60,0,-1

K,5,0,-a

K,6,0,-a

K,7,D,0

K,8,D+1,0

K,9,D,1

K,10,D-1,0

K,111,D,-1

K,112,D,-1

K,11,D,-a

K,12,D,-a

K,13,-v,-a

K,14,D+v,-a

K,15,D+v,W-a

K,16,-v,W-a

K,20,0,W-a

K,21,D,W-a

!-----

!Lines

!-----

L,1,2 !L1

L,1,3 !L2

L,1,4 !L3

arc,2,3,1,1 !L4

arc,3,4,1,1 !L5

L,1,50 !L6 Left crack Left side

L,1,60 !L7 Left crack Right side

L,50,5 !L8

L,60,6 !L9

arc,4,50,1,1 !L10

arc,2,60,1,1 !L11

L,7,8 !L12

L,7,9 !L13
 L,7,10 !L14
 L,7,111 !L15 Right crack Left side
 L,7,112 !L16 Right crack Right side
 L,111,11 !L17
 L,112,12 !L18
 arc,8,9,7,1 !L19
 arc,9,10,7,1 !L20
 arc,10,111,7,1 !L21
 arc,8,112,7,1 !L22
 L,12,14 !L23
 L,14,15 !L24
 L,15,21 !L25
 L,21,20 !L26
 L,20,16 !L27
 L,16,13 !L28
 L,13,5 !L29
 L,6,11 !L30
 L,9,21 !L31
 L,3,20 !L32

!-----

!Areas

!-----

AL,1,2,4 !A1
 AL,2,3,5 !A2
 AL,3,10,6 !A3
 AL,1,11,7 !A4
 AL,19,12,13 !A5
 AL,13,14,20 !A6
 AL,12,22,16 !A7
 AL,14,21,15 !A8
 AL,19,22,18,23,24,25,31 !A9
 AL,20,21,17,30,31,26,32,4,11,9 !A10
 AL,32,27,28,29,8,10,5 !A11

!-----

!Parameters for mesh refinement

!-----

Q=0.5
 J=2
 I=10

Kesize,1,Q
Kesize,2,Q
Kesize,3,Q
Kesize,4,Q
Kesize,5,J
Kesize,6,J
Kesize,7,Q
Kesize,8,Q
Kesize,9,Q
Kesize,10,Q
Kesize,11,J
Kesize,12,I
Kesize,13,I
Kesize,14,I
Kesize,15,I
Kesize,16,I
Kesize,50,Q
Kesize,60,Q
Kesize,111,Q
Kesize,112,Q
Kesize,21,I
Kesize,22,I
Lesize,1,1
Lesize,2,1
Lesize,3,1
Lesize,4,1
Lesize,5,1
Lesize,6,1
Lesize,7,1
Lesize,8,1
Lesize,9,1
Lesize,10,1
Lesize,11,1
Lesize,12,1
Lesize,13,1
Lesize,14,1
Lesize,15,1
Lesize,16,1
Lesize,17,1
Lesize,18,1

```

Lesize,19,1
Lesize,20,1
Lesize,21,1
Lesize,22,1
Lesize,23,J
Lesize,24,J
Lesize,25,J
Lesize,26,J
Lesize,27,J
Lesize,28,J
Lesize,29,J
Lesize,30,J
Lesize,31,J
Lesize,32,J
!-----
!Meshing
!-----
KSCON,1,r_c,1,n,0.75 !Nodes to mesh from
KSCON,7,r_c,1,n,0.75 !Nodes to mesh from
AMESH,1
AMESH,2
AMESH,3
AMESH,4
AMESH,5
AMESH,6
AMESH,7
AMESH,8
AMESH,9
AMESH,10
AMESH,11
!-----
!Load and Boundary conditions
!-----
lsl,s,line,,23           !Selecting lines
lsl,a,line,,29
nsl,s,1
d,ALL,uy,0             !Boundary condition uy
KSEL,S,KP,,21          !Selecting KP number 21
NSLK,S,1
d,all,ux,0            !Boundary condition ux

```



```

nsel,all
nset,S,loc,Y,W-a,W-a      !selecting nodes in specified coordinates
nset,R,loc,X,0,D          !reselecting nodes in specified coordinates
SF,ALL,PRES,P            !Pressure in selected nodes
allsel,all
!-----
!Solving the problem
!-----
/solu
solve
!-----
!Postprocessing
!-----
FINISH
/POST1
CSKP,14,0,1,3,4,1,1,      !New coordinate system
RSYS,14
!Selecting new coordinate system 14 because the path must be parallel to x axis
LPATH,1,144,145,208,209    !Path of the right crack on the origin
!LPATH,273,411,412,475,476 !Path of the left crack
Kcalc,0,1,3,0
!Definition of the calculation of SIF, on the third place 0(zero) means half of the model
at 3 places 0-for half-body 3-because it's a whole body path
*get,ux,node,1,u,x        !Obtain the ux displacement in node 1 (crack tip)
*get,uy,node,1,u,y        !Obtain the uy displacement in node 1 (crack tip)
*get,ux,node,144,u,x
!Obtain the ux displacement in node 144 (left side of the crack)
*get,uy,node,144,u,y
!Obtain the uy displacement in node 144 (left side of the crack)
*get,ux,node,208,u,x
!Obtain the ux displacement in node 208 (right side of the crack)
*get,uy,node,208,u,y
!Obtain the uy displacement in node 208 (right side of the crack)
!ALL THIS DISPLACEMENTS ARE OBTAINED IN CS14, THE AXIS ARE EXCHANGED
!-----
!Stress results into file
!-----
FLST,2,2,1
FITEM,2,node(0, 0, 0) !node position x,y,z
FITEM,2,node(4, 0,0)

```

```

PATH,PATH1,2,20,50,
PPATH,P51X,1
PDEF,sx,S,X,AVG      !stress SX
PDEF,sy,S,Y,AVG      !stress SY
PAGET,bbb,TABLE
PAGET,III,LABELS
/nopr
/outp,temp,inp
/com, *cfoopen,tryconcrete41,out      !file name
/com, *vwwrite
/com, (5x,'LENGHT',10x,'SX',15x,'SY')  !label
/com, *vwwrite,bbb(1,4),bbb(1,5),bbb(1,6)
/com, (3E15.6)                !number of decimal numbers
/com, *cfclos
/outp
/inp,temp,inp
/gopr
finish

```

Annexe II: Results.

Stress Intensity Factors for mixed Mode I/II and *T*-Stress.

Table 15: Results for $D/S=0.33$

D/S	S/W	a/W	K_I	K_{II}	T-Stress
0,33	1	0,1	-3,0121	7,51	-2,2730
0,33	1	0,2	-4,5419	7,7712	-2,1390
0,33	1	0,3	-6,2232	8,012	-1,9669
0,33	1	0,35	-7,2537	8,2574	-2,0046
0,33	1	0,4	-8,4688	8,5974	-2,1767
0,33	1	0,45	-9,945	9,072	-2,1740
0,33	1	0,5	-11,733	9,7179	-2,0758
0,33	1	0,6	-16,602	11,803	-2,1387
0,33	1	0,7	-23,799	15,824	-2,0111
0,33	1	0,8	-32,379	23,796	-1,1150
0,33	2	0,1	-3,2371	8,4644	-2,5087
0,33	2	0,2	-6,121	10,087	-1,7919
0,33	2	0,3	-7,9558	11,41	-1,6238
0,33	2	0,35	-8,809	12,105	-1,4944
0,33	2	0,4	-9,6537	12,886	-1,3877
0,33	2	0,45	-10,448	13,799	-1,3977
0,33	2	0,5	-11,203	14,884	-1,2583
0,33	2	0,6	-12,295	17,735	-1,0583
0,33	2	0,7	-12,4	21,977	-0,8014
0,33	2	0,8	-10,959	28,907	-0,5898
0,33	3	0,1	-0,42342	9,0666	-2,7012
0,33	3	0,2	-3,2668	10,899	-1,8530
0,33	3	0,3	-4,7321	12,667	-1,4646
0,33	3	0,35	-5,1718	13,567	-1,4055
0,33	3	0,4	-5,503	14,519	-1,1522
0,33	3	0,45	-5,6835	15,541	-1,1934
0,33	3	0,5	-5,7796	16,68	-1,1981
0,33	3	0,6	-5,6543	19,504	-0,9702
0,33	3	0,7	-5,1243	23,608	-0,4316
0,33	3	0,8	-4,0971	30,201	-0,5965
0,33	4	0,1	2,2639	9,2082	-2,7539
0,33	4	0,2	-0,27557	10,961	-1,9696
0,33	4	0,3	-1,6763	12,846	-1,5287
0,33	4	0,35	-2,0959	13,837	-1,5087
0,33	4	0,4	-2,4052	14,9	-1,0795
0,33	4	0,45	-2,54	16,033	-1,2855
0,33	4	0,5	-2,5997	17,277	-1,1688
0,33	4	0,6	-2,5209	20,219	-0,7682
0,33	4	0,7	-2,1509	24,31	-0,7066
0,33	4	0,8	-1,6272	30,815	-0,6093
0,33	6	0,1	6,6859	9,7972	-2,9583
0,33	6	0,2	4,669	11,37	-2,2006
0,33	6	0,3	3,2816	13,222	-1,7866
0,33	6	0,35	2,7573	14,243	-1,3851
0,33	6	0,4	2,3519	15,346	-1,2924
0,33	6	0,45	2,0557	16,535	-1,2875
0,33	6	0,5	1,8235	17,829	-1,1620
0,33	6	0,6	1,5205	20,877	-0,7676
0,33	6	0,7	1,3855	24,972	-0,5690
0,33	6	0,8	1,3033	31,407	-0,7294

Table 16: Results for $D/S=0.4$

D/S	S/W	a/W	K_I	K_{II}	T-Stress
0,4	1	0,1	-2,9587	8,3628	-2,4976
0,4	1	0,2	-4,7822	8,8718	-2,0210
0,4	1	0,3	-6,4155	9,1459	-1,8350
0,4	1	0,35	-7,4065	9,4086	-1,8304
0,4	1	0,4	-8,5733	9,793	-1,9376
0,4	1	0,45	-9,968	10,319	-1,8964
0,4	1	0,5	-11,707	11,039	-1,8826
0,4	1	0,6	-16,467	13,344	-1,7827
0,4	1	0,7	-23,734	17,698	-1,4044
0,4	1	0,8	-33,361	25,867	-0,4895
0,4	2	0,1	-2,4789	8,9248	-2,6568
0,4	2	0,2	-5,7906	10,758	-2,0456
0,4	2	0,3	-8,0091	12,407	-1,4588
0,4	2	0,35	-8,9789	13,225	-1,2884
0,4	2	0,4	-9,9123	14,125	-1,2157
0,4	2	0,45	-10,78	15,115	-1,4555
0,4	2	0,5	-11,639	16,263	-1,2974
0,4	2	0,6	-12,995	19,152	-0,7240
0,4	2	0,7	-13,312	23,246	-0,3431
0,4	2	0,8	-11,914	29,806	-0,4148
0,4	3	0,1	0,71479	9,6561	-2,9359
0,4	3	0,2	-2,4236	11,492	-2,0658
0,4	3	0,3	-4,2572	13,378	-1,6113
0,4	3	0,35	-4,8554	14,34	-1,3957
0,4	3	0,4	-5,3097	15,355	-1,1632
0,4	3	0,45	-5,5711	16,434	-1,1678
0,4	3	0,5	-5,7483	17,572	-1,0578
0,4	3	0,6	-5,6981	20,375	-0,5405
0,4	3	0,7	-5,119	24,305	-0,2915
0,4	3	0,8	-4,0607	30,704	-0,5909
0,4	4	0,1	3,9237	9,8142	-2,9553
0,4	4	0,2	1,34	11,496	-2,1565
0,4	4	0,3	-0,25371	13,357	-1,6154
0,4	4	0,35	-0,78375	14,345	-1,4989
0,4	4	0,4	-1,1877	15,411	-1,1559
0,4	4	0,45	-1,4085	16,551	-1,3543
0,4	4	0,5	-1,5942	17,779	-0,8192
0,4	4	0,6	-1,6099	20,713	-0,5761
0,4	4	0,7	-1,3596	24,733	-0,3607
0,4	4	0,8	-0,96986	31,14	-0,0534
0,4	6	0,1	9,3373	10,364	-3,1209
0,4	6	0,2	7,7009	11,807	-2,4286
0,4	6	0,3	6,437	13,581	-2,0940
0,4	6	0,35	5,9028	14,562	-1,7715
0,4	6	0,4	5,4716	15,653	-1,6777
0,4	6	0,45	5,0995	16,82	-1,5530
0,4	6	0,5	4,7772	18,098	-1,3923
0,4	6	0,6	4,2422	21,119	-0,8053
0,4	6	0,7	3,8055	25,2	-0,5089
0,4	6	0,8	3,3496	31,613	-0,7198

Table 17: Results for $D/S=0.5$

D/S	S/W	a/W	K_I	K_{II}	T-Stress
0,5	1	0,1	-2,8288	9,5812	-2,8099
0,5	1	0,2	-5,144	10,356	-2,0993
0,5	1	0,3	-6,7133	10,693	-1,8906
0,5	1	0,35	-7,6096	10,959	-1,7705
0,5	1	0,4	-8,654	11,344	-1,7869
0,5	1	0,45	-9,9058	11,885	-1,9177
0,5	1	0,5	-11,479	12,645	-1,6203
0,5	1	0,6	-15,874	15,061	-1,3541
0,5	1	0,7	-22,969	19,543	-0,6833
0,5	1	0,8	-34,269	27,751	0,9418
0,5	2	0,1	-1,4285	9,5005	-2,8815
0,5	2	0,2	-5,1775	11,403	-2,1244
0,5	2	0,3	-7,8621	13,277	-1,5008
0,5	2	0,35	-9,0212	14,231	-1,5612
0,5	2	0,4	-10,179	15,253	-1,3052
0,5	2	0,45	-11,321	16,373	-0,9726
0,5	2	0,5	-12,448	17,613	-0,6998
0,5	2	0,6	-14,526	20,59	-0,3274
0,5	2	0,7	-15,871	24,558	0,1722
0,5	2	0,8	-15,312	30,726	0,1801
0,5	3	0,1	1,4097	10,606	-3,2720
0,5	3	0,2	-2,1476	12,385	-2,3687
0,5	3	0,3	-3,7692	14,281	-1,8391
0,5	3	0,35	-4,6533	15,271	-1,4822
0,5	3	0,4	-5,3704	16,305	-1,2063
0,5	3	0,45	-5,8946	17,39	-1,1036
0,5	3	0,5	-6,2982	18,55	-0,7449
0,5	3	0,6	-6,57	21,27	-0,4251
0,5	3	0,7	-6,16	25,013	-0,1066
0,5	3	0,8	-5,0392	31,181	-0,3452
0,5	4	0,1	6,1484	10,947	-3,3840
0,5	4	0,2	3,4301	12,494	-2,5400
0,5	4	0,3	1,5592	14,237	-1,9855
0,5	4	0,35	0,87802	15,176	-1,8028
0,5	4	0,4	0,32266	16,182	-1,4035
0,5	4	0,45	-0,05186	17,27	-1,4687
0,5	4	0,5	-0,33663	18,443	-1,2012
0,5	4	0,6	-0,55671	21,255	-0,9403
0,5	4	0,7	-0,48474	25,16	-0,3444
0,5	4	0,8	-0,16124	31,454	-0,6301
0,5	6	0,1	13,122	11,317	-3,4819
0,5	6	0,2	12,085	12,572	-2,8920
0,5	6	0,3	11,092	14,166	-2,3366
0,5	6	0,35	10,636	15,081	-2,2360
0,5	6	0,4	10,196	16,105	-1,9425
0,5	6	0,45	9,8198	17,222	-2,0126
0,5	6	0,5	9,447	18,449	-1,7838
0,5	6	0,6	8,6948	21,412	-1,3106
0,5	6	0,7	7,8734	25,44	-0,9608
0,5	6	0,8	6,8438	31,794	-1,5493

Table 18: Results for $D/S=0.8$

D/S	S/W	a/W	K_I	K_{II}	T-Stress
0,8	1	0,1	-5,3637	16,246	-5,5084
0,8	1	0,2	-8,9482	16,968	-3,7120
0,8	1	0,3	-10,568	17,401	-2,7929
0,8	1	0,35	-11,144	17,566	-2,4447
0,8	1	0,4	-11,677	17,775	-2,2733
0,8	1	0,45	-12,227	18,053	-2,1558
0,8	1	0,5	-12,922	18,46	-1,8199
0,8	1	0,6	-12,922	18,46	-1,1620
0,8	1	0,7	-18,287	22,574	-0,0621
0,8	1	0,8	-25,872	28,209	1,9788
0,8	2	0,1	-0,5119	12,584	-4,2515
0,8	2	0,2	-4,7867	13,617	-2,8438
0,8	2	0,3	-7,5856	14,858	-1,8918
0,8	2	0,35	-8,7572	15,558	-1,7223
0,8	2	0,4	-9,9273	16,356	-1,4316
0,8	2	0,45	-11,128	17,253	-0,9564
0,8	2	0,5	-12,454	18,265	-0,4282
0,8	2	0,6	-15,709	20,889	0,2616
0,8	2	0,7	-21,07	24,9	1,3423
0,8	2	0,8	-31,896	31,783	3,0132
0,8	3	0,1	4,0851	13,735	-4,6719
0,8	3	0,2	-1,1365	14,692	-3,2529
0,8	3	0,3	-4,8025	15,989	-2,2826
0,8	3	0,35	-6,3894	16,781	-1,7121
0,8	3	0,4	-7,8772	17,687	-1,4642
0,8	3	0,45	-9,3894	18,705	-0,9940
0,8	3	0,5	-10,94	19,867	-0,7401
0,8	3	0,6	-14,61	22,758	0,2037
0,8	3	0,7	-19,597	26,825	0,9619
0,8	3	0,8	-26,146	32,943	1,4913
0,8	4	0,1	10,418	16,751	-5,7969
0,8	4	0,2	4,6648	17,408	-4,3666
0,8	4	0,3	0,43126	18,382	-3,2248
0,8	4	0,35	-1,3429	19,014	-2,5579
0,8	4	0,4	-2,936	19,771	-2,4112
0,8	4	0,45	-4,4478	20,633	-2,1503
0,8	4	0,5	-5,9324	21,624	-1,5931
0,8	4	0,6	-8,8371	24,071	-0,7927
0,8	4	0,7	-11,609	27,45	-0,1750
0,8	4	0,8	-13,361	32,879	0,6432
0,8	6	0,1	24,483	21,534	-7,3791
0,8	6	0,2	20,784	21,659	-6,1916
0,8	6	0,3	17,754	21,752	-5,0620
0,8	6	0,35	16,552	21,85	-4,3630
0,8	6	0,4	15,575	22,055	-4,0114
0,8	6	0,45	14,827	22,373	-4,0493
0,8	6	0,5	14,216	22,804	-3,4734
0,8	6	0,6	13,465	24,27	-2,5913
0,8	6	0,7	13,046	27,021	-2,0118
0,8	6	0,8	12,341	32,467	-2,2509

Displacements.

Table 19: Displacements for D/S=0.33

D/S	S/W	a/W	Node 1 ux	Node 1 uy	Node 144 ux	Node 144 uy	Node 208 ux	Node 208 uy	uy_208-uy_144	SIGN
0,33	1	0,1	-0,0021	0,0022	-0,002	0,0023	-0,0021	0,0022	-0,000100	-
0,33	1	0,2	-0,0034	0,0031	-0,0033	0,0031	-0,0035	0,0031	-0,000030	-
0,33	1	0,3	-0,0048	0,0042	-0,0047	0,0043	-0,0049	0,0041	-0,000200	-
0,33	1	0,35	-0,0055	0,005	-0,0054	0,0051	-0,0056	0,0049	-0,000200	-
0,33	1	0,4	-0,0063	0,006	-0,0062	0,0061	-0,0064	0,0058	-0,000300	-
0,33	1	0,45	-0,0072	0,0072	-0,0071	0,0073	-0,0074	0,0071	-0,000200	-
0,33	1	0,5	-0,0083	0,0088	-0,0082	0,0089	-0,0084	0,0086	-0,000300	-
0,33	1	0,6	-0,011	0,013	-0,01	0,014	-0,011	0,0130	-0,001000	-
0,33	1	0,7	-0,015	0,023	-0,015	0,023	-0,015	0,0230	0,000000	-
0,33	1	0,8	-0,022	0,041	-0,022	0,041	-0,023	0,0400	-0,001000	-
0,33	2	0,1	-0,0022	0,0041	-0,0021	0,0041	-0,0023	0,0040	-0,000100	-
0,33	2	0,2	-0,0038	0,0049	-0,0036	0,0049	-0,0039	0,0048	-0,000100	-
0,33	2	0,3	-0,0053	0,0063	-0,0052	0,0064	-0,0054	0,0062	-0,000200	-
0,33	2	0,35	-0,0061	0,0071	-0,006	0,0072	-0,0063	0,0070	-0,000200	-
0,33	2	0,4	-0,0071	0,008	-0,0069	0,0082	-0,0072	0,0079	-0,000300	-
0,33	2	0,45	-0,0081	0,0091	-0,0079	0,0092	-0,0082	0,0090	-0,000200	-
0,33	2	0,5	-0,0091	0,01	-0,0089	0,01	-0,0093	0,0100	0,000000	-
0,33	2	0,6	-0,011	0,012	-0,011	0,013	-0,011	0,0120	-0,001000	-
0,33	2	0,7	-0,014	0,015	-0,0144	0,0159	-0,015	0,0150	-0,000900	-
0,33	2	0,8	-0,0184	0,0182	-0,0181	0,018	-0,0188	0,0180	0,000000	-
0,33	3	0,1	-0,0023	-0,00047	0,00	0,00	0,00	0,00	-0,000010	-
0,33	3	0,2	0,00	0,00	0,00	0,00	-0,004	-0,00095	-0,000080	-
0,33	3	0,3	-0,0053	-0,0011	-0,0051	-0,001	-0,0055	-0,0012	-0,000200	-
0,33	3	0,35	-0,006	-0,0012	-0,0059	-0,0011	-0,0062	-0,0013	-0,000200	-
0,33	3	0,4	-0,0068	-0,0013	-0,0066	-0,0013	-0,007	-0,0014	-0,000100	-
0,33	3	0,45	-0,0076	-0,0015	-0,0074	-0,0014	-0,0078	-0,0016	-0,000200	-
0,33	3	0,5	-0,0085	-0,0017	-0,0083	-0,0016	-0,0087	-0,0018	-0,000200	-
0,33	3	0,6	-0,01	-0,0023	-0,01	-0,0022	-0,01	-0,0024	-0,000200	-
0,33	3	0,7	-0,01	-0,0033	-0,012	-0,0033	-0,013	-0,0034	-0,000100	-
0,33	3	0,8	-0,015	-0,0054	-0,015	-0,0053	-0,016	-0,0054	-0,000100	-
0,33	4	0,1	-0,0023	-0,0004	-0,0022	-0,00042	-0,0024	-0,00037	0,000050	+
0,33	4	0,2	-0,0037	-0,0011	-0,0036	-0,0011	-0,0039	-0,0011	0,000000	-
0,33	4	0,3	-0,0051	-0,0016	-0,0049	-0,0015	-0,0052	-0,0016	-0,000100	-
0,33	4	0,35	-0,0058	-0,0018	-0,0056	-0,0018	-0,0059	-0,0018	0,000000	-
0,33	4	0,4	-0,0065	-0,002	-0,0063	-0,002	-0,0066	-0,0021	-0,000100	-
0,33	4	0,45	-0,0065	-0,002	-0,0063	-0,002	-0,0066	-0,0021	-0,000100	-
0,33	4	0,5	-0,008	-0,0026	-0,00777	-0,0026	-0,0082	-0,0026	0,000000	-
0,33	4	0,6	-0,0097	-0,0035	-0,0094	-0,0034	-0,0099	-0,0035	-0,000100	-
0,33	4	0,7	-0,011	-0,0049	-0,011	-0,0048	-0,012	-0,0049	-0,000100	-
0,33	4	0,8	-0,014	-0,0073	-0,014	-0,0073	-0,015	-0,0073	0,000000	-
0,33	6	0,1	-0,0024	0,0046	-0,0023	0,0045	-0,0025	0,0047	0,000200	+
0,33	6	0,2	-0,0038	0,0035	-0,0036	0,0035	-0,0039	0,0036	0,000100	+
0,33	6	0,3	-0,0051	0,0027	-0,0049	0,0026	-0,0052	0,0027	0,000100	+
0,33	6	0,35	-0,0057	0,0023	-0,0055	0,00231	-0,0059	0,00236	0,000050	+
0,33	6	0,4	-0,0064	0,002	-0,0062	0,0019	-0,0066	0,002	0,000100	+
0,33	6	0,45	-0,0071	0,0016	-0,0069	0,00161	-0,0073	0,00168	0,000070	+
0,33	6	0,5	-0,0078	0,00128	-0,0076	0,00126	-0,0081	0,0013	0,000040	+
0,33	6	0,6	-0,0095	0,00044	-0,0092	0,00043	-0,0098	0,00046	0,000030	+
0,33	6	0,7	-0,011	-0,00068	-0,011	-0,00069	-0,011	-0,00066	0,000030	+
0,33	6	0,8	-0,014	-0,0024	-0,014	-0,0024	-0,014	-0,0023	0,000100	+

Table 20: Displacements for D/S=0.4

D/S	S/W	a/W	Node 1 ux	Node 1 uy	Node 144 ux	Node 144 uy	Node 208 ux	Node 208 uy	uy_208-uy_144	SIGN
0,4	1	0,1	-0,0023	0,0025	-0,0022	0,0026	-0,0024	0,0025	-0,000100	-
0,4	1	0,2	-0,0038	0,0035	-0,0037	0,0035	-0,0039	0,0034	-0,000100	-
0,4	1	0,3	-0,0052	0,0047	-0,0051	0,0048	-0,0054	0,0047	-0,000100	-
0,4	1	0,35	-0,006	0,0056	-0,0059	0,0057	-0,0062	0,0055	-0,000200	-
0,4	1	0,4	-0,0069	0,0066	-0,0068	0,0067	-0,007	0,0065	-0,000200	-
0,4	1	0,45	-0,0078	0,0079	-0,0077	0,008	-0,008	0,0078	-0,000200	-
0,4	1	0,5	-0,0089	0,0096	-0,0087	0,0097	-0,009	0,0094	-0,000300	-
0,4	1	0,6	-0,011	0,014	-0,011	0,015	-0,011	0,014	-0,001000	-
0,4	1	0,7	-0,015	0,025	-0,015	0,025	-0,016	0,024	-0,001000	-
0,4	1	0,8	-0,023	0,045	-0,023	0,045	-0,023	0,045	0,000000	-
0,4	2	0,1	-0,0024	-0,00065	-0,0022	-0,00062	-0,0025	-0,00068	-0,000060	-
0,4	2	0,2	-0,004	-0,00092	-0,0038	-0,00085	-0,0041	-0,001	-0,000150	-
0,4	2	0,3	-0,0056	-0,001	-0,0054	-0,00094	-0,0058	-0,0011	-0,000160	-
0,4	2	0,35	-0,0065	0,0079	-0,0063	0,008	-0,0067	0,0078	-0,000200	-
0,4	2	0,4	-0,0075	0,009	-0,0073	0,0091	-0,0076	0,0088	-0,000300	-
0,4	2	0,45	-0,0085	0,01	-0,0083	0,01	-0,0087	0,01	0,000000	-
0,4	2	0,5	-0,0097	0,011	-0,0095	0,011	-0,0099	0,011	0,000000	-
0,4	2	0,6	-0,012	0,014	-0,012	0,014	-0,012	0,014	0,000000	-
0,4	2	0,7	-0,015	0,017	-0,015	0,018	-0,016	0,017	-0,001000	-
0,4	2	0,8	-0,019	0,02	-0,019	0,021	-0,02	0,02	-0,001000	-
0,4	3	0,1	-0,0025	-0,00046	-0,0024	-0,00047	-0,0026	-0,00045	0,000020	+
0,4	3	0,2	-0,0041	-0,0011	-0,0039	-0,001	-0,0042	-0,0011	-0,000100	-
0,4	3	0,3	-0,0056	-0,0015	-0,0055	-0,0014	-0,0058	-0,0015	-0,000100	-
0,4	3	0,35	-0,0064	-0,0017	-0,0062	-0,0016	-0,0066	-0,0017	-0,000100	-
0,4	3	0,4	-0,0073	-0,0019	-0,0071	-0,0018	-0,0074	-0,0019	-0,000100	-
0,4	3	0,45	-0,0081	-0,0021	-0,0079	-0,002	-0,0083	-0,0022	-0,000200	-
0,4	3	0,5	-0,009	-0,0024	-0,0088	-0,0023	-0,0092	-0,0024	-0,000100	-
0,4	3	0,6	-0,011	-0,0032	-0,01	-0,0031	-0,011	-0,0032	-0,000100	-
0,4	3	0,7	-0,013	-0,0044	-0,013	-0,0044	-0,013	-0,0045	-0,000100	-
0,4	3	0,8	-0,016	-0,0067	-0,016	-0,0067	-0,016	-0,0068	-0,000100	-
0,4	4	0,1	-0,0025	-0,00044	-0,0023	-0,00049	-0,0026	-0,00039	0,000100	+
0,4	4	0,2	-0,0039	-0,0014	-0,0038	-0,00144	-0,0041	-0,0014	0,000040	+
0,4	4	0,3	-0,0054	-0,0022	-0,0052	-0,0022	-0,0055	-0,0022	0,000000	-
0,4	4	0,35	-0,0061	-0,0025	-0,0059	-0,0025	-0,0062	-0,0025	0,000000	-
0,4	4	0,4	-0,0068	-0,0029	-0,0066	-0,0029	-0,007	-0,0029	0,000000	-
0,4	4	0,45	-0,0075	-0,0033	-0,0073	-0,0033	-0,0077	-0,0033	0,000000	-
0,4	4	0,5	-0,0083	-0,0037	-0,0081	-0,0037	-0,0085	-0,0038	-0,000100	-
0,4	4	0,6	-0,01	-0,0049	-0,0098	-0,0049	-0,01	-0,0049	0,000000	-
0,4	4	0,7	-0,012	-0,0066	-0,011	-0,0066	-0,012	-0,0066	0,000000	-
0,4	4	0,8	-0,015	-0,0093	-0,014	-0,0093	-0,015	-0,0093	0,000000	-
0,4	6	0,1	-0,0025	0,0056	-0,0024	0,0055	-0,0026	0,0057	0,000200	+
0,4	6	0,2	-0,0039	0,0042	-0,0038	0,0041	-0,0041	0,0043	0,000200	+
0,4	6	0,3	-0,0052	0,0028	-0,0051	0,0027	-0,0054	0,0029	0,000200	+
0,4	6	0,35	-0,0059	0,0021	-0,0057	0,0021	-0,0061	0,0022	0,000100	+
0,4	6	0,4	-0,0066	0,0015	-0,0064	0,0014	-0,0068	0,0015	0,000100	+
0,4	6	0,45	-0,0073	0,00081	-0,0071	0,00075	-0,0075	0,00088	0,000130	+
0,4	6	0,5	-0,008	0,000088	-0,0078	0,000032	-0,0083	0,00015	0,000118	+
0,4	6	0,6	-0,0097	-0,0015	-0,0094	-0,0015	-0,01	-0,0014	0,000100	+
0,4	6	0,7	-0,011	-0,0035	-0,011	-0,0035	-0,012	-0,0034	0,000100	+
0,4	6	0,8	-0,014	-0,0061	-0,014	-0,0061	-0,014	-0,006	0,000100	+

Table 21: Displacements for D/S=0.5

D/S	S/W	a/W	Node 1 ux	Node 1 uy	Node 144 ux	Node 144 uy	Node 208 ux	Node 208 uy	uy_208-uy_144	SIGN
0,5	1	0,1	-0,0026	-0,00051	-0,0025	-0,00047	-0,0028	-0,00054	-0,000070	-
0,5	1	0,2	-0,0044	-0,00052	-0,0043	-0,00045	-0,0045	-0,00058	-0,000130	-
0,5	1	0,3	-0,0061	-0,00051	-0,0059	-0,00043	-0,0062	-0,0006	-0,000170	-
0,5	1	0,35	-0,0069	0,0064	-0,0068	0,0065	-0,0071	0,0063	-0,000200	-
0,5	1	0,4	-0,0078	0,0075	-0,0077	0,0076	-0,008	0,0074	-0,000200	-
0,5	1	0,45	-0,0088	0,0089	-0,0087	0,009	-0,009	0,0088	-0,000200	-
0,5	1	0,5	-0,0099	0,0107	-0,0098	0,0108	-0,01	0,0105	-0,000300	-
0,5	1	0,6	-0,0127	0,0162	-0,0125	0,0164	-0,0129	0,016	-0,000400	-
0,5	1	0,7	-0,0169	0,026	-0,016	0,027	-0,017	0,026	-0,001000	-
0,5	1	0,8	-0,024	0,05	-0,024	0,05	-0,0248	0,0496	-0,000400	-
0,5	2	0,1	-0,0025	-0,00058	-0,0024	-0,00056	-0,0026	-0,00059	-0,000030	-
0,5	2	0,2	-0,0042	-0,001	-0,0041	-0,00098	-0,0043	-0,0011	-0,000120	-
0,5	2	0,3	-0,006	-0,0012	-0,0058	-0,0012	-0,0061	-0,0014	-0,000200	-
0,5	2	0,35	-0,0069	0,0089	-0,0067	0,009	-0,0071	0,0088	-0,000200	-
0,5	2	0,4	-0,0079	0,01	-0,0077	0,01	-0,0081	0,01	0,000000	-
0,5	2	0,45	-0,0091	0,011	-0,0089	0,011	-0,0093	0,011	0,000000	-
0,5	2	0,5	-0,01	0,013	-0,01	0,013	-0,01	0,013	0,000000	-
0,5	2	0,6	-0,013	0,017	-0,013	0,017	-0,013	0,016	-0,001000	-
0,5	2	0,7	-0,017	0,021	-0,016	0,022	-0,017	0,021	-0,001000	-
0,5	2	0,8	-0,021	0,026	-0,021	0,027	-0,022	0,026	-0,001000	-
0,5	3	0,1	-0,0028	-0,0006	-0,0026	-0,00062	-0,0029	-0,00056	0,000060	+
0,5	3	0,2	-0,0045	-0,0015	-0,0043	-0,0015	-0,0046	-0,0015	0,000000	-
0,5	3	0,3	-0,0062	-0,0022	-0,006	-0,0022	-0,0064	-0,0023	-0,000100	-
0,5	3	0,35	-0,0071	-0,0026	-0,0069	-0,0025	-0,0073	-0,0026	-0,000100	-
0,5	3	0,4	-0,008	-0,0029	-0,0078	-0,0029	-0,0082	-0,003	-0,000100	-
0,5	3	0,45	-0,0089	-0,0033	-0,0087	-0,0032	-0,0092	-0,0034	-0,000200	-
0,5	3	0,5	-0,0099	-0,0037	-0,0097	-0,0037	-1,00E-02	-0,0038	-0,000100	-
0,5	3	0,6	-1,20E-02	-0,0048	-0,011	-0,0047	-0,012	-0,0049	-0,000200	-
0,5	3	0,7	-0,014	-0,0064	-0,014	-0,0063	-0,015	-0,0065	-0,000200	-
0,5	3	0,8	-0,017	-0,0089	-0,017	-0,0089	-0,018	-0,009	-0,000100	-
0,5	4	0,1	-0,0028	-0,00062	-0,0026	-0,00069	-0,0029	-0,00053	0,000160	+
0,5	4	0,2	-0,0044	-0,002	-0,0042	-0,002	-0,0045	-0,0019	0,000100	+
0,5	4	0,3	-0,0059	-0,0032	-0,0057	-0,0033	-0,0061	-0,0032	0,000100	+
0,5	4	0,35	-0,0067	-0,0038	-0,0065	-0,0038	-0,0069	-0,0037	0,000100	+
0,5	4	0,4	-0,0075	-0,0045	-0,0073	-0,0045	-0,0077	-0,0044	0,000100	+
0,5	4	0,45	-0,0083	-0,0051	-0,0081	-0,0051	-0,0085	-0,0051	0,000000	-
0,5	4	0,5	-0,0091	-0,0058	-0,0089	-0,0058	-0,0094	-0,0058	0,000000	-
0,5	4	0,6	-0,01	-0,0074	-0,01	-0,0074	-0,011	-0,0074	0,000000	-
0,5	4	0,7	-0,013	-0,0096	-0,012	-0,0096	-0,013	-0,0096	0,000000	-
0,5	4	0,8	-0,016	-0,012	-0,015	-0,012	-0,016	-0,012	0,000000	-
0,5	6	0,1	-0,0027	0,0074	-0,0026	0,0073	-0,0028	0,0076	0,000300	+
0,5	6	0,2	-0,0042	0,0055	-0,004	0,0054	-0,0043	0,0057	0,000300	+
0,5	6	0,3	-0,0056	0,0034	-0,0054	0,0033	-0,0058	0,0036	0,000300	+
0,5	6	0,35	-0,0063	0,0023	-0,0061	0,0021	-0,0065	0,0024	0,000300	+
0,5	6	0,4	-0,007	0,0011	-0,0068	0,00099	-0,0072	0,0012	0,000210	+
0,5	6	0,45	-0,0077	-0,00016	-0,0075	-0,00028	-0,0079	-0,000032	0,000248	+
0,5	6	0,5	-0,0084	-0,0015	-0,0082	-0,0016	-0,0087	-0,0014	0,000200	+
0,5	6	0,6	-0,01	-0,0045	-0,0098	-0,0046	-0,01	-0,0044	0,000200	+
0,5	6	0,7	-0,012	-0,008	-0,011	-0,0081	-0,012	-0,0079	0,000200	+
0,5	6	0,8	-0,014	-0,012	-0,014	-0,0129	-0,015	-0,0126	0,000300	+

Table 22: Displacements for D/S 0.8

D/S	S/W	a/W	Node 1 ux	Node 1 uy	Node 144 ux	Node 144 uy	Node 208 ux	Node 208 uy	uy_208-uy_144	SIGN
0,8	1	0,1	-0,0053	0,0015	-0,0051	0,0016	-0,0055	0,0014	-0,000200	-
0,8	1	0,2	-0,0090	0,001	-0,0087	0,0011	-0,0092	0,00093	-0,000170	-
0,8	1	0,3	-0,012	0,00082	-0,012	0,00097	-0,012	0,0007	-0,000270	-
0,8	1	0,35	-0,014	0,00071	-0,013	0,00086	-0,014	0,00058	-0,000280	-
0,8	1	0,4	-0,015	0,00056	-0,015	0,00072	-0,016	0,00042	-0,000300	-
0,8	1	0,45	-0,017	0,00036	-0,017	0,00053	-0,017	0,00021	-0,000320	-
0,8	1	0,5	-0,019	0,0001	-0,019	0,00028	-0,019	-0,000047	-0,000327	-
0,8	1	0,6	-0,022	-0,00067	-0,022	-0,00047	-0,023	-0,00085	-0,000380	-
0,8	1	0,7	-0,027	-0,0021	-0,026	-0,0018	-0,027	-0,0023	-0,000500	-
0,8	1	0,8	-0,032	-0,005	-0,032	-0,0047	-0,032	-0,0053	-0,000600	-
0,8	2	0,1	-0,0037	0,00011	-0,0035	0,00012	-0,0038	0,00011	-0,000010	-
0,8	2	0,2	-0,006	-0,001	-0,0058	-0,00099	-0,0062	-0,0011	-0,000110	-
0,8	2	0,3	-0,0082	-0,002	-0,008	-0,0019	-0,0084	-0,0021	-0,000200	-
0,8	2	0,35	-0,0093	-0,0024	-0,0091	-0,0023	-0,0095	-0,0025	-0,000200	-
0,8	2	0,4	-0,01	-0,0029	-0,01	-0,0028	-0,01	-0,0031	-0,000300	-
0,8	2	0,45	-0,011	-0,0035	-0,011	-0,0034	-0,011	-0,0037	-0,000300	-
0,8	2	0,5	-0,013	-0,0042	-0,012	-0,004	-0,013	-0,0043	-0,000300	-
0,8	2	0,6	-0,015	-0,006	-0,015	-0,0057	-0,016	-0,0061	-0,000400	-
0,8	2	0,7	-0,019	-0,0086	-0,019	-0,0083	-0,02	-0,0088	-0,000500	-
0,8	2	0,8	-0,026	-0,012	-0,026	-0,012	-0,027	-0,013	-0,001000	-
0,8	3	0,1	-0,0038	-0,0015	-0,0037	-0,0016	-0,004	-0,0015	0,000100	+
0,8	3	0,2	-0,0061	-0,0038	-0,0059	-0,0038	-0,0063	-0,0038	0,000000	-
0,8	3	0,3	-0,0082	-0,0059	-0,008	-0,0058	-0,0084	-0,0059	-0,000100	-
0,8	3	0,35	-0,0093	-0,0069	-0,0091	-0,0068	-0,0095	-0,007	-0,000200	-
0,8	3	0,4	-0,01	-0,008	-0,01	-0,0079	-0,01	-0,0081	-0,000200	-
0,8	3	0,45	-0,011	-0,0092	-0,011	-0,009	-0,011	-0,0093	-0,000300	-
0,8	3	0,5	-0,012	-0,01	-0,012	-0,01	-0,013	-0,01	0,000000	-
0,8	3	0,6	-0,016	-0,013	-0,015	-0,013	-0,016	-0,013	0,000000	-
0,8	3	0,7	-0,02	-0,016	-0,019	-0,016	-0,02	-0,016	0,000000	-
0,8	3	0,8	-0,027	-0,02	-0,026	-0,02	-0,027	-0,021	-0,001000	-
0,8	4	0,1	-0,004641	0,02528	-0,0044	0,025166	-0,0048	0,02543	0,000264	+
0,8	4	0,2	-0,0072	0,02242	-0,007	0,02237	-0,0074	0,02249	0,000120	+
0,8	4	0,3	-0,0095	0,01972	-0,0093	0,0197	-0,009802	0,01975	0,000050	+
0,8	4	0,35	-0,0107	0,018552	-0,0146	0,01859	-0,01095	0,01855	-0,000040	-
0,8	4	0,4	-0,011	0,01752	-0,0116	0,01758	-0,01212	0,017505	-0,000075	-
0,8	4	0,45	-0,013	0,0166	-0,012	0,0167	-0,013	0,0166	-0,000100	-
0,8	4	0,5	-0,014	0,016	-0,014	0,0161	-0,0146	0,0159	-0,000200	-
0,8	4	0,6	-0,017	-0,021	-0,016	-0,021	-0,017	-0,021	0,000000	-
0,8	4	0,7	-0,021	-0,025	-0,02	-0,025	-0,021	-0,025	0,000000	-
0,8	4	0,8	-0,025	-0,03	-0,025	-0,03	-0,026	-0,031	-0,001000	-
0,8	6	0,1	-0,0057	-0,004	-0,0054	-0,0043	-0,0059	-0,0036	0,000700	+
0,8	6	0,2	-0,0088	-0,0098	-0,0085	-0,01	-0,0091	-0,0095	0,000500	+
0,8	6	0,3	-0,011	0,0211	-0,011	0,0209	-0,011	0,0213	0,000400	+
0,8	6	0,35	-0,012	0,01773	-0,012	0,01755	-0,013	0,01797	0,000420	+
0,8	6	0,4	-0,013	-0,023	-0,013	-0,023	-0,014	-0,022	0,001000	+
0,8	6	0,45	-0,014	0,01025	-0,014	0,010091	-0,015	0,01047	0,000379	+
0,8	6	0,5	-0,015	0,00615	-0,015	0,005998	-0,016	0,006362	0,000364	+
0,8	6	0,6	-0,017	-0,038	-0,017	-0,039	-0,018	-0,038	0,001000	+
0,8	6	0,7	-0,019	-0,048	-0,019	-0,048	-0,02	-0,047	0,001000	+
0,8	6	0,8	-0,022	-0,02444	-0,021	-0,02456	-0,022	-0,02425	0,000310	+



BRNO UNIVERSITY OF TECHNOLOGY UNIVERSIDAD DE OVIEDO

FACULTY OF CIVIL ENGINEERING

ESCUELA POLITÉCNICA DE GIJÓN

ANÁLISIS NUMÉRICO DEL CAMPO DE TENSIONES EN LAS PROXIMIDADES DE DOS MUESCAS EN UN ENSAYO DE FLEXION DE CUATRO PUNTOS: MODO MIXTO I+II

RESUMEN DE TRABAJO FINAL DE GRADO

AUTOR

José Antonio Rodríguez Valdés

SUPERVISOR

Prof. Stanislav Seitl

SUPERVISOR ESPECIALISTA:

Ing. Petr Miarka

COORDINADORA ERASMUS:

Prof. María Jesus Lamela

Introducción y objetivo

Si hablamos de mecánica de la fractura, la principal forma de estudiar el comportamiento de un material es controlar su crecimiento de grieta. Con este propósito se deben considerar dos parámetros característicos de la mecánica de la fractura elástico lineal como el factor de intensidad de tensiones y la T-Stress.

Actualmente, el hormigón es el material más utilizado en ingeniería civil, por esta razón es muy importante conocer en profundidad todo lo relacionado con el crecimiento de grietas en vigas con diferentes geometrías. En esta tesis, se ha estudiado el crecimiento de grietas en un espécimen de hormigón con cuatro soportes y dos muescas. Para definir el material, se han utilizado dos propiedades elásticas del hormigón, el módulo de Young y el coeficiente de Poisson. Los resultados de este trabajo podrían usarse como referencia para diferentes estudios en mecánica de la fractura o para un uso didáctico, pero esta tesis no es útil para estructuras reales o en un campo diferente de la ingeniería, porque considera la teoría elástica lineal. Además, en una estructura real se utiliza hormigón armado y es el acero el material que soporta la flexión.

Con un conjunto de gráficos, se ha comparado como afectan los parámetros geométricos a este tipo de muestras. Esta forma de trabajar se ha mejorado con el tiempo, desde las pruebas reales de laboratorio hasta el software de simulación actual utilizando el método de elementos finitos. En realidad, antes de realizar el análisis de laboratorio, debe modelarse y estudiarse cómo funciona en un ordenador para ahorrar tiempo y dinero. En este trabajo, las diferentes geometrías se han probado solo en el software de elementos finitos, ANSYS. ANSYS proporciona directamente los valores del factor de intensidad de tensiones y los valores de tensión necesarios para calcular la T-Stress.

El factor de intensidad de tensiones K es un parámetro fundamental en el campo de la mecánica de la fractura, expresa el estado tensional en la punta de grieta, cuando llega a un valor crítico que hace que la grieta colapse, se llama tenacidad a la fractura K_c . Hay tres modos de fisuración, KI, KII y KIII, cada uno representa una dirección de tensión en la punta de la grieta. En los resultados se demuestra que en este trabajo solo se ha obtenido KI y KII.

La T-Stress es también un concepto que está estrechamente relacionado con la mecánica de la fractura; se utiliza para diferentes funciones en este campo, pero principalmente se puede considerar como un parámetro para controlar la estabilidad tensional de la grieta.

El objetivo de esta tesis es extraer algunos resultados y conclusiones, que pueden ser útiles en un futuro en este campo de la mecánica de la fractura del hormigón.

Fundamentos teóricos.

Mecánica de la fractura.

Toda la tesis está basada en la mecánica de la fractura, existen dos teorías básicas en este campo; Mecánica de fractura elástico lineal y Mecánica de la fractura elástico-plástica. En esta tesis, el estudio introducido se realiza en Mecánica de fractura elástico lineal.

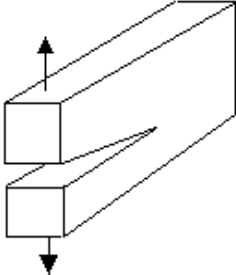
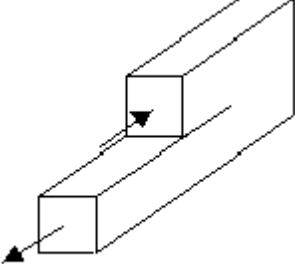
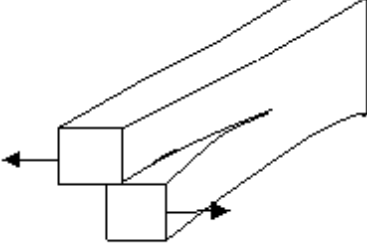
Factor de intensidad de tensiones.

El factor de intensidad de tensiones (K) define el estado tensional en la punta de grieta. Es decir, las tensiones cerca de la punta de grieta aumentan en proporción a K. Además, el factor de intensidad de tensiones define las condiciones de la punta de la grieta, si se conoce K, es posible obtener tensiones y desplazamientos en función de r y θ . Esta descripción mediante un solo parámetro de las condiciones de la punta de grieta resulta ser uno de los conceptos más importantes en la mecánica de fracturas.

El factor de intensidad de tensiones es una expresión que solo depende de la tensión aplicada σ , la longitud de la grieta a y la geometría C de la muestra.

$$K = C\sigma\sqrt{\pi a}$$

Cuando se aplica una presión a un cuerpo agrietado, la superficie de la grieta se mueve en diferentes direcciones, depende del tipo de carga, la dirección de la carga, etc. Hay tres modos posibles de desplazamiento de la superficie de la grieta. El factor de intensidad de tensiones se evalúa en cada modo (KI, KII, KIII).

Mode I (Opening mode)	
Mode II (Edge sliding mode)	
Mode III (Shear mode)	

Modos de desplazamiento del frente de grieta.

Para los materiales elásticos lineales, las tensiones y desplazamientos son aditivos, el factor de intensidad de la tensión también es aditivo en cada modo, pero no es correcto sumar un K_I con un K_{II} .

$$K_I^{Total} = K_I^{(A)} + K_I^{(B)} + K_I^{(C)}$$

$$K_{Total} \neq K_I + K_{II} + K_{III}$$

Para el Modo I, el signo es importante, si K_I es positivo, la grieta se abrirá, si K_I es negativo, la grieta se cerrará. Para los modos II y III el signo generalmente se toma como positivo. En esta tesis solo se obtienen factores de intensidad de tensión del Modo I y Modo II, es decir, debido a la dirección de la carga, la superficie de la grieta no se mueve fuera del plano de presión.

T-Stress.

El valor de T-Stress es el término independiente en r de las ecuaciones del campo de tensiones obtenidas de la expansión de Williams. Ha sido estudiada por muchos investigadores diferentes y se utiliza para muchas cosas diferentes en el campo de la FM.

La T-Stress se utiliza como una corrección de la solución de Westergards para eliminar el efecto de la tensión transversal que surge en la carga uniaxial.

La T-Stress se usa como predicción de la trayectoria de grietas en ensayos de tensión compacta, pero hay varios estudios que contradicen esta teoría.

La zona plástica (PZ) se ve afectada por la T-Stress, se usa para corregir la PZ como consecuencia del mecanismo de restricción de la punta de grieta.

En estudios de T-Stress en materiales piezoeléctricos y sensibles a la presión, se demostró que estaban afectados por las constantes elásticas y eléctricas (la carga positiva aumentó con la tensión T-Stress), también afectaron el desplazamiento de la fisura y las formas de la PZ.

La T-Stress no es útil para predecir trayectorias de grietas en crecimiento dinámico.

Uno de los métodos para calcular la T-Stress es el siguiente:

$$T = \lim_{r \rightarrow 0} (\sigma_{xx} - \sigma_{yy})_{\theta=0}$$

donde σ_{xx} y σ_{yy} son los componentes de la tensión y θ es el ángulo de la coordenada polar. En esta tesis, T-Stress se calcula por la diferencia entre σ_{xx} y σ_{yy} .

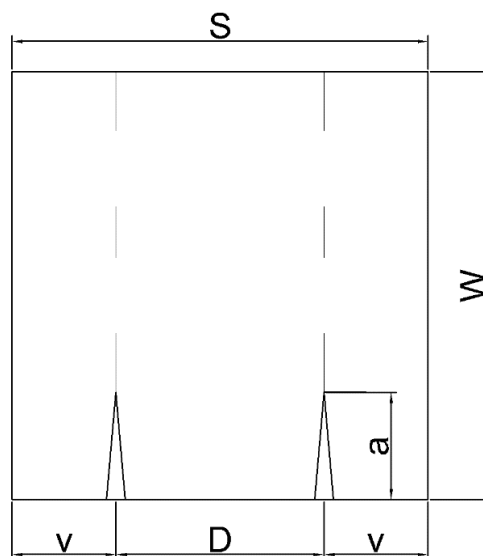
Modelado.

Geometría y restricciones.

Esta tesis expone los resultados de una prueba de flexión de cuatro puntos con una probeta con dos muescas paralelas. El modelo se ha realizado con dimensiones relativas que han sido variadas para obtener los factores de intensidad de tensiones y la T-Stress para cada geometría.

La dimensión principal es el ancho (W), las otras dimensiones variables son el espacio (S), la longitud de la grieta (a) y la distancia entre las grietas (D).

Lo importante es que solo hay una dimensión con un valor constante, el ancho (W), cuyo tamaño es siempre de 100 mm, todos los demás están relacionados entre sí; a/W es la relación entre el ancho y la longitud de la grieta, S/W es la relación entre el ancho y el largo y D/S es la relación entre el ancho y la separación entre las dos grietas.



Esquema de la geometría

Ratio	Valores
a/W	0.1, 0.2, 0.3, 0.35, 0.4, 0.45, 0.5, 0.6, 0.7, 0.8
S/W	1, 2, 3, 4, 6
D/S	0.33, 0.4, 0.5, 0.8

Valores de los ratios.

Propiedades del material.

Después de definir los parámetros iniciales, el siguiente paso consiste en configurar las propiedades del material. En ANSYS, se necesitan dos valores para definir un material isotrópico lineal, el Módulo de Young y el coeficiente de Poisson. Para el Módulo de Young, un valor aceptado es 30000 MPa, que corresponde a un hormigón C20 / 25, siguiendo el Eurocódigo 2. El coeficiente de Poisson para el hormigón es 0.2 .

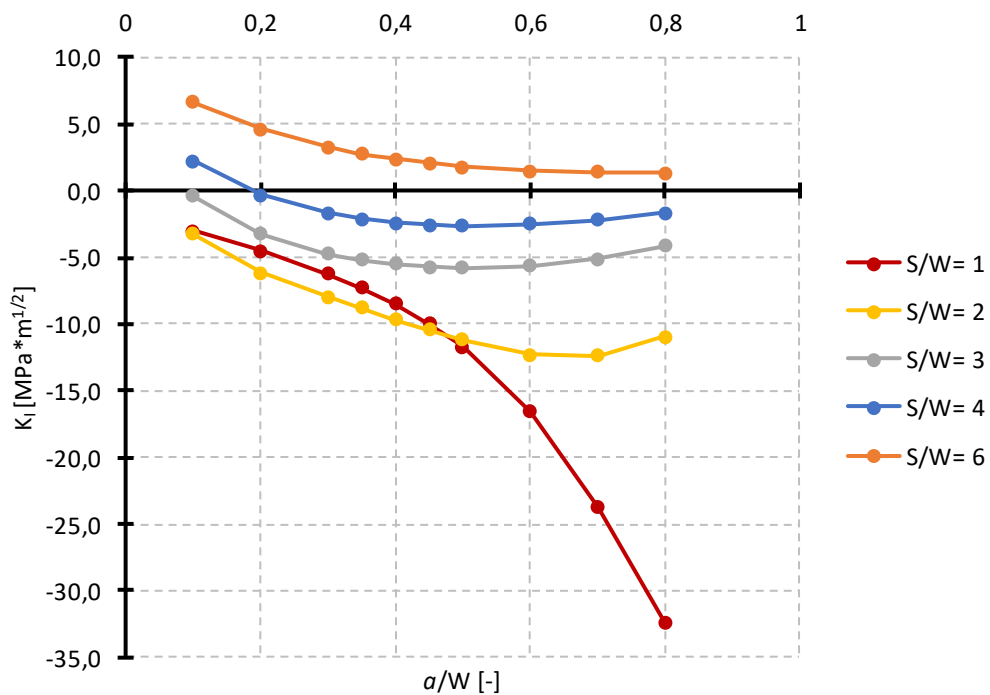
En la macro se utiliza el comando UIMP, para definir estos valores.

	Young`s Modulus	Poisson`s ratio
Concrete C20/25	30000 MPa	0.2

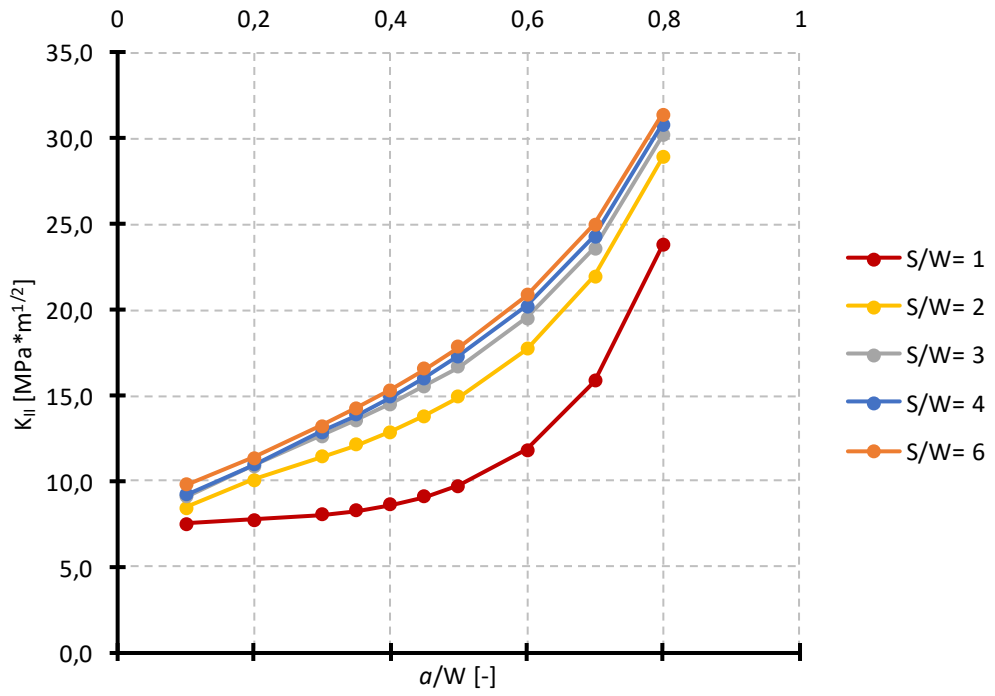
Propiedades del material en ANSYS.

Resultados

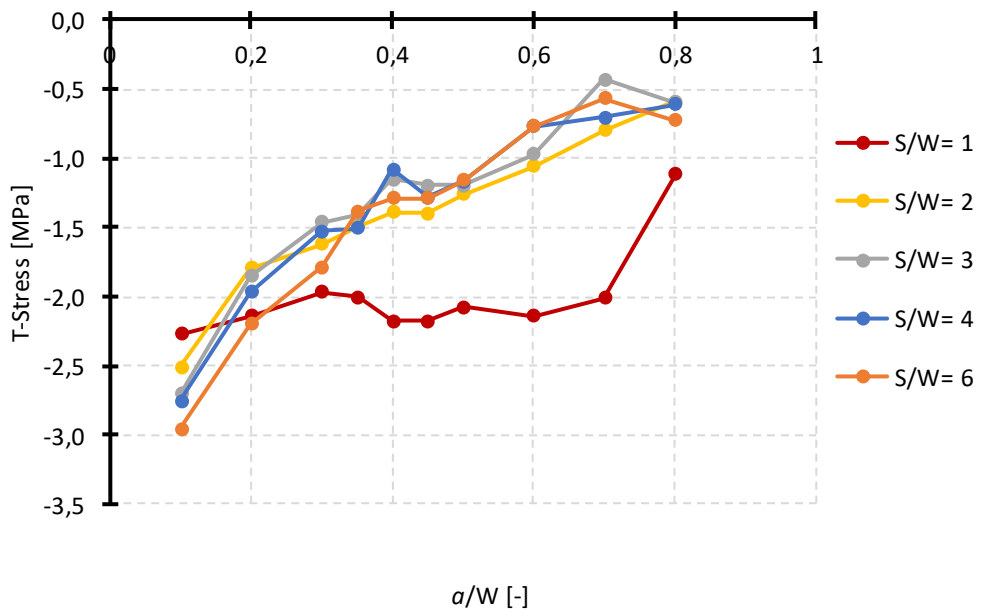
Curvas de D/S constante.



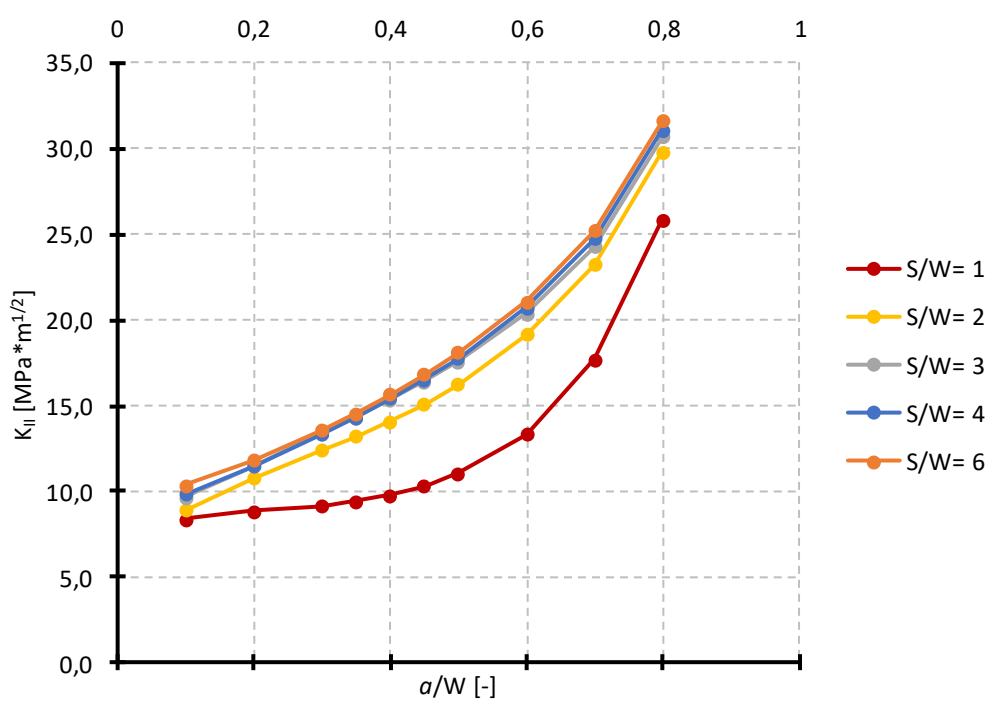
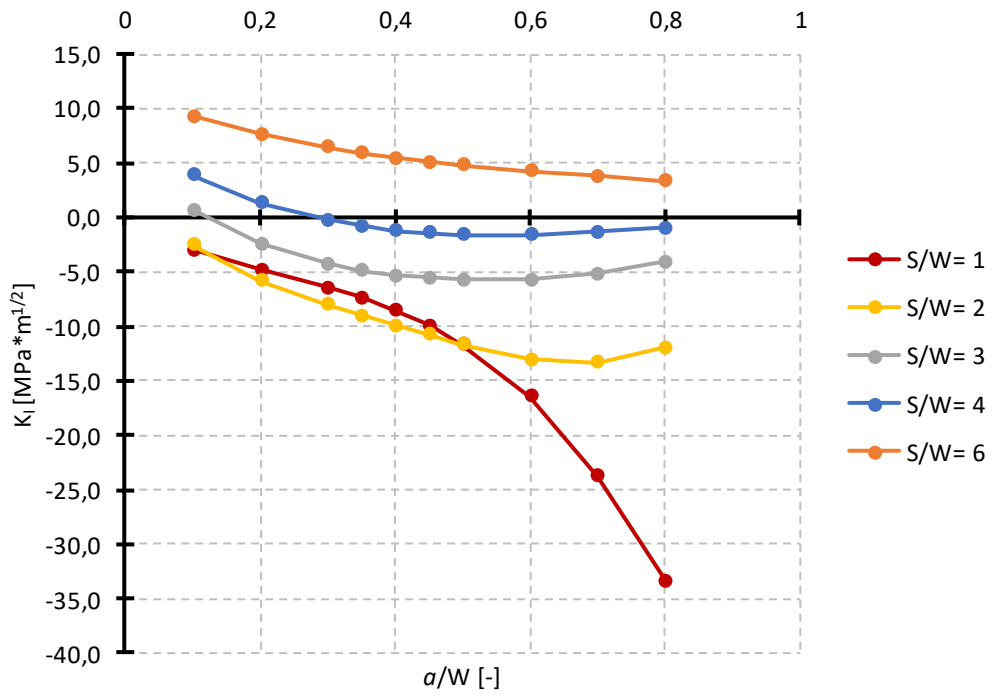
K_I para D/S=0.33

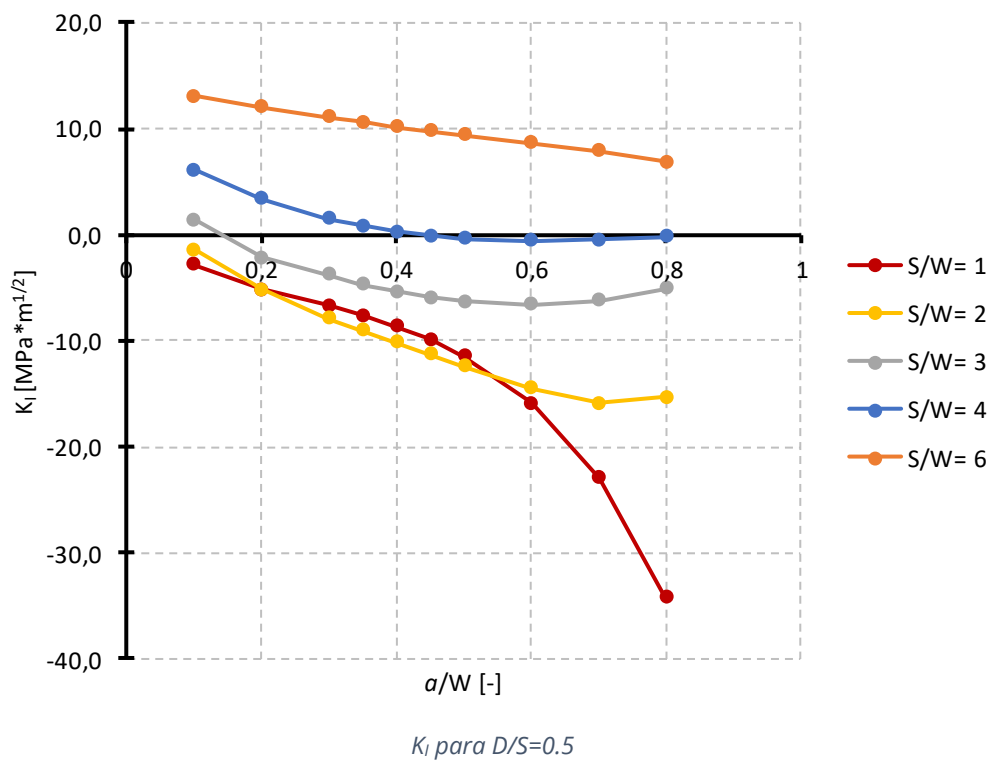
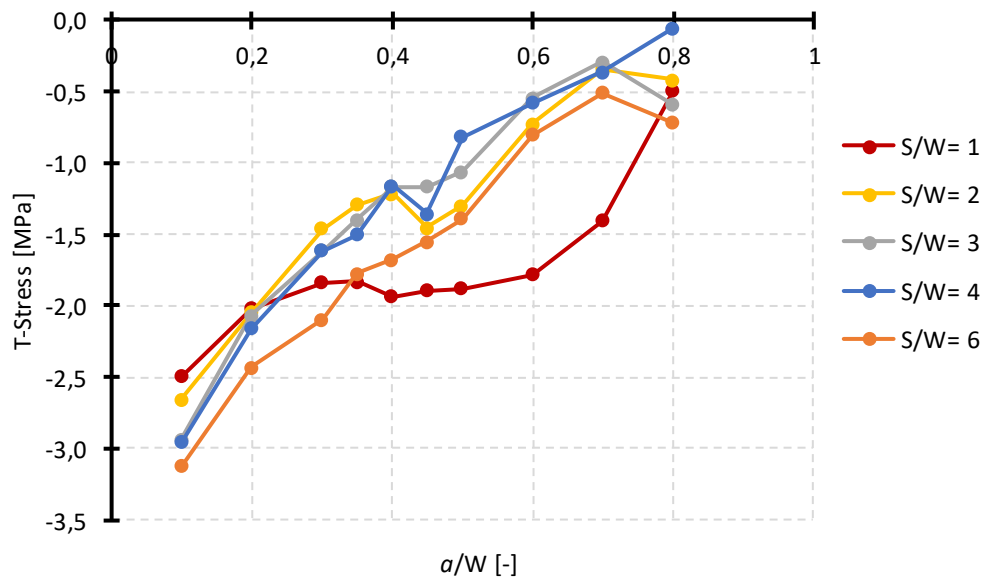


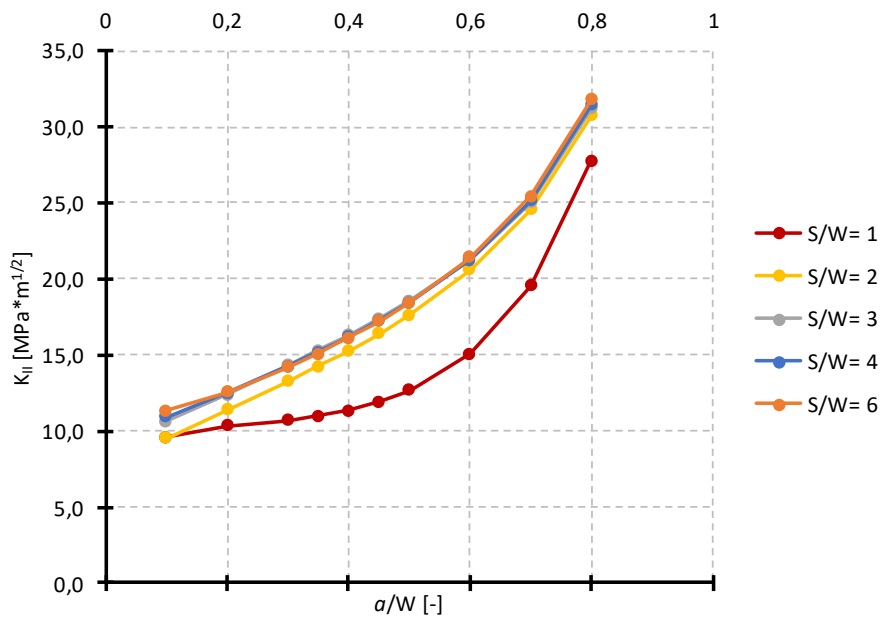
K_{II} para $D/S=0.33$



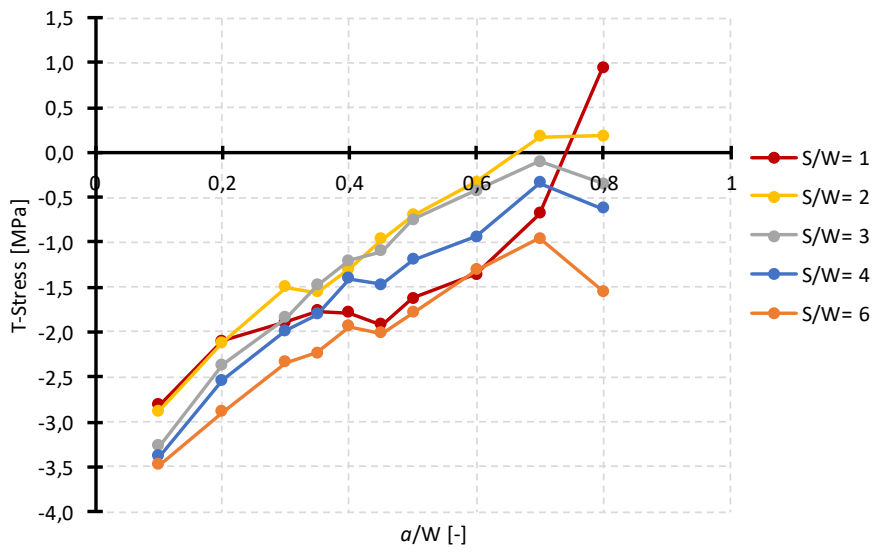
T-Stress para $D/S=0.33$



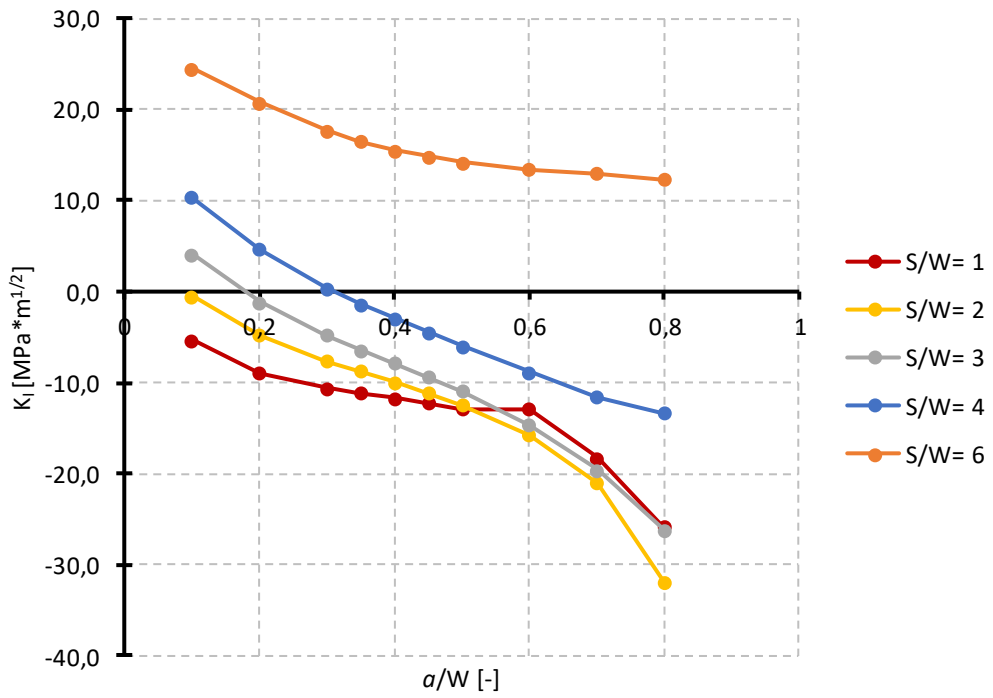




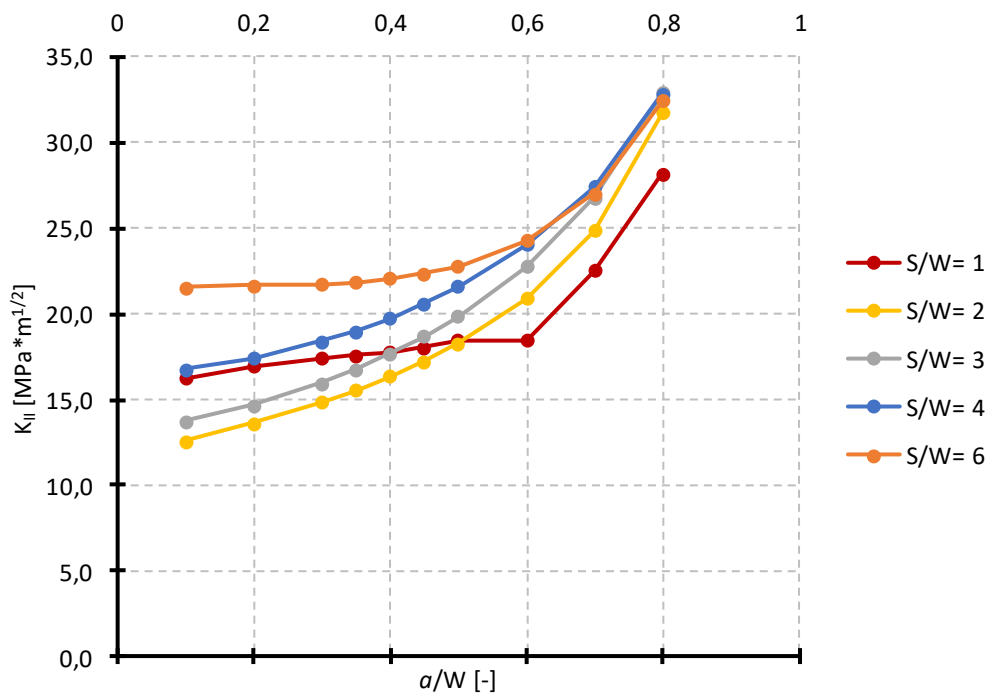
K_{II} para $D/S=0.5$



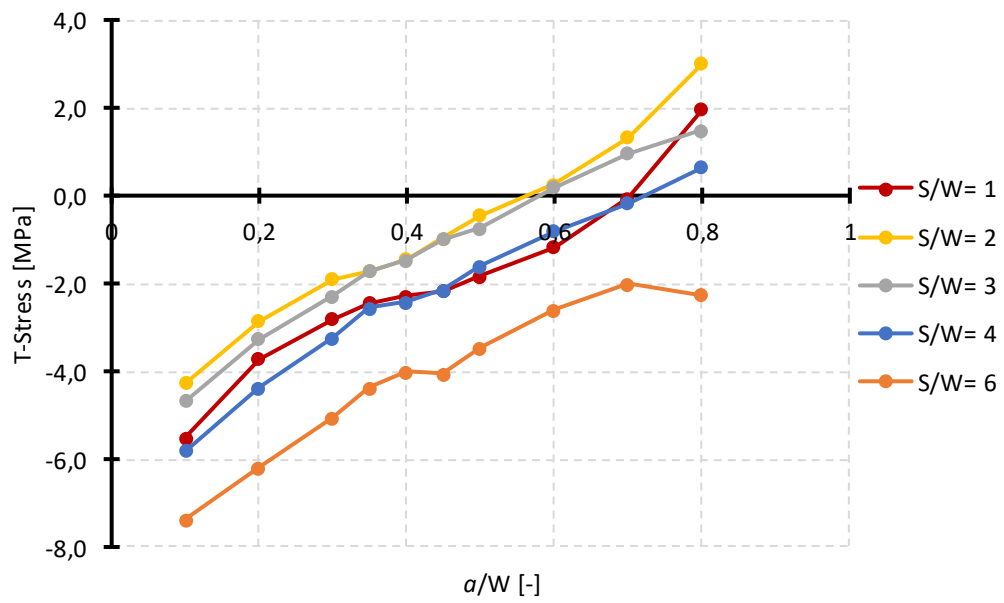
T-Stress para $D/S=0.5$



K_I para $D/S=0.8$

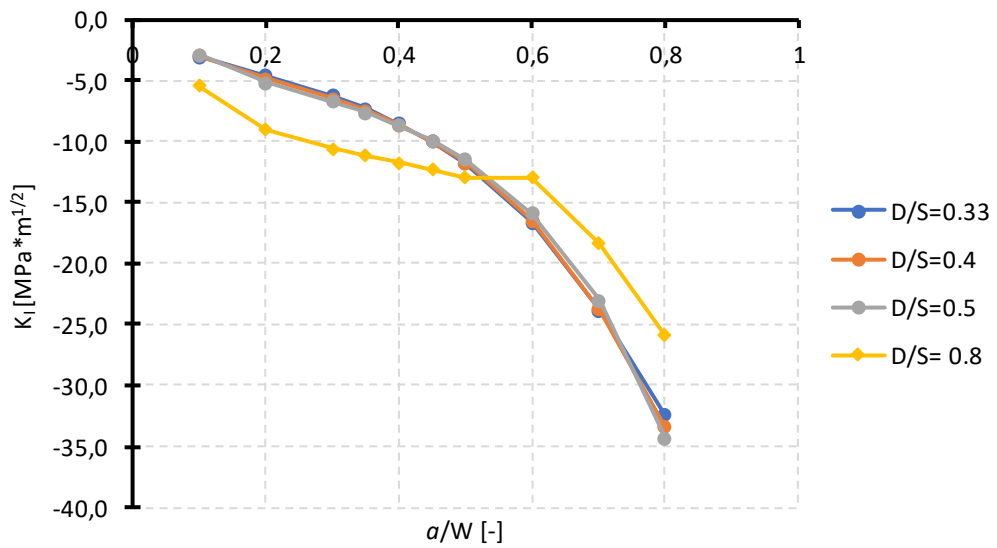


K_{II} para $D/S=0.8$

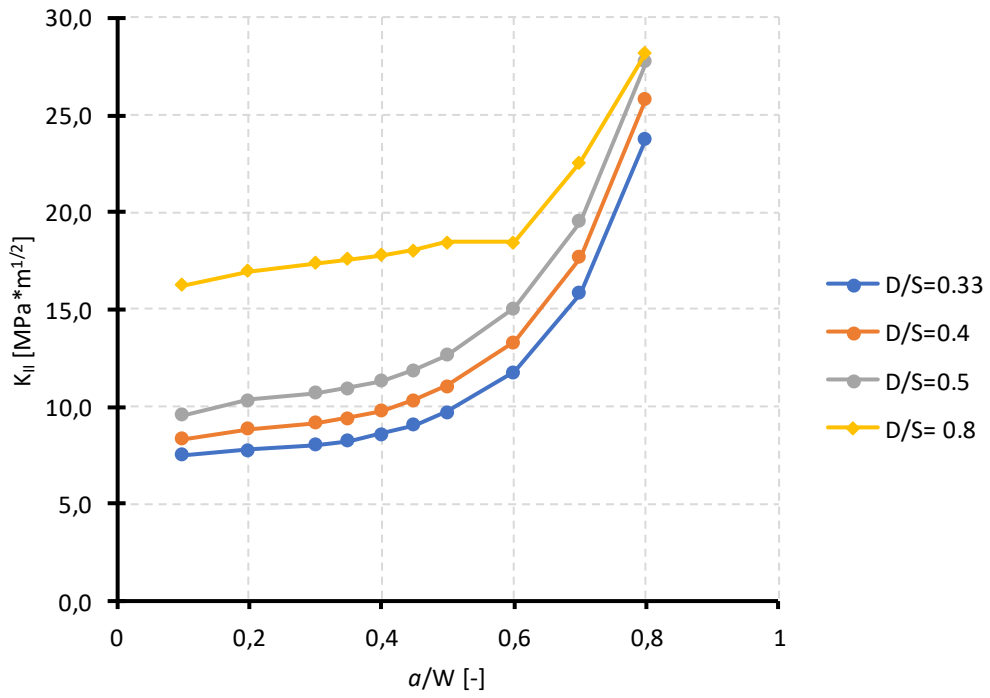


T-Stress para D/S=0.8

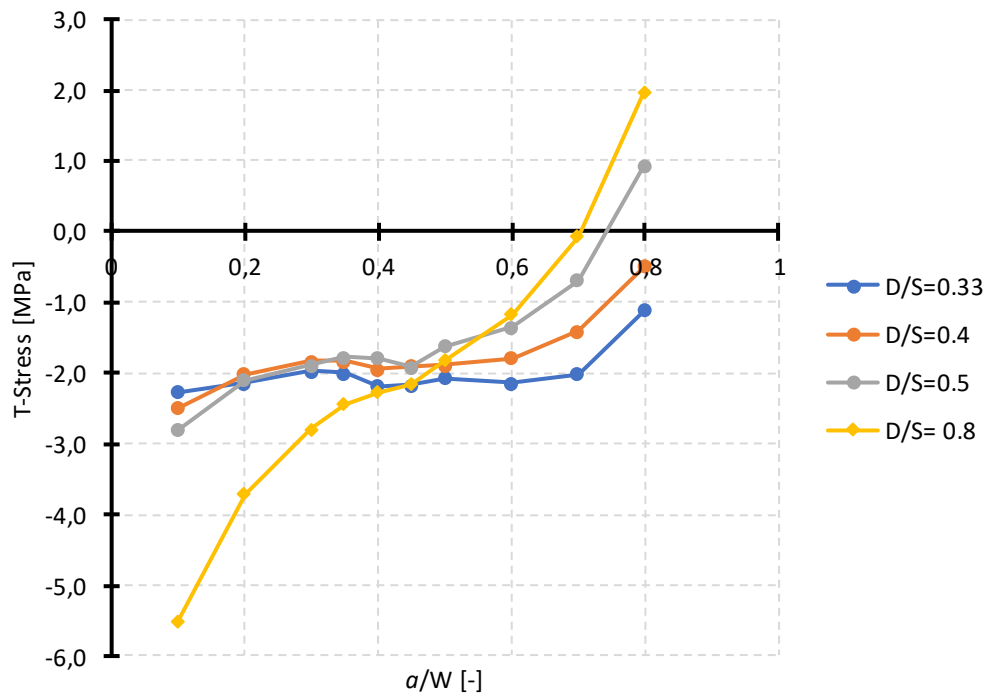
Curvas de S/W constante.



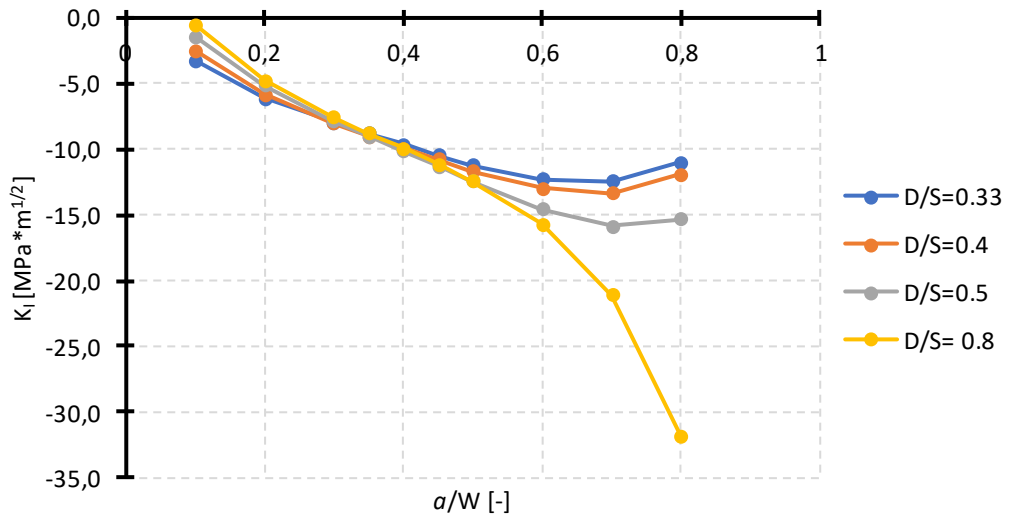
K_I para S/W=1



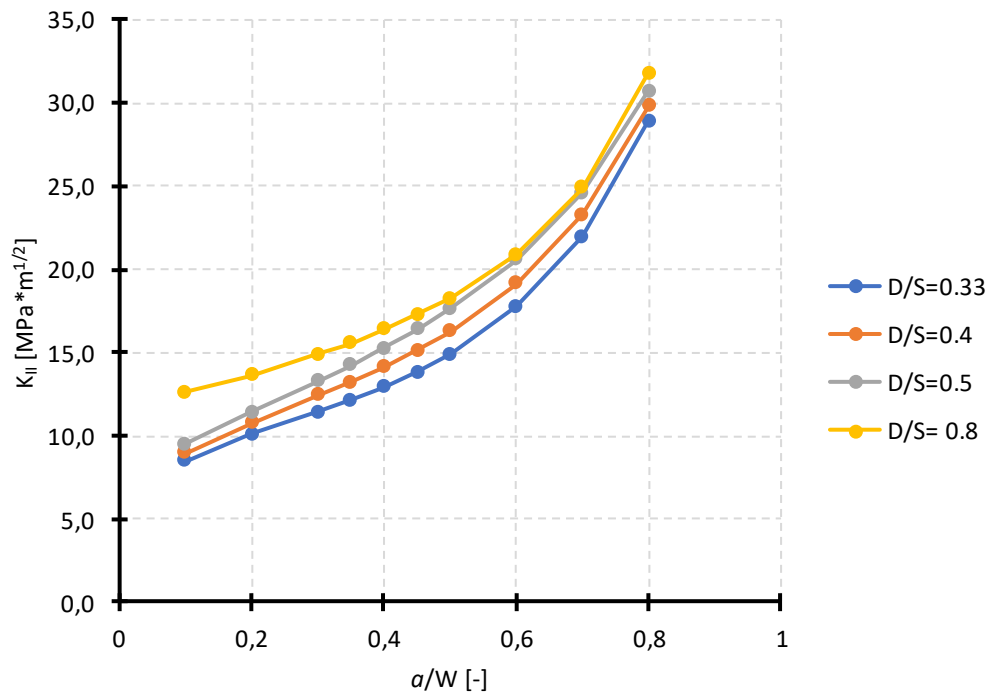
K_{II} para $S/W=1$



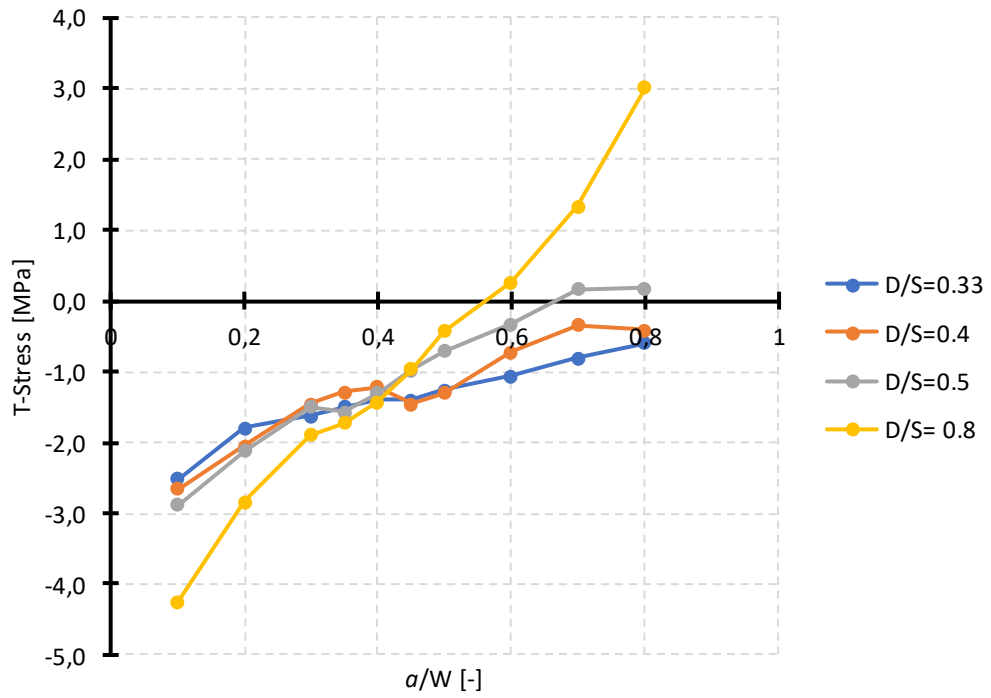
T-Stress para $S/W=1$



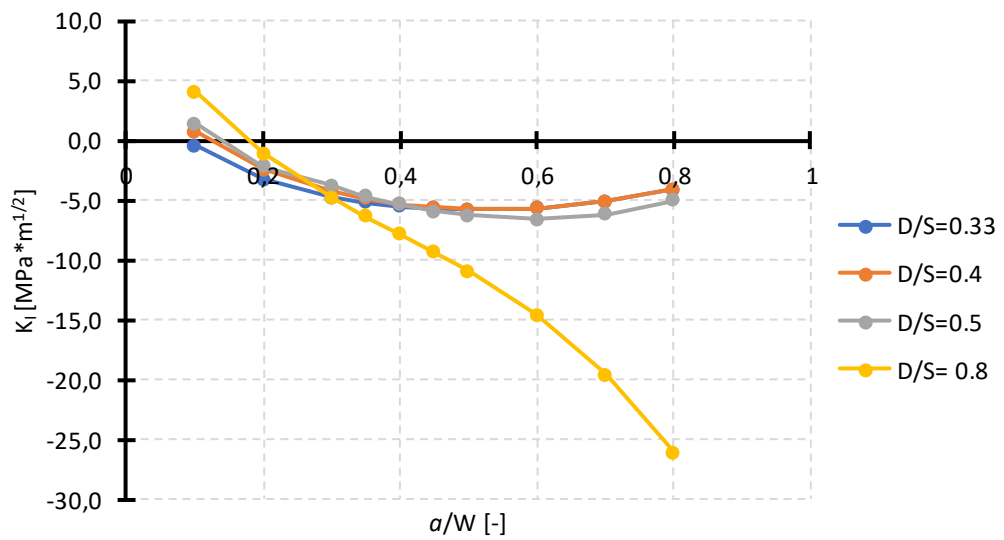
K_I para $S/W=2$



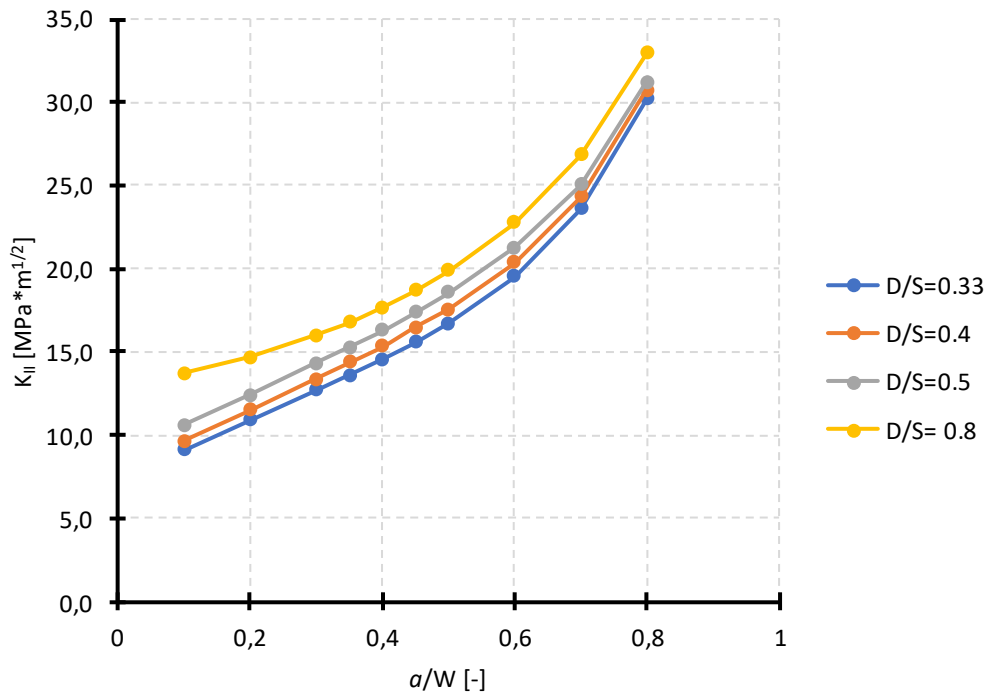
K_{II} para $S/W=2$



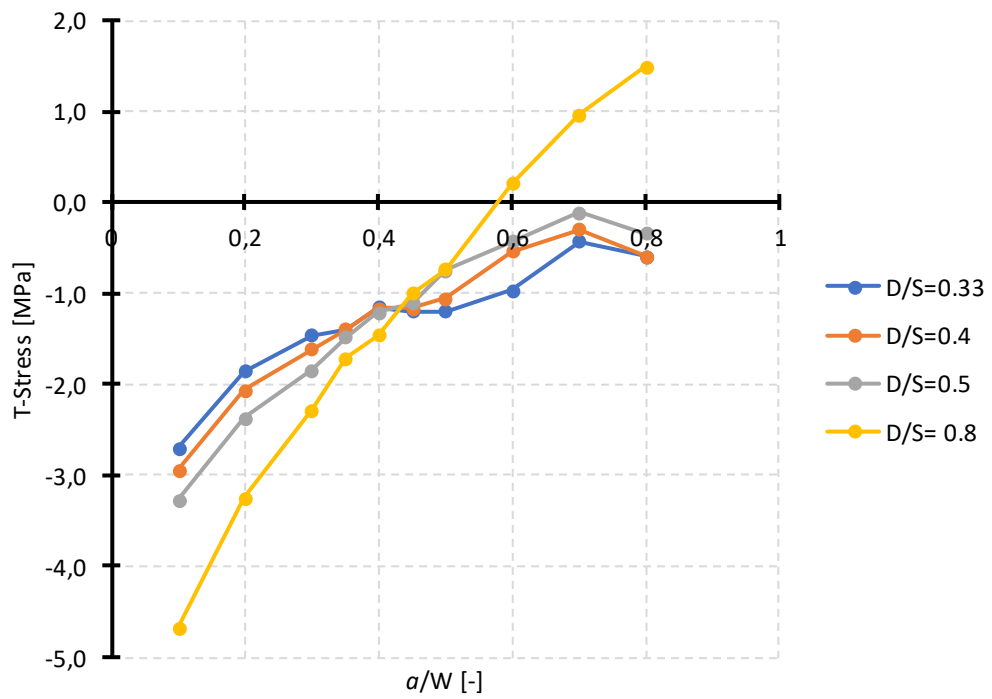
T-Stress para $S/W=2$



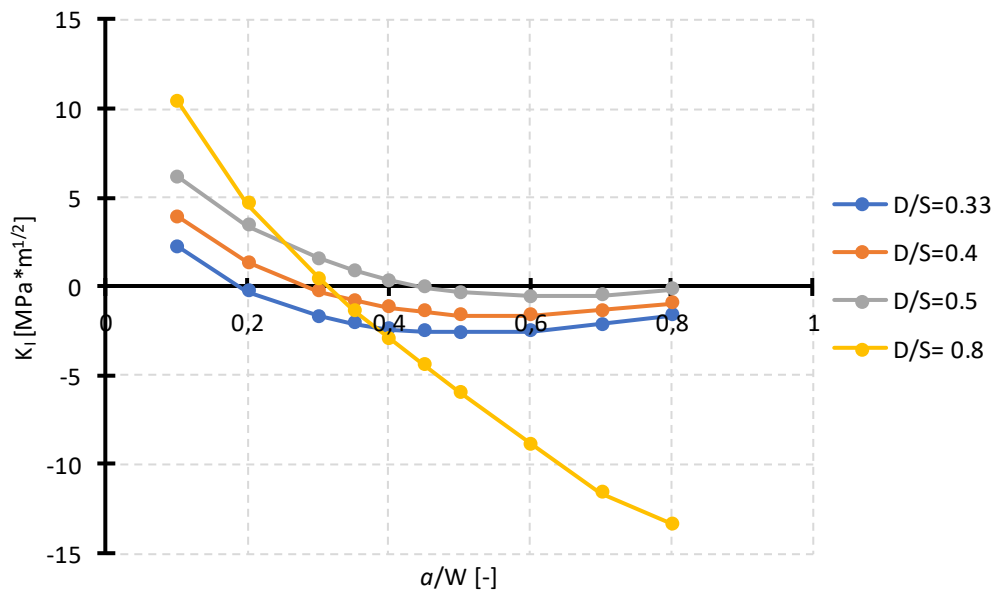
K_I para $S/W=3$



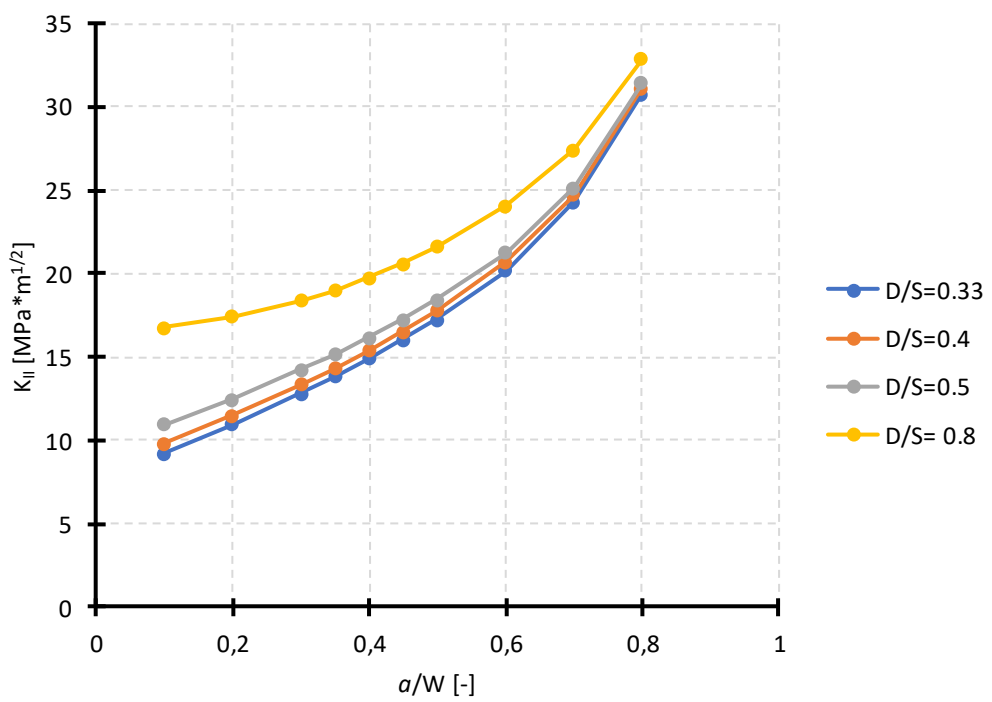
K_{II} para $S/W=3$



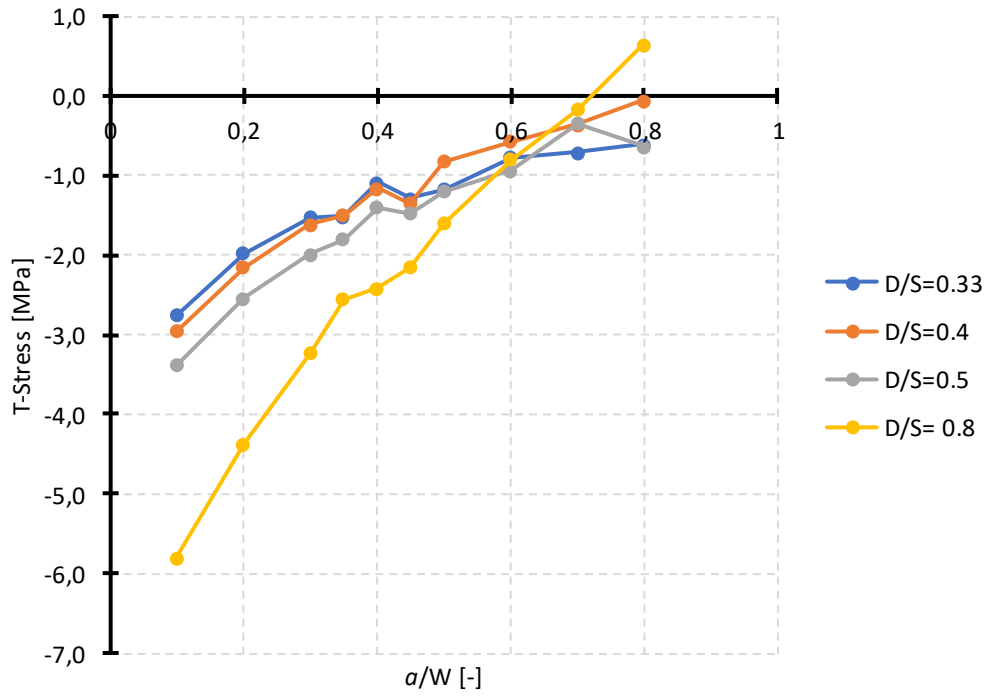
T-Stress para $S/W=3$



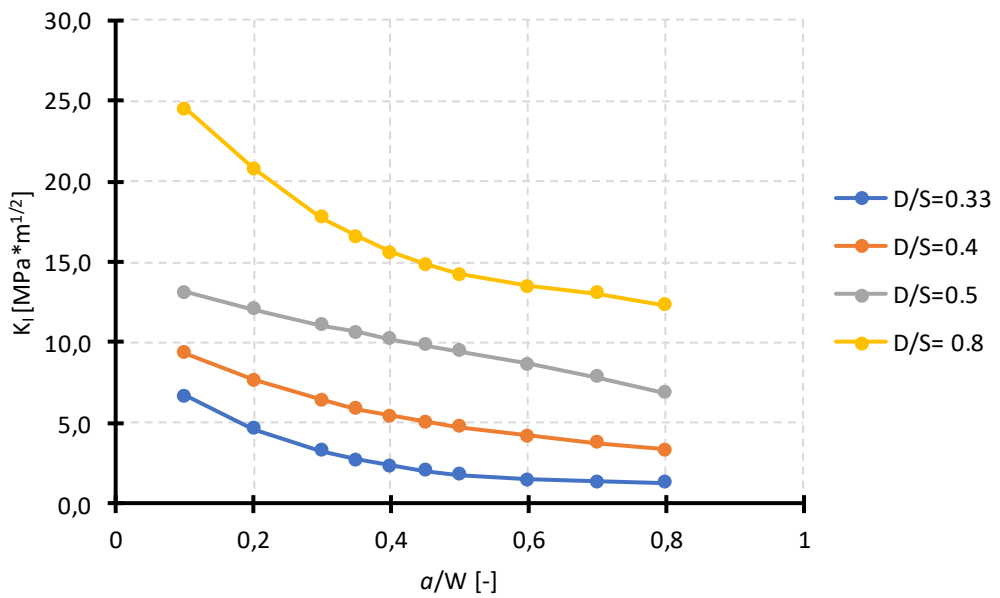
K_I para $S/W=4$



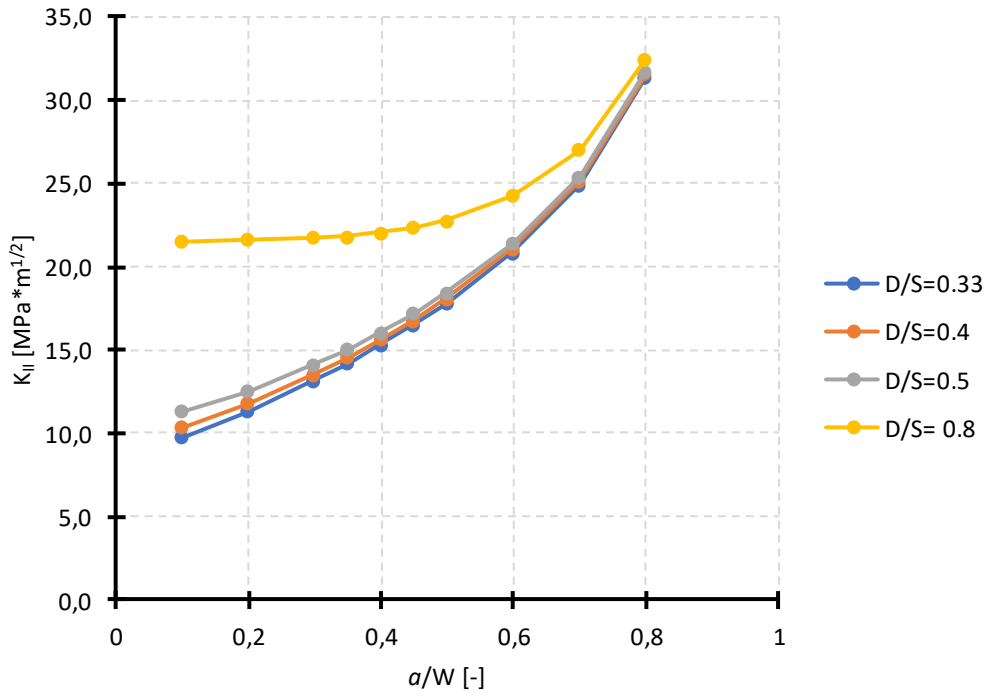
K_{II} para $S/W=4$



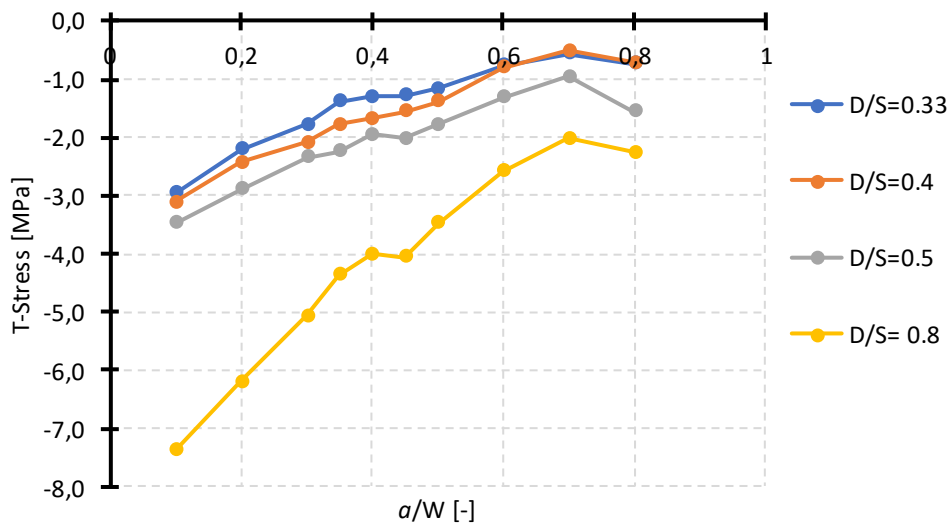
T-Stress para S/W=4



K_I para S/W=6



K_{II} para $S/W=6$



T-Stress para $S/W=6$

Conclusión.

En esta tesis, se estudiaron tres parámetros para definir el estado tensional en la punta de grieta para diferentes dimensiones en la prueba de flexión de cuatro puntos, el factor de intensidad de tensiones para Modo I y II, y la T-Stress. Los resultados se obtuvieron en el software del método de elementos finitos, ANSYS, y luego se representaron en gráficos. Comparando las curvas es posible obtener algunas conclusiones.

Para especímenes cuadrados ($S/W=1$), las curvas tienen diferentes comportamientos porque se trata de un caso especial.

La KI cambia su comportamiento dependiendo de las dimensiones, pero se ha demostrado que para mayores longitudes de grietas, el Modo I tiende a valores negativos, lo que significa que la grieta se está cerrando.

Para KII, las curvas son muy claras, siempre con la misma forma. La curva siempre crece para mayores longitudes de grietas.

T-Stress también tiene líneas de tendencia claras, y como KII, las curvas siempre crecen para grietas mayores.

Los valores obtenidos en ANSYS son solo resultados matemáticos, que deben analizarse para demostrar su veracidad, como se ha hecho con el signo de KI utilizando los desplazamientos.

Todos los resultados extraídos en esta tesis podrían mejorarse en el futuro o usarse en diferentes documentos para obtener más conclusiones en la prueba de flexión de cuatro puntos. Para probar la exactitud de estos valores, deben compararse con los números reales obtenidos en el laboratorio.